Wear of High-Technology Coatings, Deposited by High-Velocity Oxygen Flame (HVOF)

Mara Kandeva , Zhetcho Kalitchin and
Yana Stoyanova

B P International

Wear of High-Technology Coatings, Deposited by High-Velocity Oxygen Flame (HVOF)

Wear of High-Technology Coatings, Deposited by High-Velocity Oxygen Flame (HVOF)

Author(s)

Mara Kandeva [a], Zhetcho Kalitchin [b*] and Yana Stoyanova [a]

[a] Faculty of Industrial Engineering, Tribology Center, Technical University – Sofia, 8, Kl. Ohridski Blvd, 1756 Sofia, Bulgaria.
[b] SciBulCom2 Ltd., 2A, Yakubitza Str., 1164 Sofia, Bulgaria.
[*] Corresponding author: E-mail: kalitchin@gmail.com;

9 789355 478856

9 789355 478863

Contents

PREFACE

The tribology is a fundamental interdisciplinary science and technology for the contacts and the contact interactions in technical systems. The term "contact interactions" (tribological interactions) unites in combination all the phenomena and processes within the zone of touching the bodies, independently of their nature – physical, mechanical, chemical, electrical, thermo-dynamical, acoustical, and technological [1-6]. Carriers of these interactions are regions having specific structures, characteristics, and states, named „contact". The contacts as objects of the tribology have no analogue in the fields of science. They cannot exist as separate independent physical objects without the presence of the contacting bodies, but they have decisive importance to the functional characteristics of the contacting systems. It is for this reason the contacts are considered in the tribology as independent functional objects of the systems [7-9].

The basic tribological phenomena and processes are friction, wearing, and lubrication, which determines the exploitation characteristics and resources of the details, the mechanisms, and the machines. The friction to a great extent is connected with energy losses, consuming 30-40% of the energy produced in the world. The wearing is accompanying the process of friction and it leads to losses of material and human resources. It is the reason for the termination of the exploitation process of more than 80% of the details and the machines taken as one whole. Simultaneously with this, friction as a driving process is of essential importance for the functioning of a series of systems such as mechanical brakes, and friction devices, as well as in many technological processes – ignition, welding by friction, and some others. The utilization of the achievements of the contemporary tribology enables decreasing many times the losses arising from friction and decreasing the wearing process in machines, which would lead to economic effectiveness at values ranging from 2 up to 4% of the national income of the developed countries in the world. The object of the tribology is the elaboration and controlling of surface layers, coatings, construction, and lubrication materials having appropriate physicomechanical and mechano-chemical characteristics, which ensure adaptation and optimization of the regime of occurring the tribological interactions in various operational regimes.

The exploitation period of a machine represents the calendar duration of its exploitation until the destruction or loss of its functional indices. The expenses for the repairing work of the machines, the equipment, and the transportation expenses represent in developed countries tens of billions of dollars per year. In the course of the development of the industry, these figures are growing up continuously. The expenses for repair and technical servicing of the machines exceed several times their original prices. The investigations show that for example, for automobiles the expenses for these losses are about 6 times higher, for airplanes – up to 5 times, for the metal processing and wood processing machines – up to 8 times higher. The different machines are repaired a different number of times during their exploitation period, for example, the road construction machines are to be repaired up to 15 times. The greatest wearing degree is for details and functional parts of machines and equipment, which are

being exploited in abrasive or aggressive media, as well as details of transportation machines operating, in a dust-contaminated environment. Such fields of exploitation are the following – machines in agriculture, the mining industry, energy production, chemical industry, cement production, and others.

The problem of increasing the life cycle of the machines is connected with the enhancement of the wear resistance of the contacting joints. This is a complicated problem. In most cases, it requires combining high antifriction effectiveness and high wear resistance. The high antifriction effectiveness means a low coefficient of friction, which is achieved by the plasticity of the surface layers, while the high wear resistance implies great resistance of the surface layer against splitting, impact interactions, and vibrations, which is achieved by the higher hardness of the surfaces. Usually, the plastic (the soft) layers have lower hardness, while the layers with great hardness have lower plasticity and high brittleness. The compromise is achieved by precision analysis of the mutual influence of three main groups of factors: *working medium* – with or without lubricating material, presence of abrasive material, aggressive compounds, etc.; *dynamic conditions* – velocities, loadings, type of the movement, presence of vibrations; *contacting materials* - composition, structure, physical-mechanical properties, compatibility [4,10-12].

It is very important to point out the circumstance, that during the exploitation of the machines the tribological processes influence one another and they change the time-space characteristics of the contact, and this in its turn determines its behavior and the functional characteristics of the contacting joints, respectively those of the machines, taken as one whole.

Many years of practice in creating protective layers and coatings of the metals have shown that the highest quality wear-resistant coatings are obtained by using concentrated flows of energy. One can observe in the current literature a large number of developments, in which different aspects are considered for the creation of protective coatings by applying gas-thermal methods and concentrated energy flows [13-17].

The subject of the present book is the essence and the mechanisms of wearing of composite powder coatings, consisting of superalloys, deposited by supersonic flame jet - HVOF (High-Velocity Oxy-Fuel) as a new generation of tribology materials. These coatings have been obtained at the velocity of the flame jet 1000 m/s of powder composites, containing micro-particles of different chemical compositions – nickel, tungsten, boron, silicon, manganese, and others having different content percentages. The coatings have been obtained upon a substrate of steel in two cases – without preliminary thermal treatment of the substrate and with preliminary thermal treatment of the substrate. The wearing process characteristics have been studied – mass wear, wear rate, wearing intensity, absolute and relative wear resistance. It is known that the mechanisms and the dynamics of the wearing process and the wear resistance depend on the conditions of interaction. The tribological behavior of such coatings is of special interest under extreme exploitation conditions– the presence of solid-state

particles, high loadings and velocities, impacts and vibrations, high temperatures, presence of aggressive media, vacuum, radioactive irradiation, and others.

The book represents the results of HVOF-coatings for three cases: wearing process during dry abrasive friction over the surface with solid attached abrasive particles (abrasion); erosion wear process under the effect of the air stream, carrying solid abrasive particles (erosion), and wearing process under the influence of vibration normal loading during sliding along the surface having solid attached abrasive particles (vibration-abrasive wear).

The investigations have been carried out in the Center for Tribology at the Faculty for Industrial Technologies (FIT) in the Technical University- Sofia under the leadership of Prof. Ph.D. Mara Kandeva with some already known and other newly elaborated methods and devices.

The results from the studies on supersonic flame coatings were reported at the world congresses in Italy (Torino) and China (Beijing), at the international conferences BALKANTRIB of the Balkan Tribological Association in Turkey, Serbia, Romania, Greece, Bulgaria and they have been published in journals, indexed in Scopus and Web of Science.

_____

Wear of High-Technology Coatings, Deposited by High-Velocity Oxygen Flame (HVOF)

Mara Kandeva [a], Zhetcho Kalitchin [b*] and Yana Stoyanova [a]

ABSTRACT

One of the methods for decreasing the wearing degree in contacting joints and increasing the resource of the machines and the mechanisms is the deposition of composite powder coatings of super-alloys using the supersonic flame jet (HVOF –High-Velocity Oxy-Fuel). Using this contemporary technology one obtains coatings, which have considerably improved mechanical and tribological characteristics – high adhesion strength of bonding with the substrate, density, hardness, wear resistance, and corrosion stability.

The subject of the present book is the processes and the mechanisms of wearing the composite powder coatings of super-alloys, deposited by a high-velocity flame jet - HVOF at a velocity of the flame jet 1000 m/s of powder composites, containing micro-particles having different chemical compositions – nickel, tungsten, boron, silicon, manganese, and others. in various percentages of their content and different sizes of the powder particles.

The structure of the book includes an preface, nine chapters, and references.

The first chapter reveals the essence and the mechanisms for obtaining the HVOF coatings, it describes the basic powder materials and composites for their preparation, the physical-mechanical characteristics of the coatings, their advantages, and disadvantages, and the fields of their applications.

The second chapter describes the technology for the preliminary preparation of the samples and the parameters of the technological regime for the deposition of the coatings. The methods and the devices are described, serving for the investigation of the wearing process of the HVOF coatings under 3 different sets of conditions the contact interaction: abrasive wearing in case of dry friction over the surface of solid attached abrasive particles using tribo-tester „pin-disk“;

_____

[a] _Faculty of Industrial Engineering, Tribology Center, Technical University – Sofia, 8, Kl. Ohridski Blvd, 1756 Sofia, Bulgaria._
[b] _SciBulCom2 Ltd., 2A, Yakubitza Str., 1164 Sofia, Bulgaria._
*Corresponding author: E-mail: kalitchin@gmail.com;

erosion wearing under irradiation with the air stream, carrying the solid abrasive particles; wearing under the impact of cyclic normal loading with various frequency during sliding along the surface with solid attached abrasive particles using the tribotester „pin-drum".

The third chapter represents the results of the mass wear, the rate of the wearing process, the specific intensity of the wearing process, and the wear resistance The HVOF coatings have two kinds of powder composites –a matrix of tungsten carbide and a matrix of nickel with different sizes of the powder particles in the case of dry abrasive friction and erosion caused by the air stream, carrying the solid particles. It has been established that there is non-linear dependence of the characteristics of the abrasive wearing process depending on the path length and the influence of the sizes of the powder particles upon the wear resistance of the coatings. It has been ascertained that the abrasive wear resistance of the two types of coatings – with tungsten matrix and with nickel matrix, is greater in the case of smaller sizes of the powder particles, respectively for the coatings with tungsten matrix of 11 microns, while for the coatings with the nickel matrix it is 20 microns. The same coatings in the case of erosion have lower wear resistance, i.e. lower resisting ability under the impact influence of abrasive particles in the air stream. This can be explained based on the different mechanisms of the wearing process of the coatings. It is observed that the wear resistance of the tested coatings and that of the substrate is greater in the case of erosion in comparison with that of the abrasive friction.

The fourth Chapter represents the results of the abrasive wearing process of 11 types of HVOF coatings with metal, ceramic and metal-ceramic composites and their mixtures. Results have been obtained about the influence of the normal loading, the preliminary thermal treatment of the substrate, and the type of the substrate upon the characteristics of the abrasive wearing process. It has been established that the dependence of the abrasive wearing process on the magnitude of the normal loading has a different character for the various types of coatings. At small values of the loading, this dependence is straight proportional, while at high values of the loading it becomes non-linear. The magnitude of the wear degree depends on the nature and the type of the preliminary thermal treatment of the substrate. For coatings, deposited on a substrate of steel the wear degree is lower, compared to that for coatings, deposited on aluminum. The preliminary thermal treatment of the substrate leads to a decrease in the wear degree for all the coatings, but a different extent. The lowest wear degree among all the studied coatings is demonstrated by the coating, deposited using a powder composite of WC-12Co on a steel substrate. The coating WC-12Co is a combination of very hard dicarbides and a plastic matrix of cobalt. The high abrasive wear resistance of the coating is due to the high degree of wetting of the tungsten carbides in the cobalt matrix, as a result of which in the bulk phase of the coating an internal contact network is being formed having high cohesion strength of the metal-ceramics WC-Co.

The fifth Chapter represents the comparative results of the abrasive wearing process of four types of coatings without and with preliminary thermal treatment

of the substrate under conditions of dry vibration-abrasive friction. It has been found that the magnitude of the vibration rate influences the size and the character of the changes in the mass wear of the coatings. Up to a certain value of the vibration rate, the wear degree is decreased, but thereafter it grows up and at vibration rates w>16,88 mm/s the wear degree reaches greater values than those in the absence of vibration. The dependence between the wear degree and the vibration rate has a non-linear character with expressed minimum. The minimal wear among all the studied samples for the entire range of vibration rates is shown by the coating WC-12Co, which is an order of magnitude lower than that of the remaining coatings. The preliminary thermal treatment of the substrate up to a temperature of $650^{o}C$ for 5 minutes during deposition of the coating 602P leads to a lowering of the wear degree with 55% for the entire range of changes in the vibration rates. Upon analyzing the microstructure of the coatings after the wearing process at a vibration rate of 21.08 mm/s, it is seen that in the case of the coating WC-12Co the basic mechanism of the wearing process is the mechanical scratching by the abrasive particles during relative motion. The worn coating has the homogeneous texture of the type of flat plane network of scratches, obtained by the planar movement of the samples. The high wear resistance of the coating is due to the strictly differentiated functions, which fulfill the components in its structure: the particles WC ensure the great resistance of the coating against the cutting tangential action of the abrasive particles and the fatigue vibration strength of the coating; The cobalt (Co) fulfills contacting role in the structure of the coating – it builds up internal boundary network between the particles of WC and this guarantees remaining of the whole coating. The wear resistance of the composite coatings to a great extent is determined by the thickness and the physical-mechanical properties of this network. The internal contact network in many cases determines the damper properties of the coating under impulse action and periodic actions. In the case of coatings, obtained from ceramic mixtures 602P and 602P+WC-12Co (1:1) the basic mechanism of the wearing process is the fatigue caused destruction of the surface, as a consequence of the cyclic loading at a high vibration rate.

Chapter six represents comparative results for the characteristics of the wearing process and the wear resistance of composite powder coatings, deposited by High-Velocity Flame jet (HVOF), which contain composite mixtures Ni-Cr-B-Si having various concentrations of chromium – 9.9%; 13.2%; 14%; 16% and 20%, at the same size of the particles 45 µm and identical contents of the rest of the elements boron and silicon. Results have been obtained about the dependence of the mass wear on the path length of friction, the variation of the intensity of the wearing process on the concentration of chromium for coatings without thermal treatment of the substrate, and with thermal treatment of the substrate. It was established that for all the coatings the preliminary thermal treatment of the substrate leads to a decrease in the intensity of the wearing process. It is shown that upon increasing the concentration of chromium the intensity of the wearing process is decreasing non-linearly, whereupon it reaches minimal values at 16% Cr. In the case of coatings with a 20% concentration of Cr the intensity of the wearing process grows up, which is due to the absence of the components B and Si in the composite mixture, whereupon no new inter-metalloid structures are

formed of high hardness and wear resistance. A diagram has represented the interconnection between the hardness of the coatings and the abrasive wear resistance. Based on regression analysis analytical dependences have been obtained for the intensity of the wearing process on the concentration of chromium for coatings without thermal treatment and with thermal treatment of the substrate, represented as polynomials of second order and third order.

Chapter seven illustrates comparative results about the erosion-wearing process of the same composite Ni-Cr-B-Si coatings at two angles of irradiation with the air stream, containing solid particles – 60° and 90°. It has been ascertained that for all the coatings the preliminary thermal treatment of the substrate leads to a diminishing of the intensity of the wearing process, i.e. increase in the erosion wear resistance. The angle of the jet stream influences the wear resistance of all the coatings. At an irradiation angle of 60^{o,} the wear resistance grows up within the interval from 1.5 up to 2.6 times higher for the coatings without thermal treatment of the substrate and within the interval from 1.6 up to 3.5 times higher for the coatings with thermal treatment of the substrate in comparison to the wear resistance at angle 90°. This effect is the greatest - 3.5 times higher for the coating with 16%Cr. At jet angle 90° the wear resistance grows up to 10% and this increase is the same for all the coatings. The dependence of the erosion wear resistance on the concentration of chromium has a strongly expressed non-linear character. It increases with the increase in the concentration of chromium and it reaches a maximum for coatings with 16% Cr having thermal treatment of the substrate at jet angle 60°. Regression models have been obtained for the intensity of the erosion process for the two jet angles 60° and 90° for the coatings without thermal treatment and for the coatings having thermal treatment of the substrate.

Chapter 8 represents results for the influence of the size of the micro-particles in super-alloys upon the abrasive wearing process of 12 kinds of HVOF coatings. All the composites have identical chemical compositions, but they contain particles having different sizes – 5 µm, 11 µm, 22 µm, 35 µm, 45 µm, and 55 µm. Results have been obtained for the dependences of the mass wear and linear wear, the intensity of the wearing process, the absolute and the relative wear resistance versus the path length of friction, the normal loading, and the size of the powder particles for all the tested coatings – with and without thermal treatment of the substrate. It has been established that the preliminary thermal treatment of the substrate exerts influence upon the magnitude and the mechanism of the abrasive wearing process, consisting in diminishing the intensity of the wearing process of all tested coatings, which is due to an increase in the hardness of the coatings. The increase in the abrasive wear upon increasing the path length of friction has linear character for all tested coatings. Upon increasing the normal loading the abrasive wear grows up linearly for all tested coatings. The sizes of the composite particles exert an effect upon the magnitude of the abrasion wear degree. Upon increasing the size of the particles the wearing degree grows up and the dependence acquires a wave-like character. The degree of non-linearity depends on the magnitude of the normal loading. The sizes of the composite particles influence the mechanisms of the

abrasion wearing process combined with the influence of the normal loading: in the cases of coatings having small sizes of the particles from 5 μm up to 35 μm and low loading values up to15 N, the prevailing mechanisms of the wearing process is micro-splitting, while at greater loading of 20 N and 25 N one observes for these coatings traces of micro-splitting and plastic deformation. In the cases of coatings having larger sizes of the particles ranging from 35 μm up to 55 μm under great loadings the prevailing mechanism is the plastic deformation, while under small or medium loadings a mixed mechanism is observed for the abrasion wearing process – both micro-splitting and plastic deformation.

Chapter 9 illustrates results from the comparative investigation of the abrasion wearing process and the coefficient of friction of galvanic chromium coatings without any nano-size particles, galvanic chromium coatings, modified with different concentrations of the nano-sized diamond particles, and tungsten carbide HVOF coating WC/Co (88/12), under identical conditions of friction. As a summary of the obtained results for galvanic chromium, chromium-nano-size-diamond coatings, and composite coating WC/Co (88/12), deposited by HVOF technology, it can be stated that the coating WC/Co (88/12) has the highest wear resistance among all the electrolytic chromium coatings without and with NDDS, obtained in the three regimes R1, R2 and R3. The wear resistance of the WC/Co coating is 7,2 times higher than that of the chromium coating without NDDS in the case of regime R1 and from 5,4 times up to 15,4 times, higher wear resistance compared to the chromium coatings having NDDS within the entire range of varying their concentration. The high wear resistance of the WC/Co coating is due to its high density and the homogeneous fine-grain structure, consisting of fine grains of WC, bonded between each other by the internal contacting network of cobalt (Co). The properties and the thickness of this network play an extraordinarily important role in the contact interaction of the coating during friction – small tangential resistance and respectively small wearing degree. The results of the carried out comparative investigation give us the reason to draw the main conclusion, that the composite coating WC/Co (88/12), deposited by the HVOF technology, can replace the non-ecological chromium and chromium-nano-diamond coatings in the tribological systems.

The book is intended for research workers, engineers, technologists, and specialists, working in the field of preparation of new types of tribology materials and coatings, and also for enriching the knowledge of students, diploma students, and Ph.D. degree students in the field of technical sciences.

Keywords: Wear; high-velocity oxygen flame; contacting materials.

_____

INTRODUCTION

The tribology is a fundamental inter-disciplinary science and technology for the contacts and the contact interactions in technical systems. The term „contact interactions" (tribological interactions) combines in one all the phenomena and processes inside the zone of touching between bodies, whatever their nature is – physical, mechanical, chemical, electrical, thermodynamic, acoustic, technological [1-6]. The place of location of these interactions is a region of some specific structures, characteristic features and states, named „contact area". The contacts as the subject of the tribology have no analogue in science. They cannot exist as independent physical objects without the involvement of some contact bodies, but they have decisive importance for the functional characteristics of the contact systems. For this re, ason the contacts are considered in the tribology to be independent functional objects of the systems [7-9].

The asic tribological phenomena and processes are friction, wear and lubrication, which determine the operational characteristics and the resource of the details, the mechanisms and the machines. The friction is connected to a great extent with some energy losses, consuming 30-40% of the energy, produced in the world. The wear is an accompanying process of friction and it leads to losses of material and human resources. It is the reason for disrupting the exploitation of more than 80% of the details and the machines taken as a whole. In addition to this the friction as driving process is of essential importance for the functioning of a number of systems such as mechanical brakes, and friction devices, as well as in many technological processes – ignition, soldering by friction and others. The utilization of the achievements of contemporary tribology enables many times to decrease the losses resulting from friction and wear in the machines, which would leadan to an economical effect amounting to a value of 2 up to 4% of the national income of the developed countries in the world. The object of tribology is the elaboration and regulation of surface layers, coatings, construction and lubrication materials having appropriate physico-mechanical and mechano-chemical characteristics, which ensure adaptation and optimal regime of occurring of the tribological interactions under different exploitation regimes.

The exploitation time period of a machine is the calender duration of its explotation until disruption or loss of its functional indices. The expenses for the repair of the machines, the equipment and the transportation means amount to billions of dollars per year in the developed countries. In the course of development of the industry this amount grows up. The losses for the repair work and the technical servicing of the machines exceed several times their value. The investigations show, for example, that in the case of automobiles these losses are about 6 times, for the airplanes – up to 5 times, for the metal processing and for the wood processing machines – up to 8 times higher. The various machines are to be repaired different number of times during their exploitation period, for example the road construction machines are to be repaired up to 15 times [1,2,3]. The greatest wear is that of details and operational parts of machines and equipment, which are exploited in abrasive and aggressive media, as well as

details of transportation machines, working in polluted powder medium. Such fields of exploitation appear to be – machines in the agriculture, in the mining industry, energy production, chemical industry, cement production and some others.

The problem to increase the life time cycle of the machines is connected with the enhancement of the wear resistance of the contacting joints. This is a difficult and complicated problem. Inmost of the cases it requires to combine high antifriction ability and high wear resistance.The high antifriction ability means small coefficient of friction, which is achieved by plasticity of the surface layers, a high wear resistance, which implies great resistance of the surface layer against splitting, impact action and vibrations, wjich is achieved by greater hardness of the surfaces. Usually the plastic (soft) layers possess smaller hardness, while the layers with great hardness have loer plasticity and high fragility. The compromise is achieved based on precision analysis of the mutual influence between three basic groups of factors: *working medium* – with or without lubricating material, the presence of abrasive, aggressive components etc.; *dynamic conditions* – veocities, loadings, type of movement, presence of vibrations; *contacting materials* - composition, structure, physical-mechanical properties, compatibility.

It is important to notice the circumstance, that during the exploitation of the machines the tribological processes are influencing each other and they change the time-space characteristics of the contact, while this in its turn determines the behaviour and the functional characteristics of the contacting joints, and respectively the machine as one whole.

The many years practice for creating protective layers and coatings of the metals prove that the highest quality wear resistance coatings are obtained in case of using concentrated energy flows. The current literature reports a large number of developments, in which various aspects are considered to form protective coatings by using some gas-thermal methods and concentrated flow of energy.

_____

High-Velocity Gas Flow Thermal Coatings (HVOF)

1.1 ESSENCE OF THE GAS FLOW –THERMAL TECHNOLOGIES

The composite powder coatings, deposited by HVOF (High-Velocity Oxy-Fuel) are a new generation of tribo-materials, using which one can achieve a wide range of combining the mechanical and tribological characteristics – high adhesion strength, density, hardness, wear resistance, corrosion stability. The powder particles, obtaining high kinetic and thermal energy in the flame jet, pass over into semi-plastic and/or plastic state and in the form of droplets or particles interacting with the substrate, whereupon they are deformed forming thin lamellar platelets. Upon their impact with roughness sections of the substrates, the particles-droplets are cooled down, forming adhesion bondings with the surface and cohesion bonds between one another thereby forming the laminar structure of the composite coatings. Due to the high velocity and the small contact time of the particles with the oxygen under definite conditions they do not form oxides, which is a prerequisite for good tribological properties of the coatings [18-23]. The HVOF coatings have been the object of intensive studies and they are continuously being improved. The results of the investigations of the present authors and some other researchers show that the mechanical and the tribological characteristics of the HVOF-coatings, besides the parameters of the technological regime of deposition, depend to a great extent on the chemical composition and the concentration of the elements in the powder composite, the size of the particles, the temperature of the substrate [17,24-31].

Fig. 1.1 represents the principal scheme of the structure of the coating, deposited by the HVOF process. The formed coating is not homogeneous and it usually contains a definite amount of pores, metal oxides, inter-metallic compounds, and some others [14].

The initial material for depositing the coating can be any substance, which undergoes melting, including metals, metallic compounds, types of cement, oxides, glasses, and polymers. The contact bonding between the substrate and the coating could be mechanical, chemical, or metallurgical, or most often a combination of these three. The properties of thermally deposited coating depend on the initial material, the type of the applied process for thermal deposition, and its parameters, as well as the consecutive treatment of the prepared coating.
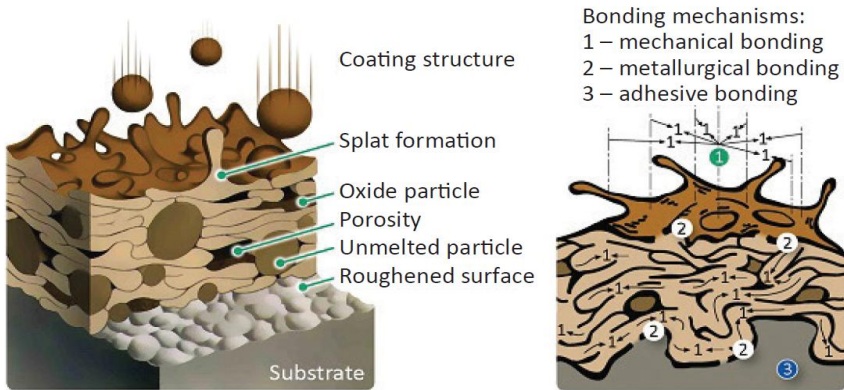
Fig. 1.1. Schematic structure of a thermal sprayed coating and bonding mechanisms [28]

1.2 POWDER MATERIALS AND COMPOSITES FOR HVOF COATINGS

In the current literature, the most widely used high-quality powder metal composites are also known as „super-alloys". They are divided into two big groups [4,9]:

- Powder composites based on nickel, nickel-chromium-boron silicon;

- Powder composites based on cobalt, tungsten-chromium-cobalt-alloys;

There exist powder composites based on technically pure iron.

The passage below indicates some of the most often used in the industry powder composites for the deposition of supersound high-velocity gas-thermal coatings:

Ni-Al95/5 - Nickel-Aluminium – they are used for making an *underlayer*, which has high adhesion strength with the upper deposition layer – 65-75 KP/cm^2. This is the result of partial welding ability, which occurs in the course of the exothermal reaction. Having its role as an intermediate layer it possesses high plasticity, which implies high wear resistance.

15E – Chromium-Nickel –is used under the conditions of impact, thermal loading, and in corrosive aggressive media. The obtained coatings have low ruggedness, which fact decreases the expenses for additional mechanical treatment and ensures a low coefficient of dry friction. It operates at high-temperature loadings. *Chemical composition:* Ni-70,5%; Cr-17%; B-3,5%; Si-4%; Fe-4%; C-1%.

18C- Cobalt-Nickel-Chromium –is used in chemically aggressive and abrasive media at high thermal loadings. *Chemical composition:* Ni-26,8%; Cr-18%; B-3%; Si-3,5%; Fe-2,5%; C-0,2%; Co-40%; Mo-6%.

34F- Tungsten carbide-Cobalt (plated), 50/12% - it consists of a chromium-nickel matrix with a fine grain structure, hardness of 60 HRC, and hardness of the carbide particles 72 HRC. The coating has low ruggedness.

36C- Tungsten carbide - Nickel (plated), 35/8%- matrix of particles of self flux chromium-nickel alloy of hardness 60 HRC and large particles of tungsten carbide of hardness 75 HRC.

WC-Co - Tungsten carbide -Cobalt, 88/12%- at an average size of the powder particles 1-2 μm high density is achieved, as well as adhesion strength, bearing ability under loading, and wear resistance. It is used as a counter-body of metal-ceramic coatings in sliding bearings upon achieving a hardness of 71 HRC.

WC-Co - Tungsten carbide -Cobalt, 83/17%- wear-resistant plastic coating, which is used in operational conditions – abrasion, cavitation, dry friction, and high mechanical loadings. It possesses high stability concerning scratching unlike the coating WC-Co 88/12. It enables the deposition of coatings having a great thickness. The maximal temperature of operation is 500°C.

WC-Co-Cr - Tungsten carbide-Cobalt -Chromium, 86/10/4%- Co-Cr matrix gives higher wear resistance in cases of abrasion and corrosion in comparison to WC-Co coatings. These coatings are used in the paper production industry for protection against corrosion in the presence of sulfur and abrasive wear. The stability against oxidation is up to 650°C.

Cr_2C_2Ni-Cr – Chromium carbide - Nickel carbide, 75/25%- High wear resistance in case of abrasion up to 900°C. This is the best coating against abrasive erosion and hot gas erosion. It has high stability concerning sulfur and sulfur oxides, low roughness, and low coefficient of dry friction. There are options for application in nuclear reactors. It replaces the WC-Ni 88/12 coating.

Ni-Cr-Mo– Hastel B- High adhesion strength. High stability concerning corrosion and oxidation stability up to 870°C. An application under operating conditions in the presence of seawater, acids, bases, and salt solutions.

WC-CrC-Ni – Tungsten carbide - Chromium carbide -Nickel, 73/20/7% (LW5) – Good wear resistance in an environment of bases and organic acids at high temperatures. Very good friction properties. It does not contain cobalt. It is used in the nuclear power industry.

Ni-Cr-Mo – Hastel C – Very high wear resistance in cases of dry friction and corrosion stability in aggressive media. Mechanical treatment only by polishing.

As far as some basic interactions are concerned, which occur between the separate components of the powder composite in the process of formation of the coating, the following statements can be said in brief:

* **The chromium** *(Cr)* at high temperatures interacts with the carbon *(C)*, silicon *(Si),* and boron *(Br)* forming metalloids. It forms a solid hard-to-melt structure with carbon *(Cr$_3$C$_2$)* of green colour, which is not soluble in acids. Chromium has an atomic weight of 52,01 and valencies +VI, +III, +II and it has isotopes 52, 53, 50, 54. The presence of admixtures makes it fragile. Chromium forms with oxygen some oxides *(CrO$_3$;Cr$_2$O$_3$)*. At temperatures above 196°C, the oxide *CrO$_3$* liberates *O$_2$* and forms a hard-to-melt, solid-state structure.

* **Boron** *(B)* at high temperatures combines with some metals *(Fe, Ni)* and also with carbon *(C)*, forming respectively borides and carbides *(B4C),* distinguished with great hardness;

* **Nickel** *(Ni)* of atomic weight 58,69 and valencies +II, +III has isotopes 58, 60, 62, 61, 64. It is included in the composition of super-hard powder composites, manifesting ferromagnetic properties. It is weakly attacked by acids, the strong bases do not affect it. In the oxidative medium and at high temperatures it is bonded to oxygen and it forms solid state oxides (NiO) having a green color.

* **The cobalt** *(Co)* and **the iron** *(Fe)*, similar to nickel, display ferro-magnetic properties, and they are used for the preparation of super-hard alloys, having magnetic properties.

* **The molybdenum** *(Mo)* forms an alloy with the iron *(Fe)*, while at high temperatures it interacts with oxygen *(O$_2$)* forming an oxide *(MoO3);*

* **The tungsten** *(W)* at high temperatures undergoes interaction with the carbon *(C)* and it forms tungsten carbide *(WC)* – a compound having great hardness. The cobalt *(Co)* plays the role of a binding element with the tungsten matrix.

The ceramic powder composites, used for depositing high-velocity gas thermal coatings, have some specific properties like high melting temperature, great hardness, inertness towards chemical interaction, very good adhesion with the substrate, low coefficients of thermal expansion, and others.

Table 1.1. Technical data of some ceramic powder composites

№	Parameters	Oxide of aluminum	Oxide of zirconium	Silicate of zirconium	Oxide of chromium	Nickel chromium
1.	Chemical composition	98,6% Al_2O_3	98% ZrO_2	65%ZrO_2 34% SiO_2	90%Cr_2O_3	80%Ni 20%Cr
2.	Stability to acids and bases	good, without hot bases	good, without hot acids	good	good, without hot acids	
3.	Crystalline form		cubic	Cubic ZrO_2	hexagonal	
4.	Density g/cm^3	3,3	5,2	3,8	4,6	8
5.	Porosity	8-12 (7% open)	8-12 (7%open)	8-12 (4%open)	4 (2% open)	0
5.	Hardness by Moos	9,5	9,5	9,5	9,5	3
6.	Limit of strength, kg/cm^2	2600	1470	-	7380	4920-7300
7.	Adhesion to steel, N/mm^2	40-70	40-70	40-70	70	-
8.	Wear resistance	very good	good	good	Very good	-
9.	Coef. of dry friction over steel 4124	0,1	0,1	0,1	-	
10.	Relative elongation, % at layer thickness 0,5mm	0,7	1,4	0,7	1,3	0,2
11.	Roughness, μm of non-treated Polished, rubbed	20-30 around 3-5 around 2,5	20-30 around 3-5 around 2,5	20-30 around 3-5 around 2,5	20-30 around 1,5-2,5 around 1-2	
12.	Melting temperature ^{o}C	1980	2480	1650	1650	1450
13.	Resistance to thermal shock	good	Very good	good	mediocre	-
14.	The average value of the thermal conductivity at 540-1090°C, kcal/h.m.^{o}C	2,36	0,99	1,86	2,23	12,6
15.	The average value of the thermal capacity, kcal/kg	0,28 (30-1700)^{o}C	0,18 (30-1700)^{o}C	0,15	0,2 (16-17480)^{o}C	0,12 (1-100)^{o}C
16.	Coef. of linear thermal elongation, mm/mm.^{o}C	7,38x10^{-6} (20-1230)^{o}C	9,72x10^{-6} (20-1230)^{o}C	7,56x10^{-6} (20-600)^{o}C	9,00x10^{-6} (20-1100)^{o}C	18,9x10^{-6} (1-980)^{o}C
17.	Coefficient of emission at layer thickness 0,762 mm	at 1000°C 0,4	at 1000°C 0,34	at 60°C 0,78	at 1000°C 0,75	-
18.	Electro-conductivity	insulator	insulator >1200°C conductor	insulator	insulator	conductor
19.	Electro-resistance, Om	4,5x10^6 -260°C	2,7x10^4 -260°C	1,1 x10^6-260°C	-	28,3x10^6-20°C

№	Parameters	Oxide of aluminum	Oxide of zirconium	Silicate of zirconium	Oxide of chromium	Nickel chromium
		$4,5 \times 10^5$ -450°C	$2,1 \times 10^2$ -260°C	4×10^2 -260°C		$45,6 \times 10^6$ -650°C
20.	Breakthrough voltage at V/0,25mm -200/s and layer thickness 0,25-1,25 mm	90-180V	-	-	0,01-85V	
21.	Dielectric constant (0-320°C)	10	35	15	-	-
22.	Coef. of dielectric losses	0,5	5,25	1,2	-	-
23.	Coef. of leakage (0-320°C)	0,05	0,15	0,08	-	-
24.	Colour	white	light beige	light beige	black	
25.	Recommended thickness of the coating	0,12-1,3 mm	0,12-1,3 mm	0,12-1,3 mm	0,12-1,3 mm	0,05-0,1mm

13

The oxides of aluminium and zirconium are the most often used oxides. The coatings of oxide ceramics are deposited to have thicknesses of 0,1 – 1 mm or even higher and in a non-treated state, they have a roughness of 15 - 30 μm. Higher roughness is achieved using honing treatment and polishing with the diamond instrument. The maximal roughness after the treatment reaches up to 2 – 4 μm.

Almost all the materials are used in their quality as substrate, which does not allow melting upon heating with the jet stream, they are not oxidized and they do not bind carbon.

Table 1.1 represents technical data about the most often used ceramic powder composites.

1.3 PHYSICOMECHANICAL CHARACTERISTICS OF THE HVOF COATINGS

The main physicomechanical characteristics of gas thermal coatings, which bear direct relation to the tribological behavior of the contact systems, are the following:

Hardness, density, and porosity:

The hardness and the density of the thermally deposited coatings are usually higher than that of the substrate, upon which the coating has been deposited. The hardness bears relation to the abrasive and to the erosive wear resistance, which makes them especially valuable for applications under contact conditions with active abrasion and erosion. In the cases of thermally deposited metal coating, the hardness and the density of the coating depend on the nature of the material of the coating, the applied technological equipment for thermal deposition, the parameters of the technological regime, and especially on the structure and the properties of the contact zone, which is formed between the substrate and the coating.

The velocity of the particles in the different processes for thermal deposition in inverse order is the following: detonation, high-velocity gas flame process (HVOF), arc plasma, wire arc, and gas flame deposition.

The hardness and the density depend on the temperature of the particle and the type of the used atomization gas. The porosity of the coating depends mainly on the regime of thermal deposition, its parameters, and the nature of the thermally deposited material.

Corrosion stability:

The metallic thermally deposited coatings can be either anodic or cathodic concerning the substrate beneath them. Since the corrosion occurs in the anode, the anodic coatings will corrode in corrosive media, but not the cathode. The anti-corrosion coatings undergo corrosion or „they sacrifice themselves", to protect

the substrate. In many cases, the corrosion stability of the thermally deposited material is of exceptional importance – at very high temperatures and in case of interaction with aggressive media.

Adhesion:

The thermally deposited coatings in most of the cases have very high adhesion strength. The used special coatings having very high wear resistance, deposited by a process of thermal deposition with a high velocity of the particles (HVOF-process), could possess adhesion of more than 34,000 kPa (5000 psi), measured by the method *ASTM C633* "Standard method for testing the adhesion or cohesion strength of coatings deposited by flame." Most of the coatings, applied in infrastructural applications, possess values of adhesion, comparable with those of paints. The typical coatings of zinc, aluminium and zinc-aluminum alloy, deposited under open field conditions or factory available conditions have adhesion from 5440 up to 13,600 kPa (800 up to 2000 psi), measured by ASTM D4541 "Standard method for testing of the force needed for detaching the coatings using portable adhesion testing devices." [5-12].

1.4 ADVANTAGES, DISADVANTAGES, AND APPLICATIONS OF THE HVOF COATINGS

Advantages:

The first and the greatest advantage of HVOF and the plasma thermally deposited coatings consists in the ability of the contemporary technologies to modify completely the quality, the characteristics, and the performance of the surfaces of industrial machines, equipment, and their components by the addition upon them of a comparatively thin layer using the most contemporary achievements of the materials science and the tribology.

The remaining advantages consist in:

- *Diminished expenses*. The expenses for repair work of a given detail are less than those, for buying a new one. The coating has greater resources than that of the originally applied material;

- *Lower heat transfer*. With some small exceptions, the process of thermal deposition does not influence the thermal properties of the detail;

- *A rich variety* of materials for thermally deposited coatings. Almost every metal, ceramic, or polymer can be thermally deposited.

- *High wear resistance*

- *Corrosion stability*.

- *Thermal stability*. Heat protection coatings can be produced. They can be both of high thermal transmission capacity, as well as non-transmissive.
- *They are suitable for restoring the dimensions*.

- *They can copy complex surfaces*.

- *The physical characteristics* of the surface coatings are uniform equal to or better than those of the solid chromium coating concerning corrosion protection, and stability concerning abrasive or adhesion wear.

- *Ecological effect*, which is expressed in a considerable decrease in the wastes, which are dangerous for the health and the expenses, connected with them for deposition, as well as reducing the harmful and carcinogenic emissions, characteristic for the case when using electrolyte bath during the process of chromium addition.

Disadvantages:

- *Linear process* – it enables the deposition only of external surfaces, but not on the internal diameter.

- *High* capital expenses.

- *The process* must be located in closed premises, in completely closed-door halls of suitable dimensions, so that it becomes possible to process those parts, which are usually treated with solid chromium coating.

Porosity: The pores present in most of the thermally deposited coatings (except for the case of vacuum plasma deposition (VPS), the coatings having consecutive thermal treatment and alloyed coatings). Porosity from 1 up to 25% is considered to be the normal one, but it can be additionally controlled by changes in the parameters of the process or changes in materials.

The porosity can be disastrous for the coatings regarding:

- Their corrosion stability;
- Their surface treatment;
- Strength, microhardness, and wear resistance.

The porosity is of great importance for:

- The lubrication – the pores act as storage places for the lubricating material;
- Improvement of the thermal insulation properties;
- Decrease the tensions and increase the admissible thickness of the coatings;
- Improving the stability concerning an impact;
- The applications, connected with a prosthesis, surface boiling, etc.

Oxidation: Most metal coatings suffer from oxidation in the course of the normal thermal deposition in an air medium. The products from the oxidation are usually included in the coating. The oxides in principle are considerably harder than the metal itself. The coatings having a high content of oxides are usually harder and more wear resistant. The oxides in the coatings can influence negatively the corrosion stability, their strength, and their machining properties.

Surface texture: In principle, the surface of the detail after deposition of the coating is rough and it has a specific texture. The rough coatings of high strength of bonding are ideal for intermediate (interconnected) layers in cases of coatings of a lower strength of bonding. Many coatings after their deposition form surfaces with high friction and this property are used in many applications (for example in the case of roll drums for testing the brakes in automotive control centers). Some plasma-deposited ceramic coatings form a smooth surface of texture and they find important applications in the textile industry. Other applications make use of the abrasive properties of some of the coatings. The thermally deposited coatings do not lead to the formation of glittering and smooth surfaces without any additional treatment, as is the case with the galvanic coatings.

Some applications:

The coatings, deposited by the supersonic gas thermal jet stream, find wide wide applications in many fields. Many of these applications are connected with corrosion protection, for example, coatings of zinc, aluminium, and their alloys are anodic concerning steel and iron and they protect them against corrosion in several working environments, including atmospheric influence, upon immersion into the fresh or salty water, as well as under high-temperature conditions. The coatings of aluminium are most often used in the sea operating environment. They serve for corrosion protection of many sea ship details. Since these materials are anodic concerning steel, their porosity does not influence their ability to protect the substrate of ferrous metals. The coatings of zinc and zinc-aluminium alloy can undergo corrosion rapidly in the strongly contaminated industrial atmosphere or in chemical media, where pH is either too high or too low. For this reason, it is usually painted or some sealing that is deposited on these materials, which are meant to improve their characteristics.

- The cathodic coatings, such as copper-nickel alloys, can also be used for the protection of low carbon content steels against corrosion. These materials should have a protective coating, to prevent the penetration of water inside the coating. The coatings are especially hard and they are often used in applications, requiring both corrosion stability, as well as wear resistance.

- The aluminium coatings are often used for corrosion protection at temperatures up to 660°C (1220°F).

- The coatings, containing zinc and/or copper, are used for preventing the harmful effect of fresh or salty water. The zinc in zinc-aluminum alloy at a ratio of

85-15 does not allow any sticking and damage, caused by zebra shells on the steel substrates. Since these coatings are durable and they prevent corrosion, their use is recommended for all kinds of equipment. The coatings, containing copper and brass, have a well-proven effect on the sticking organisms, but they are not recommended for use upon steel, due to the galvanic reaction between the two metals.

- The zinc coatings are sometimes used for preventing the corrosion of steel reinforcements of concrete. In cases of similar applications, the zinc is deposited on the concrete and it is bonded electrically to the steel.

- The HVOF coatings are especially suitable for the renovation of worn-out surfaces. Frequent application is restoring the dimensions of worn-out rotating surfaces (shafts), whereupon simultaneously with it their resource (lifetime) is increased several times. Similarly, they can be used for restoring the outlines of casting molds, as well as for the repair of worn openings.

- These coatings are used also in electric systems and devices. Electroconducting metals, such as copper, for example, can be used as conductors. The ceramic materials can be used for electric insulation. The conducting materials are used for the electromagnetic screening of sensitive electronics.

- The high hardness and thickness coatings are used as materials stable to cavitation, combined with technologies for welding layers deposition in their quality of technics for repair works.

1.5 CONCLUSION

The composite coatings of powder-form superalloys, deposited by high-velocity jet (HVOF-coatings) are mainly used for exploitation of details under extreme conditions of abrasion and erosion.

Most of the studies on such coatings consider the influence of the parameters of the technological regime (velocity of the flame jet, ratio „fuel gas-oxygen", angle of interaction, and distance between the jet and the surface of the samples) and the chemical composition of the composite powder mixture upon the thickness, the hardness and the porosity of the coatings.

The studies on the tribological properties of the HVOF-coatings and more specifically the characteristics of the wearing process in different regimes of friction have limited character. The results from the tribological investigations of the separate authors are obtained by different methodologies and using devices having various kinematic schemes of friction in different exploitation media – water, lubricating materials, and active corrosion media. These differences in experimental arrangements make difficult the comparative analysis and the generalization of the obtained results.

The reason for this fact is that there is a lack of a united approach in the tribology and methodology for the complex investigation of contact interactions. For the quantitative evaluation and interpretation, some parameters and criteria are used, which reflect one aspect or another of the contact interaction – physical, chemical, substantial, energetic, and technological.

_____

Methods and Devices for Studying HVOF Coatings

2.1 PREPARATION OF SAMPLES FOR INVESTIGATION: TECHNOLOGICAL REGIME

The choice of the powder composites for deposition of coatings by HVOF technology is done aiming at the maximal enhancement of the exploitation resource of contact surfaces and contacting joints by promoting their wear resistance under conditions of abrasive and erosive wear for application in various fields of the Bulgarian industry – ore mining and energy production.

The coatings are deposited on a carrier (substrate) of the same material – steel with the chemical composition shown in Table 2.1a. The hardness of the substrate is within the limits of $193.6 \div 219.5$ HV.

Table 2.1a. Chemical composition (weight %) of the substrate

Element	C	Si	Mn	Ni	P	S	Cr	Fe
Percentage	0.4	0.20	0.55	0.30	0.45	0.045	0.30	Balance

The preparation and the investigation of the coatings are occurring in several consecutive steps: preparation of the powder composites, preparation of the substrate, deposition of the coatings by HVOF-technology, measurement of the thickness and the hardness of the obtained coatings, preparation of samples for testing the wearing process, abrasive/erosive wear, calculation of the characteristics of the wear degree. The scheme of the consecutive steps of a study on abrasive wear is shown in Fig. 2.1 [33, 37].
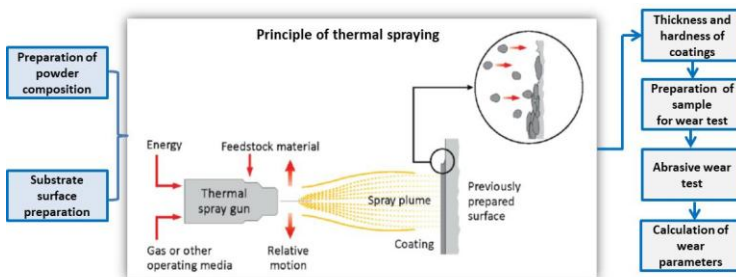

Fig. 2.1. Scheme of preparation and research of HVOF coatings

All the coatings are deposited on cylindric samples of a diameter of 15 mm and height of 25 mm of steel having a chemical composition, described in Table 2.1.a and hardness 193.6 ÷ 219.5 HV. Samples are cut out of the so-prepared samples having deposited coatings to be tested having a diameter of 5 mm – three samples for each type of coating.

The increase in the adhesion strength between the coating and the substrate is achieved by preliminary treatment of its surface. This treatment occurs in three steps: cleaning, erosion using abrasive particles (blasting), and mechanical treatment. The cleaning is done by solvent aiming at the removal of mechanical contaminants, adsorbed organic molecules, moisture, and other components. The extraction of the adsorbed gas molecules and some elements in the depth of the surface layer is achieved by burning the surface of the substrate using a flame up to 100°C at a nozzle distance of 40 mm and angle of 45° or with vapour jet apparatus. After this operation again the surface is cleaned using a solvent. Using erosion of the surface of the substrate (blasting) one can achieve a definite level of roughness of the substrate, which is of essential importance for the magnitude of the adhesion strength of the coating. Abrasive material "Grit"" is used, I accordance with the requirements of the standard ISO 11126, having grain size composition of the abrasive in ratio: 3.15 ÷ 1.4 mm – 9.32%; 1.63 ÷ 0.5 mm – 16.4%; 1.4 ÷ 1.0 mm – 15.8%; 1.0 ÷ 0.63 mm – 39.6%; 0.5 ÷ 0.315 mm – 9.32%; 0.315 ÷ 0.16 mm – 9.32%; particles of sizes below 0.15 mm of the different fractions – up to 100% of the following chemical compounds: SiO_2 – 41% , combined in the form of silicates; AlO – 8.3%, MgO – 6.6%, CaO – 5.5% and MnO – 0.4%.

The system for blasting has the following technical parameters: input pressure 8 atm; working pressure in the nozzle – 4 atm; diameter of the nozzle 7 mm; distance between the nozzle and the surface – 30 mm; angle of the interaction of the jet with the surface – 90° [20].

The coatings are deposited using the device MICROJET+Hybrid, which uses a fuel mixture of propylene ad oxygen (C_3H_8/O_2). The parameters of the technological regime for deposition of the coatings are represented in Table 2.1b.

Table 2.1b. Technological regime parameters for HVOF coating deposition

Parameter	Technological regime
Propylene/oxygen (C_3H_8/O_2) ratio, %	55/100
Particle velocity, m/s	1000
Spraying distance, mm	100
Impact angle, ^{o}	90
Air pressure from compressor, bar	5
N_2 pressure in the proportioning device, bar	4
Powder feed rate, g/min	22

In case of deposition of coatings without thermal treatment (cold HVOF process) the surface of the substrate is heated by flame up to temperature 200°C, which is

measured by Laser infrared thermometer INFRARED of accuracy 0.5^oC. The coating is deposited in several layers. For the first layer, the nozzle is situated at an angle of 45° and a distance from the substrate of 10 mm, while for the next layer – the distance is 25 mm. The thickness is measured by a portable device Pocket Leptoskop 2021Fe of accuracy 1 µm. For each coating, measurements were made in 10 spots on the surface and the arithmetic mean value is taken. The precision of the device is 1 µm. The surface of all the samples is polished to the same roughness Ra=0,450÷0,455 µm, which is measured by recording the profilogramme using the profile metering device „TESA Rugosurf 10-10G" of accuracy 0.005 µm. The hardness of each one of the tested coatings. It is measured by the hardness metering device "Bambino" based on the scale of Rockwell (HRC) as the mean arithmetic value of three measurements for each sample to eliminate possible effects of segregation.

2.2 DEVICE AND METHODOLOGY FOR STUDYING THE ABRASIVE WEAR

2.2.1 Main Concepts about the Abrasive Wear

The wearing is a contact process, directly connected with the interaction between the bodies, which leads to gradual changes in the shape, the state, and the working capacity of their surfaces and their surface layers.

The abrasive wear represents mechanical destruction of the surface layers of the details as a result of the cutting and/or scratching action of the abrasive particles, which are in a free state or bonded state [1-6]. The abrasive materials represent minerals of natural or synthetic origin, whose grains have great hardness and they possess the ability to cause cutting of the material.

Abrasive wear can occur caused by particles, which are:

- Firmly fixed solid grains in the surface layer, which form contact along the line of sliding or making some definite angle with it;
- Peaks of rugged spots on the surface layer;
- Free state abrasive particles, entering into contact with the surface, for example during transportation of mound-filling materials, abrasive particles from the soil in case of soil processing transport machines, in the ore-mining industry, and others;
- particles, fallen in loose sections of the contact compounds as wear products, through the oil or from the air. In 1 m^3 of air 5 grams of powder 5 are contained, of which 60-80% represent mineral particles of quartz, corundum, oxides, dioxides, and other compounds of Si, Al, Ca, Mg, Na, and other elements. These particles have very high hardness, for example, SiO_2 has a hardness of 10780-11700 MPa; Al_2O_3 – 20900 ÷ 22900 MPa, which considerably exceeds the hardness of the operating surfaces of machine details.

Abrasive wear is one of the most often occurring types of wear. In transportation, road vehicles, agricultural and mining machines, and mechanisms more than 60% of the cases of wear are due to abrasive wear. It is occurring in almost all branches of the industry – aviation technics, working wheels and directing devices of hydraulic turbines, blades of gas turbines, bearings of shafts in rowing wheels, snack bar swing shafts, and others [17,18,31].

The basic factors, influencing the intensity of the abrasive wear are the nature, shape, and sizes of the particles, angle of interaction between the particles and the surface, the nature and the properties of the surface layers, temperature and nature of the working environment, the force of the impact of particles, the velocity of sliding, etc.

The general aspect of the mechanisms of abrasive wear is its mechanical character. The friction in the presence of abrasive particles is characterized by discreteness and non-steady state of the contacts, wide spectrum and high concentration of the contact tensions, and physical-mechanical activation of the surface layers. The abrasive particles have a different and irregular form, and they can be orientated in different ways concerning the surface. The ability of the abrasive particle to penetrate the surface layer depends not only on the ratio between their hardnesses but also on the geometric shape of the particles – oval, having sharp cutting edges, and others. In most cases, the particles from the wear of the oxide layer have a greater hardness than the materials themselves. The highest hardness is manifested by the oxides of aluminium Al_2O_3. The shapes and the sizes of the products of abrasive wear depend on the mechanism of interaction between the particle and the surface – micro splitting, breaking off, plastic pushing away [10-11].

The abrasive particles can cause elastic deformation in the surface layers, preserving their shape and dimensions, but they can also undergo destruction. Depending on the structure of the particle and the environment, in which they interact with the surface, they can penetrate the surface layer, they can slide, roll and turn around, and exit the contact. The penetration into the surface of the material can cause scratching or splitting of microscopic particles having spiral or wedge shapes.

2.2.2 Methodology for Investigation of the Abrasive Wear

The methodology for studying the characteristics of abrasive wear is based on measuring the mass wear of the samples for some definite pathway of friction under permanently set conditions – loading, sliding rate, kind of abrasive, sizes of the samples, and thereafter one calculates the characteristics of the wearing process – wear rate, the intensity of wear, absolute and relative wear resistance [14-17].

The methodology consists of the following operations:

- Preparation of samples having identical dimensions and the same ruggedness of the contact surface. The ruggedness and the profile diagramme of the surface are determined by the profile-metering device „TESA Rugosurf 10-10G". The recording of the profile diagrammes is carried out in two mutually perpendicular directions on the surface of the coatings.
- The measurement of the initial mass m_O [mg] of the sample using electronic scales WPS 180/C/2 has an accuracy of 0,1 mg. Before each measurement on the scales, the sample is cleaned from mechanical and organic particles, and then it is dried using ethyl alcohol for preventing electrostatic effect;
- The sample is placed in the holder of the loading head of the tribotester, then a definite normal loading P is set and a definite friction path L is realized.
- Again the mass of the sample is measured after traveling the definite pathway of friction L.

Then the following characteristics of mass wear are calculated:

- *Mass wear* m, [mg] – it represents the destroyed mass of the surface layer of the sample for the definite friction pathway S, i.e.

$$m = m_O - m_i \qquad (2.1)$$

- *Rate of the mass wear* γ [mg/min] – it represents the destroyed mass during the friction per unit of time of friction *t*:

$$\gamma = \frac{m}{t} \qquad (2.2)$$

- *Specific wear intensity* i_a, [mg/N.m.mm^2] – destroyed mass during the friction from the surface layer under normal loading P=1N, per unit of the pathway of friction L=1m and unit of nominal contact area A_a=1 mm^2.

$$i_a = \frac{m}{P.L.A_a} , \qquad (2.3)$$

- *Specific wear resistance* I_a, [N.m.mm^2/mg] – it is represented as the reciprocal value of the specific intensity i_a, i.e.:

$$I_a = \frac{1}{i_a} = \frac{P.L.A_a}{m} \qquad (2.4)$$
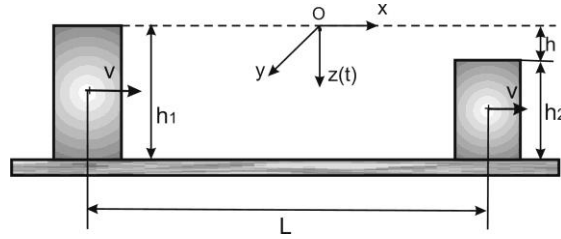
Fig. 2.2. Linear wear of the sample after definite friction path length

The connection between the linear wear h and the measured mass wear m is represented by the bulk volume wear V (Fig. 2.2) with a density ρ of the surface layer and the nominal contact area A_a, i.e.:

$$m = \rho.V \tag{2.5}$$

Since the wear bulk volume is:

$$V = A_a.h$$
(2.6)

Then one obtains using the (2.5) and (2.6) equations:

$$m = \rho.A_a h \tag{2.7}$$

Then for the linear wear h, measured based on the mass wear m, it follows that:

$$h = \frac{m}{\rho.A_a} \tag{2.8}$$

For the intensity of linear wear, it is obtained that:

$$i_h = \frac{h}{L} = \frac{m}{\rho A_a L} \tag{2.9}$$

The intensity of linear wear shows how many microns is the wear along the normal axis concerning the friction path length z per unit of friction path length L.

Then for the linear wear resistance, the following equation is used:

$$I_h = \frac{L}{h} = \frac{\rho A_a L}{m} \qquad (2.10)$$

The linear wear resistance shows how many meters of friction path length will be traveled along the coating to destroy one micron of its surface layer.

-   *Relative wear resistance* $R_{i,j}$ - it represents the ratio between the wear resistance of the tested sample $(I_{a,i})$ and the wear resistance of a sample, accepted as a reference standard $(I_{a,j})$, determined under identical conditions of friction, i.e.

$$R_{i,j} = \frac{I_{a,i}}{Ia,j} \qquad (2.11)$$

The relative wear resistance is a dimensionless quantity, which shows how many times the wear resistance of the tested sample is greater or smaller than the wear resistance of the coating/material, accepted as a reference standard under identical conditions of friction.

2.2.3 Device for Studying the Abrasive Wear

The abrasive wear of HVOF coatings is studied under conditions of dry friction along the surface with firmly attached abrasive particles using a laboratory device based on the kinematic scheme „Pin-disc". The functional scheme of the device is represented in Fig. 2.3.

The studied sample with deposited coating 1 (pin) is attached fixed in the bed of the holder 2 in the loading head 8, in such a way that the front face surface of the sample is in contact with the abrasive surface 3, firmly attached to the horizontal disc 4. Disc 4 is driven by an electric motor 6 and it is rotating around its vertical central axis at some angular velocity.

The normal loading P is applied in the center of gravity of the contact area between the sample and the abrasive surface and it is ensured by some weights using a lever system in the loading head. The friction path length is set using the number of revolutions using the revolutions metering device 7. This device enables changing the velocity of sliding by altering the angular velocity of the disc, done by the regulating block, and/or by changing the distance between the axis of rotation of disc 4 and the axis of sample 1.

The abrasive surface 3 is modeled using impregnated corundum (E) of hardness 9.0 according to the Moos scale, which guarantees the requirement of the

standard for a minimum of 60% higher hardness of the abrasive material than that of the surface layer of the tested materials.
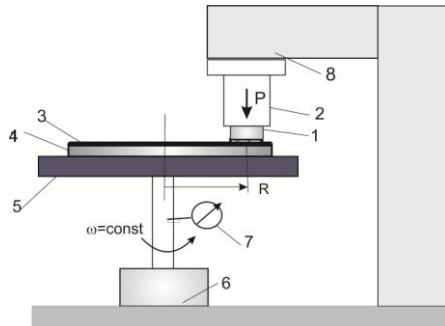
Fig. 2.3. Scheme of the device for studying the abrasive wear during friction alon surface with firmly attached abrasive particles based on «Pin-disc»

2.3 DEVICE AND METHODOLOGY FOR INVESTIGATION OF EROSIVE WEAR

2.3.1 Basic Concepts for Erosive Wear

The erosion is a process of destruction and removal of mass from the surface layer of the details as a result of their contact interaction with particles, carried by the fluid stream [3, 10, 17, 41]. The erosion is a complex process, which occurs as a result of complex actions of many factors, which can be unified into three main groups:

- Characteristics of the particles - nature, mass, velocity, angle of the interaction of the particle with the surface, hardness, geometric shape, dimensions;
- Characteristics of the surface - nature, structure, hardness, roughness;
- Characteristics of the carrying fluid – density, viscosity, presence of aggressive components, surface-active compounds, the concentration of the particles, etc.

The strongest influence upon the degree and the mechanism of the erosive wear is exerted by energy factors – mass and velocity of the particles, i.e. the impulse of the falling particle, the angle of interaction and the geometrical dimensions, and the shape of the particles [1,3,4].

The angle of interaction α is considered to be the angle, which is between the vector of the particle velocity and the tangent of the surface.

Upon assuming that the fluid medium is not aggressive regarding the surface, in the cases of different combinations of these factors, the following basic

mechanisms of erosion are possible: abrasive wear, contact fatigue, plastic deformation, and fragile destruction. The abrasive wear occurs at small angles of interaction, whereupon one does not observe any impact of the particle. At angles of interaction close to 90°, the mechanism of erosion is changed and it depends on the velocity of the article. At large angles and low velocity, the erosion is occurring slowly having a prolonged incubation period and the destruction occurs as a result of surface fatigue of the material as a consequence of periodical discrete impacts. In cases of large velocity and a large angle of interaction, the erosive wear occurs through the mechanisms of multiple plastic deformation or fragile destruction. In the case of normal contact interaction at large impact impulses and high temperature there can occur local melting of the surface, and formation of surface waves and vortices, which additionally intensify the wear process.

The surface waves in the boundary contact layer often occur in cases of tangential interaction of the particles. The turbulence and the frequency of vibrations of the contact waves depend on the geometrical shape of the surface, its roughness, and especially on the wear degree. The eroded surface becomes a generator of new surface waves and it additionally accelerates the process of erosion.

Several experimental studies show, that the dependence of the erosion intensity on the angle of the contact interaction is a nonlinear function with a clearly expressed maximum. The angle of maximal erosion is different for the various materials [3,47].

This circumstance gives the reason for some authors to accept it as a criterion for classification of the regimes of erosion such as the „plastic regime" at small angles of the contact of about 30° and the „brittle regime" of erosion wear at angles of 80° - 90°.

What is of fundamental importance for the mechanism of erosion are the geometrical shape, the dimensions, and the degree of abrasiveness of the particle. Their irregular geometric form – the presence of edges and deviations from the ideal spherical form is determined by a multitude of radii, starting with a minimal closing radius, and gradually widening in direction to a more detailed description. The geometry of the particles is characterized by two parameters – average size, which represents minimal outlining diameter, and roughness. The dimensions of the particles influence substantially the regime of the erosion. For example in cases of erosion of glass, steel, graphite, and ceramics using particles of SiC, falling at velocity 152 m/s, the regime of wear passes over from plastic regime to brittle regime depending on the average diameter value of the particles varying within the range from 8,75 μm up to 127 μm. The maximum of wear in the case of small particles is at an angle of the interaction of around 30°, while in the case of large particles it is around 80°. The size of the particles not only changes the mechanics of the wearing process but also substantially changes the classification of the materials from the viewpoint of wear resistance concerning erosion.

The difficulties to predict the erosion behaviour and the wear resistance of the materials originate from the complex nature of the contact interactions, whereupon there exists mutual influence of the described factors.

The influence of mechanical characteristics of the materials on the erosion wear process is not simple. The increase in the hardness is not always a criterion for erosion wear resistance. There exist such conditions of interaction during erosion, when the hardness of the materials exerts influence upon the wear degree and their classification regarding erosion wear resistance. Such is the case of erosion of materials at a small angle of interaction ($\alpha = 30^{o}$) when the erosive agent is particles of SiC with a diameter of around 1mm, moving at a velocity of 30 m/s. The highest wear resistance is manifested by cobalt, while copper occupies the last but one place. The nature and the characteristics of the operating carrier fluid – water, gas, lubricant, and others, show different influences on the mechanisms of erosion. In some cases, it carries the small abrasive particles away from the contact zone revealing new surfaces and intensifying the wear. In other cases the fluid plays the role of lubricant, decreasing the impulse of micro collisions. A third case should be noted as the splitting action of the fluid inside microcracks in the surface layers. Surface active compounds by the effect of Rebinder can influence two directions upon the erosion: on one side – to intensify the destruction processes, while on the other side – to decrease the intensity of the wear process by forming protective films on the surface through the passivation effect.

The erosion wear is observed in many cases of important and costly spare parts, mechanisms, and machines such as different kinds of pumps, industrial ventilators, sand-jet apparatuses, jet mills, compressors, internal combustion engines, airplanes, space devices, and others.

2.3.2 Theory of Erosive Wear due to the Air-abrasive Jet Stream

The elaboration of the theory of erosion wear, caused by the air-abrasive jet stream is based on the law for contact interaction in the tribology[47,52]. This law reflects the triple unity of interaction in tribological systems as a result of the multiplication effect of three potentials: active potential dA/A – relative external fluctuation on the tribe system; reactive potential dR/R – the relative reaction of the tribe system and communicative (contact) potential between the confusion/disturbance and the reaction, using which the interaction is realized between the active and the reactive potentials [9,10].

In the general case the law for contact interaction in symmetrical differential form is as follows:

$$\frac{dR}{R} = \eta \frac{dA}{A} \qquad\qquad (2.12)$$

In the case of erosive wear, it is assumed in the current literature that there is proportionality between the reaction and the deviation (disturbance), whereupon the communicative potential is assumed to be a constant quantity, equal to the unit, i.e.

In the considered case of erosion wear the relative deviation dA/A (the action) represents the impact of the abrasive phase in the jet stream, which is expressed by its mass flow - m_a , i.e.

$$\frac{dA}{A} = \frac{dm_a}{m_a}$$

(2.13)

It should be understood that the term mass flow of the abrasive jet m_a is the number of abrasive particles in the jet, falling on the surface of the sample per unit of time, in our case - one minute.

The dependence of the mass flow of the abrasive phase on the time interval of interaction, i.e. represents *the law for change in the mass of the abrasive particles*, attacking the surface layer of the tested material through the air stream.

The relative reaction dR/R of the surface of the sample is defined by the ratio between the mass wear for a small interval of time dm and the mass wear m for the entire period of the erosion, i.e. the relative reaction, in this case, is expressed by the relative wear of the surface layer:

$$\frac{dR}{R} = \frac{dm}{m}$$

(2.14)

The change in the mass wear over time represents *the law for the erosion of the material due to the action of particles*.

After taking into account the equations (2.13), (2.14) and $\eta = 1 = const$, the law for the contact interaction in the form of (2.12) now is reduced to:

$$\frac{dm}{m} = \frac{dm_a}{m_a}$$

(2.15)

After integrating the expression (2.15) and the anti-logarithmic transformation one finds the interconnection between the two laws – the law of wearing and the law for variation of the impact abrasive mass $m_a = m_a(t)$. After substituting in the equation (2.14) one obtains *the law for the velocity of jet-abrasive erosion* in the form:

$$\frac{dm}{dt} = k\frac{dm_a}{dt}$$

(2.16)

Based on the law (2.16) one determines *the intensity of the erosion wear*, i.e.:

$$i_e = \frac{\dot{m}}{\dot{m}_a} = k$$

(2.17)

The intensity of the erosion represents the ratio between the rate of mass wear of the surface layer and the mass flow of the abrasive phase in the jet. The intensity of the erosion is a dimensionless quantity.

The erosion wear resistance is determined as the reciprocal value of the intensity of the wearing process i_e. It represents dimensionless quantity, which shows how many grams of the abrasive mass is needed for the loss of 1 gram of mass m from the surface of the sample for a definite period of interaction, i.e.

$$I_e = \frac{1}{i_e} = \frac{\dot{m}_a}{\dot{m}}$$

(2.18)

The relative erosion wear resistance $R_{i,j}$ is determined by the formula:

$$R_{i,j} = \frac{I_i}{I_j}$$

(2.19)

Where is the erosion wear resistance of the tested sample, determined based on (2.18), while is the wear resistance of a sample, accepted as a standard for comparison, determined under the same conditions of the wearing process?

The relative erosion wears resistance is a dimensionless quantity, which shows what fraction is the wear resistance of the tested sample, compared to the wear resistance of the standard under identical conditions of jet-abrasive erosion.

The Laboratory for Tribology at the Faculty of Industrial Technologies in the Technical Unversity - Sofia has elaborated a device and a methodology, which are based on the above-described theory of jet-abrasive erosion and they are by the requirements of the modern standards [11,12].

2.3.3 Device for Studying the Erosion Wear

The erosion wear of the studied HVOF coatings is accomplished by an air stream, carrying abrasive particles in the atmospheric medium. The functional scheme of the device is represented in Fig. 2.4.
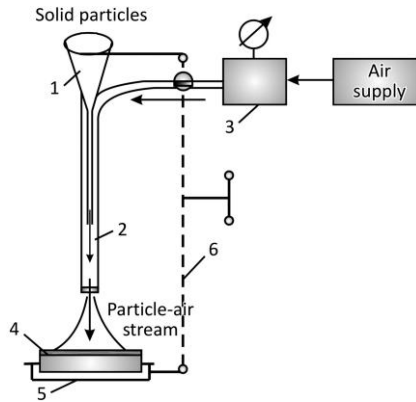
Fig. 2.4. Schematic diagram of erosive wear testing

The designation of the device is to form two-phase jet «air-abrasive particles» by independent setting and regulation of the parameters of the two independent stationary flows – air and abrasive, more specifically – air pressure and flow rate of abrasive particles.

The abrasive material having a definite flow rate flows gravitationally out of chamber 1 and enters mixing chamber 2, where it is mixed with the inlet air flow at some definite pressure. The two-phase mixture of «air-abrasive particles» flows out in the form of a two-phase jet stream and it interacts at a definite angle with the coating 4 of the sample, which is located in the holder 5. The holder 5 is attached to a stand, which enables regulating the following parameters: distance between the nozzle and the surface of the sample, angle of interaction between the axis of the jet and the surface (jet angle).

The flow of abrasive particles out of chamber 1 occurs at a constant rate through an additional chamber having a definite amount of abrasive, which is not represented in the scheme. The amount of abrasive material before placing it in chamber 1 is sieved through a set of sieves and then it is dried up in a dry box to remove the moisture from the particles. The air stream from a source of compressed air passes through the pneumo-preparation group, which contains an air filter and settler for purification of the air from mechanical particles, moisture and oil vapors; regulator and stabilizer of the pressure. The pressure is measured by a manometer, attached to chamber 3 after the pneumo-preparation group.

The mass flow of abrasive material having mass in the device is determined by measuring the time interval t_a for its gravitational outflow, i.e. without feeding air stream. It is calculated by the formula:

$$\dot{m}_a = \frac{m_a}{t_a}$$ (2.20)

At minimum 3 measurements are carried out and the mean arithmetic value is taken for the time interval t_a with an accuracy of 0.1 seconds.

2.3.4 Methodology for the Study of Erosion Wear

The methodology for studying the erosion wear and erosion wear resistance using the above-described device consists of measurement of the mass erosion wear as the difference between the mass of the sample before treating and after treatment with the two-phase jet stream at the same preset parameters: distance between the nozzle and the surface, angle of the jet α, working pressure of the air, type and average size of the abrasive particles, the mass flow rate of the abrasive $\dot{m}_a$, i.e.

$$m_e = m_e^o - m_e^i$$ (2.21)

Using the so obtained values of mass erosion wear for each experiment one calculates the parameters: rate of erosion $\dot{m}_e$, the intensity of erosion, and erosion wear resistance I_e. The rate of erosion $\dot{m}_e$ is measured in units mg/min:

$$\dot{m}_e = \frac{m_e}{\Delta t}$$ (2.22)

The intensity of erosion i_e, the erosion wear resistance, I_e and the relative wear resistance are determined respectively by the equations (2.17), (2.18), and (2.20).

The parameters of the experimental investigation of the erosion are represented in Table 2.2.

Table 2.2. Parameters used in the erosive wear testing

Test parameter	Value
Solid particles material	Black corundum (Al_2O_3)
Maximum size of the particles	600 μm
Airstream pressure	0.1 MPa
Particles flow	166.67 g/min
Particles impact angle	90°
Distance between the sample and the nozzle	10 mm
Duration of the test	5 minutes
Ambient temperature	24° C

The mass of the samples is measured by electronic balance WP-S-180/C/2 with an accuracy of 0,1 mg. Before each measurement, the sample is cleaned using a solution, neutralizing the static electricity, and then it is dried up.

2.4 DEVICE AND METHODOLOGY FOR STUDYING VIBRO-ABRASIVE WEAR

2.4.1 Influence of the vibrations on the friction and the wear of the machines

The study of the vibration processes is of special importance in the various branches of modern technical fields – metallurgy, energy production, transport machine building, rocket and space technics, and others. This imposes the elaboration of efficient methods and means for the struggle against the harmful impact of vibrational loadings. Thus, for example, based on data known from the world practice in the field of aviation technics, 60-80% of air crashes are due namely to failures as a consequence of strength fatigue and destruction of the constructions under the effect of vibrations. Due to the harmful effect of prolonged duration vibration loading, the exploitation resource of the machines becomes shorter and that of the equipment, the quality of their work deteriorates.

It is of important significance also the investigation of the vibrations in the ecological aspect, i.e. their physiological effect on human health. Harmful influence is exerted both by the direct vibration impact, as well as by the accompanying noise, the acoustic vibrations.

Modern machines, devices, transportation means, and other mechanical systems have increased values of the functional parameters, such as rate, pressure, productivity, and others. This leads to an increase in the intensiveness, and widening of the frequency spectra of the harmful vibrations, which accompany their operation. These harmful vibrations substantially deteriorate the quality and the reliability of the machines and their products, the comfortability, and the effectiveness of vehicles.

Intensive dynamic loadings destroy due to fatigue in the zone of the contact, they change the smooth functioning of the regulating appliances in metal processing machines, lead to loosening of threaded conjunctions and dynamic instability of the transition resistance of the contacts in radio-electronic devices, they increase the loose spaces as a result of wear, increased wear, which in its turn leads to enhancement of the vibration characteristics.

The main sources of harmful vibrations in the machines can be classified into the following main groups:

- Sources of vibrations, connected with different physical processes, which are occurring in the device – processes of burning in internal combustion engines, interactions of liquids and gases with the blades of the turbines, pulsations of the liquids inside the pipelines, electromagnetic phenomena

in electric motors and generators, various technological processes – cutting of metals, friction processes in kinematic pairs and others;

- Sources of vibrations, connected with the movement of the objects in the source. Forces of inertia appear in the course of these movements, often having periodic character, which are the inducing forces for the appearance of the vibrations in the systems;

- Sources of vibrations, connected with the so-called vibration technologies. They are widely distributed as highly productive modern technologies – Vibro-transportation, Vibro-feeding, Vibro-piercing, Vibro-separation, Vibro-assembling, and others. Their implementation in a given machine and equipment is done by the so-called Vibro-inducers. They have different constructions and methods of inducing vibrations.

Influence of the normal vibrations during friction

Changing the mechanical and the deformational properties of the contact, and its actual area, the vibrations influence the force and the coefficient of friction. The variation of the force and the coefficient of friction depends on the character of the distribution of the loading in the contact, the rate of sliding, and the parameters of the vibrational loading. Depending on the ratio between these factors one can observe a decrease or increase in the magnitude of the friction force.

The decrease in the force of static friction between the surfaces of vibrating quartz and the surfaces of the casing (plating) of steel, aluminum, and low-melting alloy of soft solder (tin 67%, lead 33%), was reported for the first time in a disguised form in the research work of Haikin C.E. and co-authors - „About the forces of dry friction", the year 1939. The authors set as their purpose to determine the range of shifting in the contact, characterizing the transition from friction at rest to friction during sliding (i.e. from static friction to kinetic friction). There are important conclusions in this work about the interconnection between normal and tangential shiftings, as well as about the non-linear dependence between the contact deformations and the loading. According to the opinion of the authors, the deviation from linear dependence (slower increase in the forces, than the shifting) seems to be the reason for the appearance of sliding or tearing off.

An attempt to explain the variation of the force and the coefficient of friction during interaction with the applied normal vibrations has been made as early as in the year 1955 by G. D. Lomakin, who analyzes and idealized a model, representing a solid body attached to a spring, doing forced harmonic oscillations at frequency f in normal (perpendicular) direction to the plane of friction. The body has on its end an elastic element having elasticity c in the tangential direction. The body touches a plane, which is moving at velocity v making relaxation vibrations of frequency f along the line of sliding. The change in the normal loading with time is represented by the equality:

$$N = Nc(1 - p\sin 2\pi ft) \qquad (2.23)$$

Where $p = N_a / N_c$ and N_a is the amplitude of the periodic component of the loading, while N_c is the initial loading.

The periodic variation of the normal loading causes flexible shiftings in the direction, normal concerning the plane of friction.

To simplify the analysis, the author neglects the influence of the plastic properties of the material and the difference between the coefficients of static and kinetic friction. As a result of this an expression is obtained for the dynamic coefficient of friction (in analogy also for the force of friction) of the following type:

$$\mu = \mu_o \left(1 - \alpha e^{-\frac{\alpha c}{pfNc}} \right)$$ (2.24)

where μ_o is the static coefficient of friction; α – coefficient of proportionality.

It follows from this expression, that upon increasing the amplitude of vibration of the normal loading the coefficient of friction is decreasing, whereupon, as faster as the velocity of friction becomes smaller.

At higher frequencies, within the range from 6 up to 42 kHz, the decrease in the static coefficient of friction is observed by Friedman and Level. The authors state that the transition from static to dynamic friction is accomplished within the range of tangential shiftings from 1 to 10 μm. The increase in the amplitude at fixed frequency leads to a lowering of the coefficient of friction, while at some definite amplitude it becomes zero. The decrease in the frequency makes this effect stronger. Thus at a frequency of about 6,6 кHz, even an insignificant increase of the amplitude sharply diminishes the coefficient of friction. Under the given conditions of contact the authors come closer to contact-resonance frequency, but they do not draw this conclusion.

The attempt to study the influence of roughness turns out to be unsuccessful, as far as the amplitude dependences of decrease in the coefficient of friction between two surfaces having different pretreatment have been recorded at various frequencies, i.e. the data cannot be compared.

One of the important factors, in determining the decrease in the friction force under the effect of normal vibrations, appears to be the normal contact hardness. Accounting for the effect of this factor has been realized by D.M. Tolstoy, who proposed the following: the vibrations upon the counter body of the slider should lead to its shifting upwards, i.e. the decrease in closeness Y between the surfaces, as far as its dependence on the loading Y(N) is non-linear and also asymmetric concerning the middle position Y_{cp}. Since the force of friction is an increasing function of the actual touching area, while the latter appears to be increasing function upon coming closer, then the lifting of the slider during the

process of vibration leads to a decrease in the force of friction. Other authors propose to use forced oscillation aiming at lowering the force of friction in the real friction nodes, but yet it is not clear what is the economic purposefulness of such a method. The finding of the contact-resonance decrease in the force of friction is a scientific achievement of D. M. Tolstoy and it will help in solving even more dynamic tasks in tribology. The decrease in the coefficient of friction of the indentors, sliding under the action of normal vibrations has been observed by Godfrey. The results from the experiments show, that a great decrease in the coefficient of friction is recorded at accelerations, exceeding the acceleration in case of free falling, i.e. in the case of dividing the surfaces. In this case, the vibrational loading passes over to impulse loading. Under the action of this loading,g the author explains the great plastic deformation of flat-plate samples. The lowering of the coefficient of friction in case of vibrations at ultrasound frequency in the normal direction, and also in different directions, has been observed by a number of researchers. An attempt has been made to explain, from the viewpoint of theoretical mechanics, the decrease in the coefficient of friction at rest and at sliding under the effect of normal vibrations. Despite the correctness of the logical conclusions, these research works cannot answer completely the question of the decrease in the coefficient of friction, since the physical explanation of the studied phenomena is missing them.

The decrease in the coefficient of friction in case of accelerations at normal vibrations and large accelerations in case of free falling is considered by D. M. Tolstoy to be a trivial fact, but the data, obtained by Lomakin, do not allow to have complete consensus on this opinion in the general case. Besides the acceleration of the vibrations, their frequency should also be taken into account, as well as the character of the contact between the surfaces, the physical-mechanical properties of the materials, and the loadings. Data from studies, in which one observes a decrease in the force of friction (respectively decrease in the coefficient), show that the character of the contact is mainly elastic. For this reason, the change in the loading during the process of normal vibrations leads to a decrease in the elastic closeness, and therefore to a diminishing of the actual area of touching and respectively decrease in the force of friction. This effect becomes especially noticeable in the contact-resonance range of the frequencies. If the contact is mainly plastic, then the application of vibrations will result, according to the rheological properties of the contact, in the accumulation of plastic deformations, respectively in making them nearer and the actual area of the contact. This fact, in its turn, should lead to an increase in the force of friction, which is confirmed by the results of the experiments of Weitz. In the research work of this author, metal contact surfaces are subjected to what he called "Vibro-pretreatment, ï.e. preliminary action of normal vibrational loading of definite duration, and thereafter the force of friction was measured.

The increase in the amplitude of vibrational loading leads to enhancement of the force of friction. This fact correlates with the results of studies on the origin of amplitude dependence on the effect of nearing and on the actual contact area under the action of normal vibrations.

An important circumstance seems to be taking into account the behavior of the adsorbed layers (including also the thin oxide coatings) on the contact surfaces in case of vibrational loadings. The vibrations can cause destruction of the layers due to fatigue, as a result of which some juvenile surfaces of the metals can appear and local spots of cohesion. One should understand under the term of *juvenile surfaces* surfaces without oxide layers, adsorbed organic and inorganic molecules, moisture etc. Upon increasing the amplitude and transition from vibrational loading to impulse loading brittle destruction of the surface layers is possible. This partially can explain the increase of the friction force in case of impulse loading.

Influence of tangential vibratons during friction (fretting)

The fretting-wear appears where the low-amplitude sliding between the contact surfaces is prolonged, having large number of cycles. The result is two types of destruction: surface wear and deterioration of the strength due to fatigue. Forward-reverse movements of magnitude 0.1 μm can lead to damage of the components in case the number of cycles is of the order of one million.

The fretting-wear and fretting fatigue are observed in almost all kinds of machines and they are the reason for damaging sound-state components. The studies show that unlike the other forms of wear the frequency of fretting problems in the machines is not decreasing during the last decades. The fretting fatigue remains an important factor, but still not well known in the structure of bearing components. The knowledge about fretting is of essential importance for each engineer or technologist, dealing with machine equipment, which almost always contains large number of low-amplitude sliding contacts.

The fundamental characteristics of the fretting-wear are the very small amplitude of the movements during sliding, which determine the symptoms of this wearing mechanism. Under definite conditions of normal and tangential loading of the contact, the microscopic movement inside the contact is done also without sliding. The center of the contact can remain fixed, while the edges are doing forward-reverse movements of amplitude, of the order of 1 μm, which can cause destruction. Therefore, from practical point of view, no lower limit exists for the tangential force, needed for destruction and this fact should be taken into account in the design of mechanical components. The accumulation of wear degree gradually divides the two surfaces and in some cases it can contribute to acceleration of the process of wear in case of abrasion. The process of fretting wear can be additionally accelerated by corrosion, temperature and other effects. In such cases the wear is called *fretting-corrosion*.

Studies on wear are missing in the literature in cases of simultaneous action of normal vibrational loading and abrasive dry friction. No investigations are known on the subject of vibro-abrasive wear of HVOF coatings.

2.4.2 Device and Methodology of Studies on Vibro-abrasive Wear

The study on abrasive wear, under the action of periodic loading, is made using tribo-tester „Pin-cylinder", whose scheme is represented in Fig. 2.5 [44,45].

The notations in Fig. 2.5 are as follows: 1 – electric engine; 2 - cylinder; 3 – saple with cating; 4 – loading head; 5 – abrasive surface; 6 – fixed strip; 7 – tooth ring; 8 – mechanism for attachment of the sample; 9 – vibrating frame; 10,11 – fixed stopping mechanism; 12,13 – weights and loading mechanism; 14 - vibrator; 15 – bearing construction of the vibrator; 16 – driving mechanism of the vibrator; 17 – button for switch on/off of the vibrator; 18 – regulator of the parameters of the vibrations.

The studied sample 3 (pin) contacts by its fron surface with the abrasive surface 5 of the conterbody, which represents a horizontal cylinder 2. The sample 3 has diameter of the contacting plate = 17 mm and it is attached to the holder at the loading head 4 by means of elastic bonding, which enables self-adjustment of the sample with respect to the surface 5 and it enables the option to rotate around its own verticle axis.

These circumstances guarantee conditions for consecutive uniform wear of the entire nominal contact area of the sample. The loading head 4 through horizontal tooth ring 7 is bonding to fixed strip 6, situated in parallel to the forming surface of the cylinder 2 and in this way it ensures relative translational movement of the sample along the generant surface of the cylinder 2. The sample 3 is attached by the gadget 8 to the vibtating frame 9, through which the vibrations are transferred from the vibrator 14 along the axis of the sample. The central normal loading pressure P along the axis of the sample is ensured by selecting suitable weights 12 in the loading mechanism 13. The vibrator 14 is mounted on the carrying construction 15, in which it moves translationally simultaneously with the vibratin frame 8, the loading head 4 and the sample 3 along the generant surface of the cylinder 2. The surface with firmly attached abrasive is modeled by impregnated corrundum having definite hardness and grain size, which is attached fixedly to the surface of the cylinder 2. The cylinder 2 rotates around its horizontal axis at constant angular velocity. The movement of the sample 3 represents a plane-type of movement: the nominal contact plane is doing translational movement along the generant surface of the cylinder and at the same time it rotates aroud the vertical axis, passing through its center. The spots on the contact zone have different in size and in direction velocities at a given moment of time, but in the process of contact interaction upon relative movement the separate points change periodically their position with respect to the abrasive surface of the cylinder 2. This circumstance determines the uniform distribution of wear in all the points of the contact surface, which is the main advantage of this device.
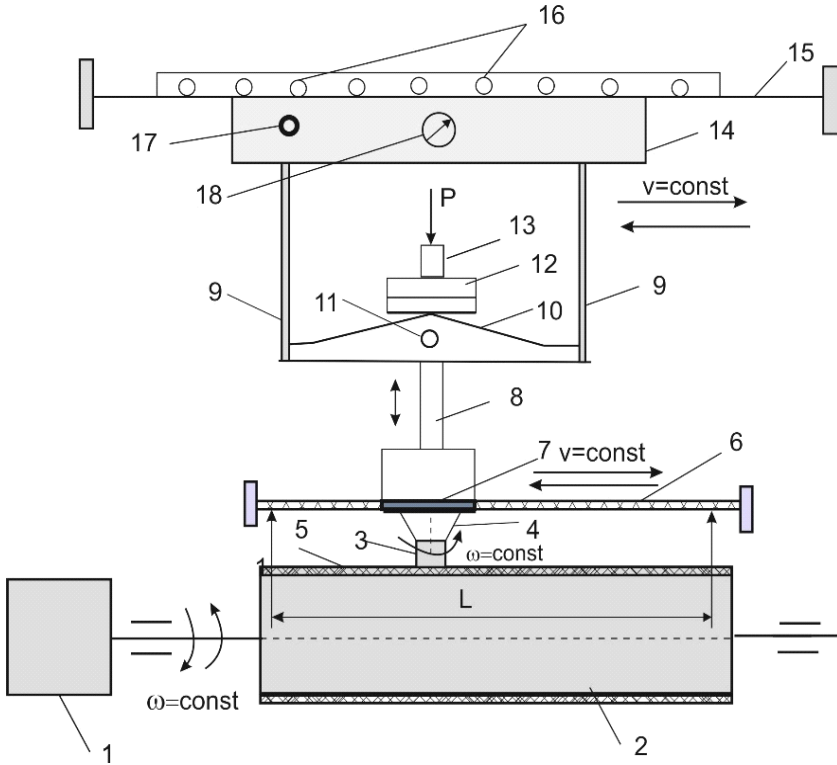
Fig. 2.5. Scheme of tribo-tester „Pin-cylinder" for studies of abrasive wear under the action of normal vibrations

Amother advantage of the device is, that the sample is contacting always with fresh abrasive surface, where products of wear are almost missing. This is the result of the movement of the sample along helix line with respect to the surface, and also the result of cleaning of the abrasive surface 5 from the fine products of wear process by means of vacuum pump. The stability of the movement is ensured by the constant ratio between the angular velocities of the drum and of the sample. The direction of rotation of the cylinder, the turning on and turning off the device is accomplished by means of regulating block. Turning on the vibrator 14 is done by the button 17, while setting of the vertical vibration velocity – by the regulator 18.
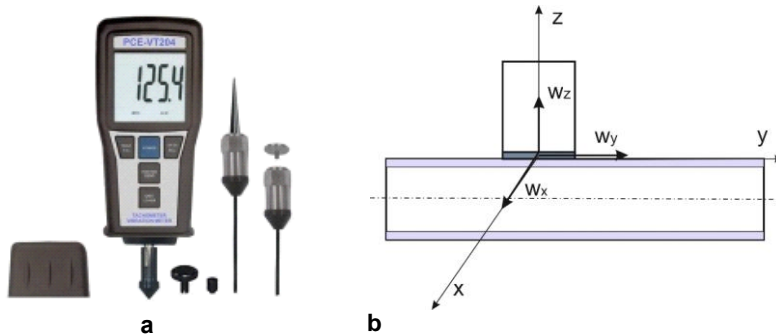
Fig. 2.6. Vibrometer „PCE-VT 204" for measuring the parameters of the vibrations: a) vibrometer „PCR-VT 204" ; b) components of the vibration velocity along the three axis

The measurement of the parameters of the vibrations – vibrational shifting [mm], vibrational velocity [mm/s] and vibrational acceleration [mm/s^2] is done by vibrometer „PCR-VT 204" (Fig. 2.6, a).

The Table 2.3 represents the values of the vibration velocity in three directions: vertical vibration - w_z, vibration in the direction of sliding - w_y and transverse vibration - w_x along direction x, for each indication of the regulator 18 (Fig. 2.6, b).

Table 2.3. Values of the components of the vibration velocity

Settings of the regulator	1	5	7	9	10
w_z mm/s	3	6	9	16	20
w_x mm/s	0,2	0,35	0,8	3,8	5
w_y mm/s	0,4	0,6	0,9	3,8	4,4
w, mm/s	3	6,04	9,08	16,87	21,08

Using the regulator of vibrations 18 one can set different values of the vibration velocity, changing within the range 3≤w≤21,08 mm/s. This interval of variation of the vibration velocity is chosen in accordance with the requirements for evaluation and classification of machines and equipments in ISO 2372 and VDI 2056. The machines and equipments are classified in four groups K, M, G and T. The velocity of sliding *V* of the sample, more specifically the center of mass of the contact plane, has two components V_y and V_x, which in accordance with Fig. 2.7 are determined by the formula:

$$V_x = \frac{L}{t}; \ \ V_y = r.\omega = r\frac{\pi.n}{30}; \ \ V = \sqrt{V_y^2 + V_x^2} \tag{2.25}$$

where L=0.6 m is the horizontal pathway along the generant line of the cylinder, the path length which the sample passes during one cycle; the time t=2,28 [min] - the time interval, during which the sample travels path length L along the generant line of the cylinder; r=0,075 [m] is the radius of the cylinder; $n = 40$ [min^{-1}] is the number of revolutions of the cylinder.
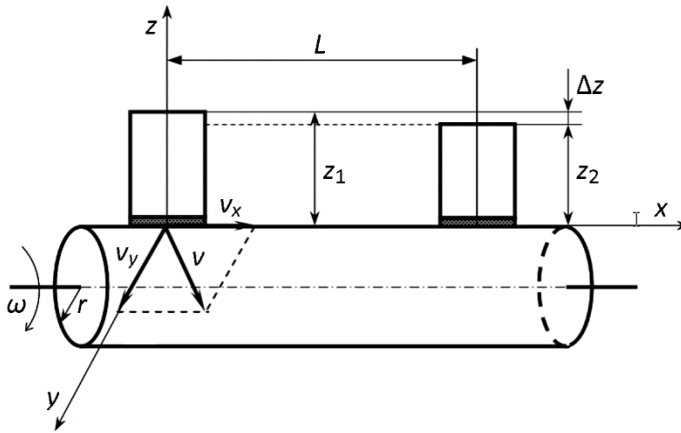
Fig. 2.7. Scheme of the sliding velocity of the center of the contact plane of the sample along the rotating cylinder

The total pathway of friction of the sample along the spiral line is calculated by the formula:

$$S = V.t.N \tag{2.26}$$

where *N* is the number of cycles of sliding.

The study is carried out under identical conditions of sliding by changing the vibrational velocity. The samples have cylindrical form of identical dimensions and roughness of the contact surface Ra=0.413 μm. The testing is done at constant values of the loading 3.92 N. Abrasive sandpaper of Corrundum 120 is used as counterbody, which is replaced when testing each separate sample.

The methodology for investigating the characteristics of wear consists of measurement of the mass wear of each sample at preset constant values of the factors: loading, friction path length, velocity of sliding, type of the abrasive surface and definite vibration velocity. Thereafter under the same conditions of sliding another value of the vibration velocity is given and again the mass wear is measured. The experiments are repeated for each sample at several values of the vibration velocity.

Based on the measured mass wear one calculates the characteristics: rate and intensity of the wear process, absolute and relative wear resistance as in the case of abrasive wear.

The relative wear resistance characterizes the influence of the vibrations upon the wear resistance and it represents the ratio between the wear resistance I_w of the sample under the action of vibrational loading and the wear resistance I_i of the sample without vibration, under one and the same conditions of friction:

$$\lambda = \frac{I_w}{I_i} \tag{2.27}$$

_____

Abrasive and Erosive Wear of HVOF Coatings with Tungsten and Nickel Matrix

3.1 MATERIALS

Two groups of coatings are studied, deposited by the HVOF technology using metal powder composites: with *tungsten matrix* denoted as SX199/11 having average size of the powder particles 11 microns and SX199/45 having average size of the powder particles 45 microns; with *nickel matrix* denoted as 1660-22/20 having average size of the powder particles 45 microns and 1660-22/45 having average size of the powder particles 45 microns. The having average size of the powder particles is denoted by Arabic numeral after the slash [40-42].

The studied coatings have been deposited using system model MICROJET+Hybrid without any preliminary thermal treatment of the substrate (cold process).

Table 3.1 represents some of the characteristics of the studied coatings – chemical composition, sizes of the powder particles and hardness of the coatings.

3.2 ABRASIVE WEAR

Using the above described methodology and device for studying the abrasive wear experimental results have been obtained on the characteristics of the abrasive wear process – mass wear, rate of wear process, specific intensity of the wear process, absolute and relative wear resistance for all the coatings and the substrate. The results are represented respectively in the Tables 3.2, 3.3, 3.4, 3.5 and 3.6.

In accordance with the results in Table 3.2 kinetic curves are plotted for the wearing process, i.e. the dependence of the mass wear on the friction path length, respectively for coatings having tungsten matrix and nickel matrix of different sizes of the powder particles – Fig. 3.1 and Fig. 3.2. It is seen in the figures that the curves have almost linear character. Certain non-linearity is observed in the cases of coatings having nickel matrix with size of the particles 45 microns in comparison with the curve for the same coating with size of the particles 20 microns. What makes impression is the fact, that for coatings of particle size 45 microns the wear of coatings having nickel matrix is less than that for coatings having tungsten matrix. In case of smaller particle size the lowest

degree of wear is observed for coatings having tungsten matrix. The same coatings having larger particles - 45 microns have greater degree of wear of the substrate – see the Fig. 3.1.

Fig. 3.1. Dependence of the mass wear on the friction path length for coatings having tungsten matrix
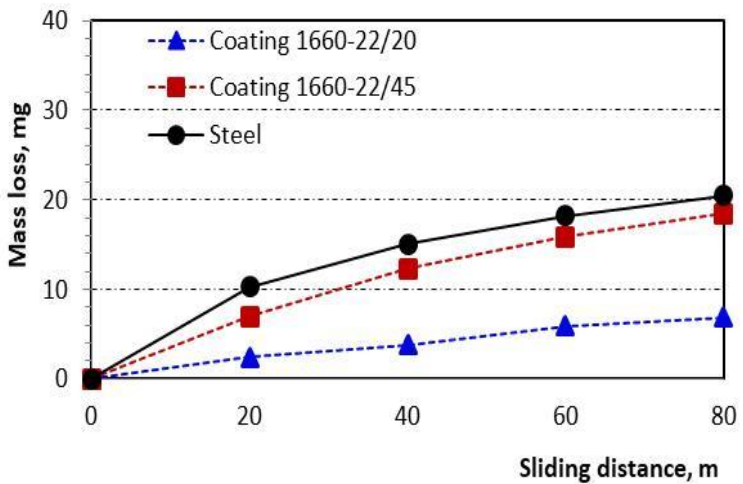
Fig. 3.2. Dependence of the mass wear on the friction path length for coatings having nickel matrix

Table 3.1. Chemical composition, particle size and hardness of coatings

Sample	Designation	Chemical composition, %	Size of particles	Hardness of coating
1	SX199/11	Cr:21; WC-Cr$_3$C$_2$-Ni:6.1; C:5.8 **W: Balance**	11 µm	HRC 64-66
2	SX199/45	Cr:21; WC-Cr$_3$C$_2$-Ni:6.1; C:5.8 **W: Balance**	45 µm	HRC 62-64
3	1660-22/20	C:0.9; Si:4.3; B:3.3; Fe:4.2; Cr:16.3 **Ni: Balance**	20 µm	HRC 58-60
4	1660-22/45	C:0.9; Si:4.3; B:3.3; Fe:4.2; Cr:16.3 **Ni: Balance**	45 µm	HRC 57-59
5	Substrate: Steel	C:0.15; Si:0.21; Mn:0.8; Ni:0.3; P:0.011; S:0.025; Cr:0.3 **Fe: Balance**	-	HRC 38-45

Table 3.2. Mass wear of the samples after different path lengths of friction (number of cycles)

Sample	Coatings	Number of cycles (N)			
		100 Sliding distance, m	200	300	400
		20 Mass loss, mg	40	60	80
1	SX199/11	0.3	0.6	1.3	2.4
2	SX199/45	13	20.2	27.1	33.2
3	1660-22/20	2.4	3.8	5.9	6.9
4	1660-22/45	7.0	12.3	15.9	18.5
5	Substrate	10.3	15.1	18.2	20.5

Table 3.3. Wear rate of the samples after different friction path length (number of cycles)

No.	Coatings	Number of cycles (N)			
		100	200	300	400
		Friction path length (m)			
		20	40	60	80
		Duration of friction (min)			
		0.47	0.94	1.41	1.88
		Wear rate (mg/min)			
1	SX199/11	0.64	0.64	0.92	1.28
2	SX199/45	27.7	21.48	19.22	17.66
3	1660-22/20	5.11	4.04	4.18	3.67
4	1660-22/45	14.89	13.09	11.28	9.84
5	Substrate	21.09	16.06	12.9	10.9

In accordance with the results for the rate of abrasive wear in Table 3.3 dependences have been plotted for the wear rate versus the friction path length for the substrate and for the tested coatings, represented in Figs. 3.3 and 3.4.
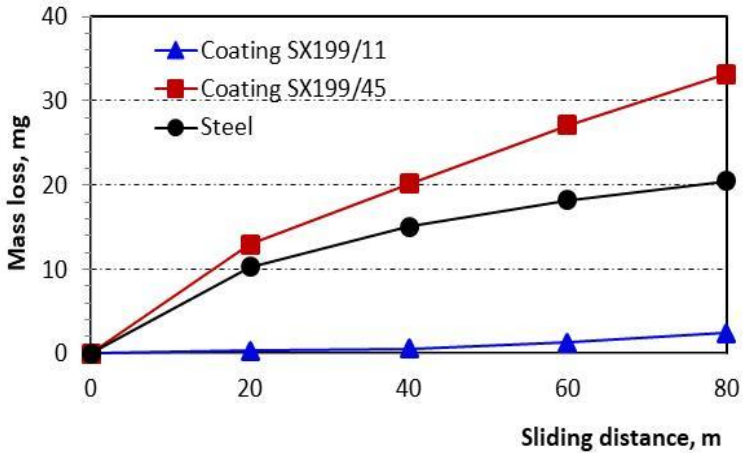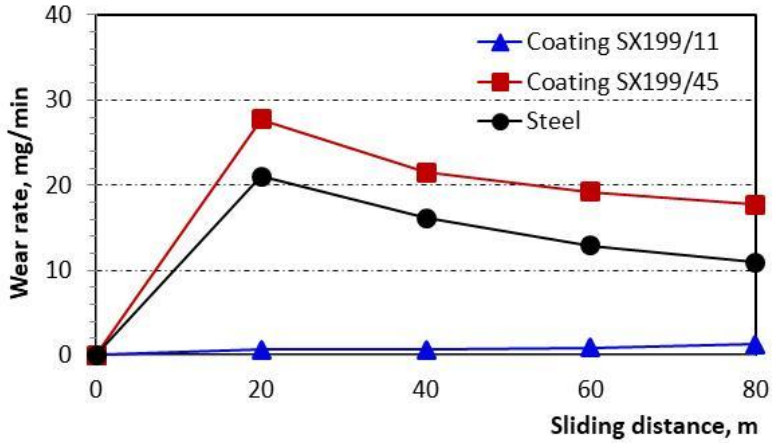

Fig. 3.3. Dependence of the wear rate on the friction path length for coatings with tungsten matrix
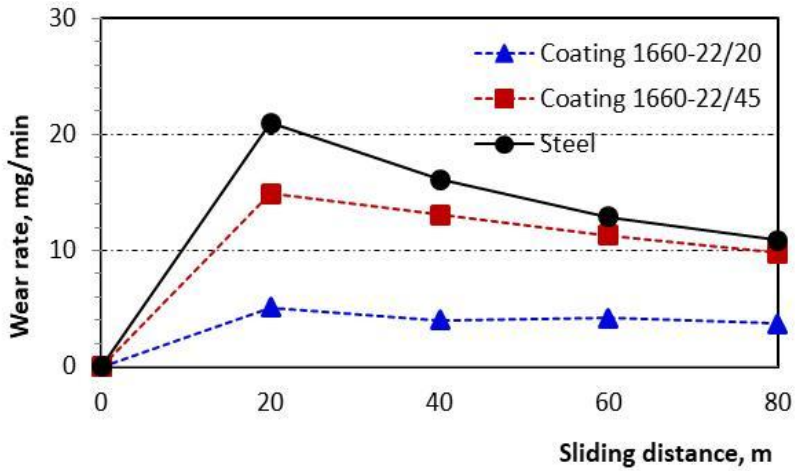
Fig. 3.4. Dependence of the wear rate on the friction path length for coatings with nickel matrix

Table 3.4. Specific wear intensiveness of the samples after different friction path length (number of cycles)

No	Coatings	Number of cycles (N)			
		100	200	300	400
		Friction path length (m)			
		20	40	60	80
		Specific intensity of wearing (mg/Nm.mm^2)			
1	SX199/11	0.1×10^{-4}	0.1×10^{-4}	0.2×10^{-4}	0.28×10^{-4}
2	SX199/45	6.28×10^{-4}	4.88×10^{-4}	4.36×10^{-4}	4.0×10^{-4}
3	1660-22/20	1.1×10^{-4}	0.9×10^{-4}	0.95×10^{-4}	0.83×10^{-4}
4	1660-22/45	1.16×10^{-4}	2.97×10^{-4}	2.56×10^{-4}	2.23×10^{-4}
5	Substrate	4.97×10^{-4}	3.64×10^{-4}	2.93×10^{-4}	2.50×10^{-4}

Table 3.5. Wear resistance of the samples for different friction path length (number of cycles)

No.	Покрития	Number of cycles (N)			
		100	200	300	400
		Friction path length (m)			
		20	40	60	80
		Wear resistance (Nm.mm^2/mg)			
1	SX199/11	10×10^4	10×10^4	5×10^4	3.6×10^4
2	SX199/45	0.16×10^4	0.20×10^4	0.23×10^4	0.25×10^4
3	1660-22/20	0.91×10^4	1.1×10^4	1.1×10^4	1.2×10^4
4	1660-22/45	0.86×10^4	0.34×10^4	0.39×10^4	0.45×10^4
5	Substrate	0.20×10^4	0.27×10^4	0.34×10^4	0.40×10^4

Table 3.6. Relative wear resistance for the coatings after friction path length 80 m

№	Coatings	Wear resistance	Relative wear resistance $R_{i,j}$	
			Influence of particle sizes	Influence of the coating upon the substrate
1	SX199/11	3.6×10^4	$R_{1,2}=14.1$	$R_{1,5}=9.0$
2	SX199/45	0.25×10^4	$R_{2,2}=1$	$R_{2,5}=0.6$
3	1660-22/20	1.2×10^4	$R_{3,4}=2.7$	$R_{3,5}=3.0$
4	1660-22/45	0.45×10^4	$R_{4,4}=1$	$R_{4,5}=1.1$
5	Substrate	0.40×10^4	-	$R_{5,5}=1$
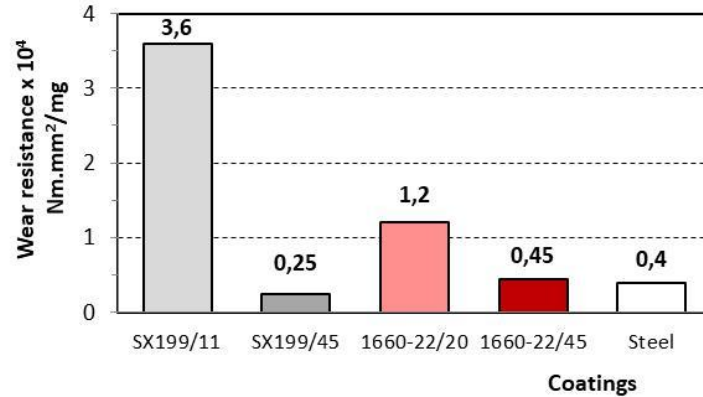
Fig. 3.5. Diagram of the abrasive wear resistance of the tested coatings and of the substrate

The Figs. 3.5, 3.6 and 3.7 represent plotted diagrams of the abrasive wear resistance and the relative wear resistance with respect to the size of the particles and in regard to the wear resistance of the substrate.

Fig. 3.6. Diagram of the influence of the particles size on the abrasive wear resistance of the tested coatings
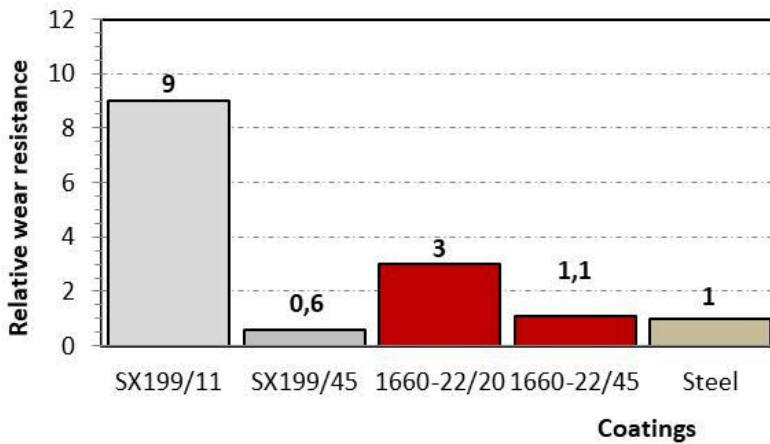
Fig. 3.7. Diagram of the relative abrasive wear resistance of the tested coatings with respect to the wear resistance of the substrate

The highest wear resistance $I_a=3.6 \times 10^4$, $Nm.mm^2/mg$ is shown by the coating with tungsten matrix (coating SX199/11) having particle size 11 microns (Table 3.6),

which is 14.1 times higher than the wear resistance of the same tungsten coating, having particle size 4 times larger – 45 microns. The relative wear resistance of this coating with respect to the substrate of steel is 9 (Fig. 3.7). The same tungsten coating having particle size 45 microns (coating SX199/45) has the lowest wear resistance - I_a=0.25x10^4,Nm.mm^2/mg in comparison to all the tested coatings, including also that of the substrate. For the coatings with nickel matrix one observes the same effect – at small sizes 20 microns (coating 1660-22/20) the wear resistance is almost three times higher than the wear resistance of the same coating, obtained using particles of size 45 microns (coating 1660-22/45).

We can summarize the above data stating, that in case of coatings with tungsten and nickel matrix the increase in the micron sizes of the powder particles leads to decrease in the abrasive wear resistance of the coatings, i.e. decrease in their resistance capability against the cutting action of the abrasive particle during friction.

3.3 EROSIVE WEAR

Using the above described device and methodology for testing of the jet-abrasive erosion results have been obtained about the mass wear, the rate and the intensity of the wear process, the absolute and the relative erosion wear resistance of all the tested coatings and of the substrate. The results are represented in the Tables 3.7 and 3.8.
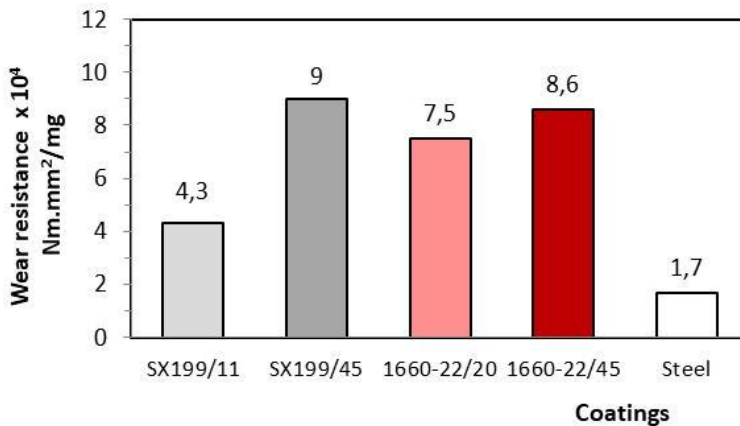
Fig. 3.8. Diagram of erosion wear resistance of the tested coatings and of the substrate

It is seen in the diagram of the erosion wear resistance of the samples, represented in Fig. 3.8, that the highest wear resistance in case of erosion is displayed by coatings with tungsten matrix having particle size 45 microns.

The decrease in the size of the particles – 11 microns - leads to decrease in the wear resistance during erosion. This result is just the opposite to the result for the abrasive wear resistance.

The lowest wear resistance in case of erosion is shown by the substrate, i.e. steel without any coating.

Upon increasing the size of the particles 4 times from 11 up to 45 microns in case of coatings with tungsten matrix the wear resistance grows up 2.1 times, while in the case of coatings with nickel matrix the increase in the erosion wear resistance is negligible – 1.2 times – see Table 3.8, Fig. 3.9.
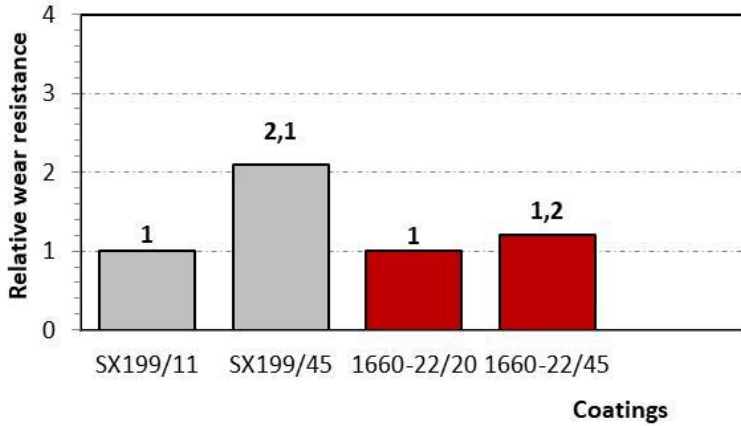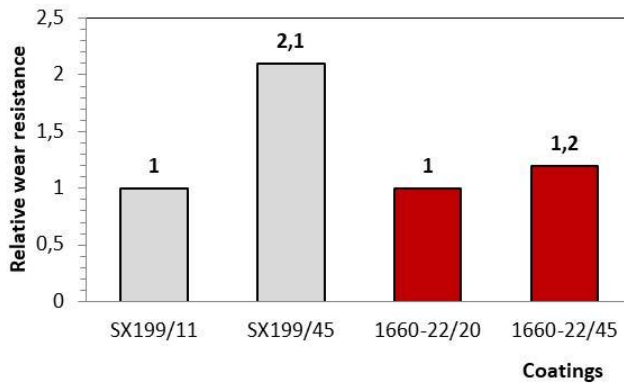

Fig. 3.9. Diagram of the influence of the particle size upon the erosion wear resistance of the tested coatings
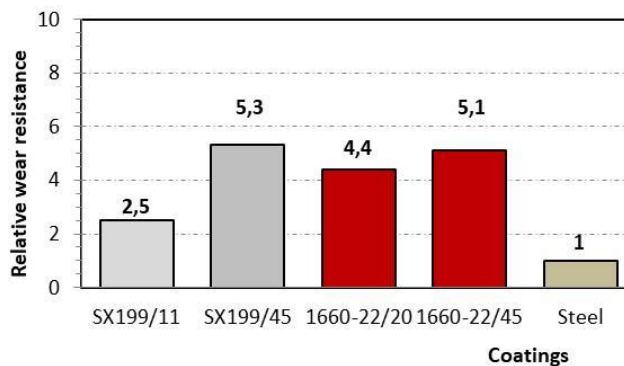
Fig. 3.10. Diagram of the relative erosion wear resistance of the tested coatings compared to the wear resistance of the substrate

Table 3.7. Characteristics of the wear and wear resistance in case of erosion

No	Coating	Wear, mg	Rate of wear, mg/min	Intensity	Wear resistance
1	SX199/11	23.3	4.66	2.33×10^{-5}	4.3×10^{4}
2	SX199/45	11.0	2.2	1.1×10^{-5}	9.0×10^{4}
3	1660-22/20	13.3	2.66	1.33×10^{-5}	7.5×10^{4}
4	1660-22/45	11.6	2.32	1.16×10^{-5}	8.6×10^{4}
5	Substrate	58.6	11.72	5.86×10^{-5}	1.7×10^{4}

Table 3.8. Relative wear resistance of the coatings in case of erosion

No	Coating	Wear resistance	Relative wear resistance	
			Influence of particle size	Total influence of the coating
1	SX199/11	4.3×10^{4}	$R_{1,1} = 1$	$R_{1,5} = 2.53$
2	SX199/45	9.0×10^{4}	$R_{2,1} = 2.1$	$R_{2,5} = 5.29$
3	1660-22/20	7.5×10^{4}	$R_{3,3} = 1$	$R_{3,5} = 4.41$
4	1660-22/45	8.6×10^{4}	$R_{4,3} = 1.2$	$R_{4,5} = 5.05$
5	Substrate	1.7×10^{4}	-	$R_{5,5} = 1$

Table 3.9. Comparative results for the wear resistance of the coatings in cases of abrasion and erosion

No.	Coating	Wear resistance in case of abrasion, I_a	Wear resistance in case of erosion, I_e	$W_{e,a} = I_e/I_a$
1	SX199/11	$3,6 \times 10^{4}$	4.3×10^{4}	1.19
2	SX199/45	0.25×10^{4}	9.0×10^{4}	36
3	1660-22/20	1.2×10^{4}	7.5×10^{4}	6.25
4	1660-22/45	0.45×10^{4}	8.6×10^{4}	19.11
5	Substrate	0.4×10^{4}	1.7×10^{4}	4.25

The increase in the wear resistance of the coatings with respect to the wear resistance of the substrate is seen from the data in the last column of the Table 3.8 and from the diagram in the Fig. 3.10. The greatest effect of enhancement of the wear resistance is obtained for the two types of coatings – with the tungsten matrix and with the nickel matrix having size of the powder particles 45 microns. The increase in the wear resistances of these coatings is very close in value - respectively 5.29 and 5.05 times.

3.4 COMPARATIVE RESULTS FOR THE ABRASIVE AND EROSIVE WEAR RESISTANCE

The Table 3.9 represents the results for the abrasive and erosive wear resistance of the tested gas-flame coatings.

It is clearly seen, that in the case of abrasive wear the wear resistance of the two types of coatings is higher at smaller sizes of the powder particles, respectively for coatings with tungsten matrix 11 microns, while for the coatings with the nickel matrix it is 20 microns. The same coatings in case of erosion have lower wear resistance, i.e. lower resistance ability under impact action of the abrasive particles in the air jet stream.

In general it can be stated, that the wear resistance of the tested coatings and of the substrate is greater in case of erosion in comparison with that in the case of abrasion friction. The comparative results are represented in the last column of Table 3.9.

Under exploitation conditions of the details in the presence of impact action of solid particles (erosion) coatings with tungsten and nickel matrix are appropriate, which have sizes of the powder particles 45 microns.

3.5 CONCLUSION

In this chapter experimental results have been obtained about the mass wear, the wear rate, the specific intensity of the wearing process and the wear resistance of HVOF coatings of two kinds of powder composites – with matrix of tungsten carbide and with matrix of nickel having different sizes of the powder particles in the cases of dry abrasive friction and erosion caused by air jet stream, carrying solid particles.

A non-linear dependence has been established for the characteristics of the abrasive wear versus the friction path length and for the influence of the sizes of the powder particles on the wear resistance of the coatings.

It has been found out that the abrasive wear resistance of the two types of coatings – with tungsten matrix and with nickel matrix, is greater in case of smaller sizes of the powder particles, respectively for coatings with tungsten matrix 11 microns, while for coatings with nickel matrix it is 20 microns. The same coatings in case of erosion have lower wear resistance, i.e. lower

resistance ability under impact action of the abrasive particles in air jet stream. This is explained by the different mechanisms of wearing of the coatings.

It has been ascertained, that the wear resistance of the tested coatings and that of the substrate is greater in case of erosion in comparison with that in the case of abrasive friction.

Abrasive Wear of HVOF Coatings with Metal, Ceramic and Metal-Ceramic Composites and Their Mixtures

4.1 MATERIALS

11 types of coatings have been studied, deposited by the HVOF technology using metal, metal-ceramic and ceramic powder composites based on nickel - 602P, 80M60); based on tungsten - 6P50W, WC-12Co, chromium oxide - Cr_2O_3 and combinations of three composites based on nickel-tungsten at the ratio 1:1:1- 602P–6P50W– (WC–12Co). The average size of the powder particles is within the limits of $45 \pm 2,5$ μm, prepared by agglomeration process including a stage of sintering [13-39,42,43].

The designations and the chemical composition (wt. %) of the studied coatings are represented in Table 4.1.

The coatings, deposited using the composites 602P, 80M60, 6P50W and the combined three composites 1:1:1 - 602P–6P50W– (WC–12Co) are investigated in two cases: without preliminary thermal treatment of the substrate and after preliminary thermal treatment. The thermal treatment consists of heating of the substrate up to a temperature of $650^{o}C$ in a chamber for 5 minutes, after which the coating is deposited. The coatings, deposited upon preliminary heat-treated substrate are denoted as PHS*. One of the coatings (80M60) is deposited upon a substrate of aluminium alloy (Al-Cu) applying preliminary heat treatment.

Table 4.2 represents the data on the thickness, porosity, hardness and roughness of the coatings without any mechanical treatment.

The samples represent square plates of dimensions 15x15x6.0 mm. The investigation is carried out under the following conditions: nominal contact area – Aa=2.25x10^{-6} m^2; velocity of sliding – V = 0.155 m/s; friction path length – L = 24.5 m; type of the abrasive surface - Corundum P 320; normal loading pressure – P = 2.5N; 5N; 7.5N; 10N.

The microstructure of the samples of the studied coatings has been obtained by transverse sections employing an optical microscope. Fig. 4.1 illustrates the microstructure of some of the studied coatings.

Table 4.1. Coating designation and appropriate powder chemical composition (wt. %)

Sample	Coating designation	Powder chemical composition, wt. %
1	602P, Substrate: Steel	Cr: 13.2; Si: 3.98; B: 2.79; Fe: 4.6; Co: 0.03; C: 0.63;
2	602P: PHS*, Substrate: Steel	**Ni: Balance**
3	80M60, Substrate: Steel	Cr: 14.2; Si: 4.37; C: 0.6; B: 2.9; Fe: 4.54; Cu: 2.36;
4	80M60: PHS*, Substrate: Steel	Mo: 2.51; Co: 0.01;
5	80M60: PHS*, Substrate: Al-Cu	**Ni: Balance**
6	6P50W, Substrate: Steel	Cr: 13.15; Si: 4.28; B: 2.87; Fe: 0.04; Ni: 29.6; Co: 0.04;C: 0.58;
7	6P50W: PHS*, Substrate: Steel	**W: Balance**
8	WC–12Co, Substrate: Steel	Co: 12; C: 5.4; Fe: < 0.1; Ni: < 0.1;
		W: Balance
9	602P–6P50W–(WC–12Co) Substrate: Steel	
10	602P–6P50W– (WC–12Co): PHS* Substrate: Steel	Mixture ratio (1:1:1)
11	Cr_2O_3, Substrate: Steel	Al2O3 < 0.03; SiO2 < 0.07; Fe2O3 < 0.02; CaO < 0.03; MgO < 0.01; TiO2 < 0.02; **Cr_2O_3: Balance**

Table 4.2. As-deposited thickness, porosity, roughness and hardness of tested coatings

Sample	Coating Designation	Thicknessµm	Porosity %	Roughness µm	Hardness HRC
1	602P Substrate: Steel	120	1.5	Ra=2,888 Rq=3,456	62
2	602P: PHS* Substrate: Steel	120	1.4	Ra=0,168 Rq=0,208	63
3	80M60 Substrate: Steel	115	3	Ra=5,798 Rq=7,298	63

Sample	Coating Designation	Thicknessµm	Porosity %	Roughness µm	Hardness HRC
4	80M60: PHS* Substrate: Steel	115	1.8	Ra=2,148 Rq=2,685	60
5	80M60: PHS* Substrate: Al-Cu	120	2.0	Ra=6,659 Rq=8,087	62
6	6P50W Substrate: Steel	110	1.6	Ra=6,832 Rq=7,514	65
7	6P50W: PHS* Substrate: Steel	115	1.4	Ra=3,832 Rq=4,561	68
8	WC–12Co Substrate: Steel	120	1.3	Ra=5,484 Rq=6,71	70
9	602P–6P50W–(WC–12Co) Substrate: Steel	120	1.5	Ra=3,028 Rq=3,765	68
10	602P–6P50W– (WC–12Co): PHS* Substrate: Steel	115	1.4	Ra=5,996 Rq=7,126	70
11	Cr_2O_3 Substrate: Steel	110	3	Ra=3,332 Rq=4,034	59
12	Substrate: Steel	-	-	Ra=0,57 Rq=0,794	-
13	Substrate: Al	-	-	Ra=0,488 Rq=0,604	-
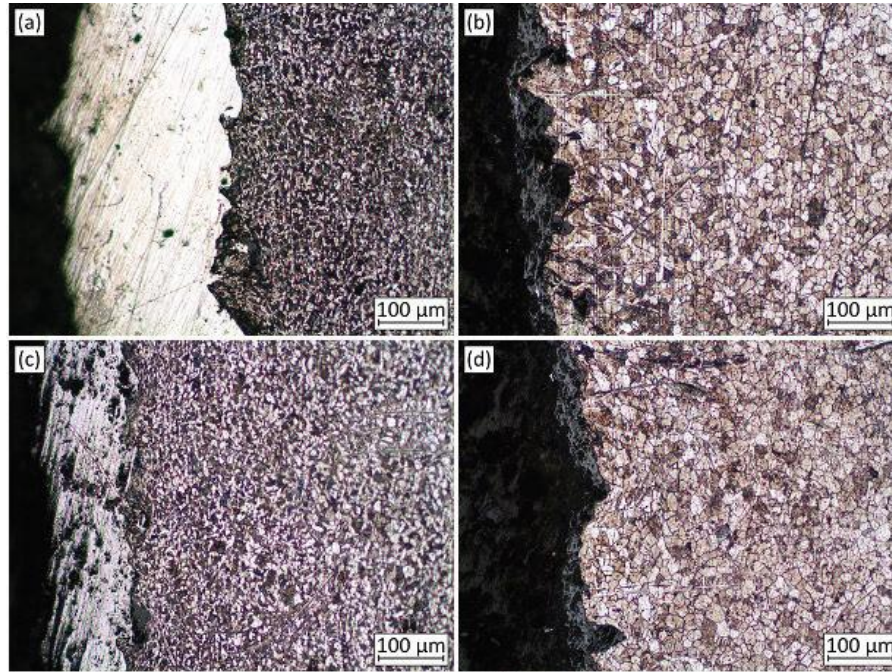
Fig. 4.1. Microstructure properties of some of the tested coatings: (a) Coating 602P, (b) Coating 80M60: PHS, (c) Coating WC–12Co, (d) Coating 6P50W–602P–(WC–12Co)

Wear of High-Technology Coatings, Deposited by High-Velocity Oxygen Flame (HVOF)
Abrasive Wear of HVOF Coatings with Metal, Ceramic and Metal-Ceramic Composites and Their
Mixtures

The relative wear ε_r is the ratio between the specific wear of the substrate i_{sb} and the specific wear of the studied sample:

$$\varepsilon_r = \frac{i_{sb}}{i_r} \tag{4.1}$$

The relative parameter is non-dimensional quantity, which shows how many times the wearing of the tested sample is lower than the wearing of the substrate under identical conditions of friction.

The influence of the preliminary heat treatment of the substrate upon the wearing degree is estimated using the factor ε_{ij}, which represents the ratio between the specific wear upon heating and the specific wear without heating of the substrate:

$$\varepsilon_{ij} = \frac{i_r^{PHS}}{i_r} \tag{4.2}$$

4.2 EXPERIMENTAL RESULTS

Table 4.3 represents the results for the mass wear, while Table 4.4 lists the data for the specific wear of the tested coatings at four values of the loading.

Table 4.5 and Table 4.6 represent the results respectively for the relative wear and the factor for the tested coatings.

Figs. 4.2, 4.3, 4.4, 4.5 and 4.6 represent graphically the plotted dependence of the mas wear on the normal loading for all the studied coatings. Figs. 4.7, 4.8 and 4.9 illustrate the diagrams of the specific wear of the coatings.

Based on the analysis of the obtained results for the abrasive wear of the composite coatings, deposited by the HVOF technology, at various values of the normal loading, we can conclude the following:

Upon increasing the normal loading the wear degree is growing up, but the dependence has a different character for the different coatings. In the cases of coatings with nickel and tungsten matrix, deposited on a substrate of steel one can observe directly proportional dependence up to the loading of P=7.5N, At higher loadings P>7.5N the dependence of the wear on the normal loading has a non-linear character, whereupon in the cases of coatings with nickel matrix the rate of wearing increases sharply, while for the coatings with tungsten matrix the wearing grows up at very low rate.

Table 4.3. Abrasive wear of tested coatings

Sample	Coating designation	Load, N			
		2.5	5	7.5	10
		Mass loss, mg			
1	602P Substrate: Steel	0.8	1.3	0.6	2.7
2	602P: PHS* Substrate: Steel	0.6	0.9	0.4	2.0
3	80M60 Substrate: Steel	2.0	3.1	4.9	7.1
4	80M60: PHS* Substrate: Steel	0.9	1.2	2.5	3.4
5	80M60: PHS* Substrate: Al-Cu	3.9	4.1	5.1	5.7
6	6P50W Substrate: Steel	0.5	1.0	1.4	1.6
7	6P50W: PHS* Substrate: Steel	0.4	0.6	0.8	0.9
8	WC–12Co Substrate: Steel	0.3	0.5	0.8	0.9
9	602P–6P50W–(WC–12Co) Substrate: Steel	1.0	1.2	1.1	1.1
10	602P–6P50W– (WC–12Co): PHS* Substrate: Steel	1.2	1.7	1.1	0.6
11	Cr_2O_3 Substrate: Steel	13.4	16.7	18.5	20.4
12	Substrate: Steel	6.4	3.7	6.6	14.1
13	Substrate: Al	5.8	12.7	19.5	26.2

Table 4.4. Specific wear of tested coatings

Sample	Coating designation	Load, N			
		2.5	5	7.5	10
		Specific wear, mg/Nm			
1	602P Substrate: Steel	1.3×10^{-2}	1.1×10^{-2}	1.0×10^{-2}	1.1×10^{-2}
2	602P: PHS* Substrate: Steel	0.9×10^{-2}	0.7×10^{-2}	0.8×10^{-2}	0.8×10^{-2}
3	80M60 Substrate: Steel	3.3×10^{-2}	2.5×10^{-2}	2.7×10^{-2}	2.8×10^{-2}
4	80M60: PHS* Substrate: Steel	1.5×10^{-2}	1.0×10^{-2}	1.4×10^{-2}	1.4×10^{-2}
5	80M60: PHS* Substrate: Al-Cu	6.4×10^{-2}	3.3×10^{-2}	2.8×10^{-2}	2.3×10^{-2}
6	6P50W Substrate: Steel	0.8×10^{-2}	0.8×10^{-2}	0.8×10^{-2}	0.7×10^{-2}
7	6P50W: PHS* Substrate: Steel	0.7×10^{-2}	0.5×10^{-2}	0.4×10^{-2}	0.4×10^{-2}
8	WC–12Co Substrate: Steel	0.5×10^{-2}	0.4×10^{-2}	0.4×10^{-2}	0.4×10^{-2}
9	602P–6P50W–(WC–12Co) Substrate: Steel	1.6×10^{-2}	1.0×10^{-2}	0.6×10^{-2}	0.5×10^{-2}
10	602P–6P50W– (WC–12Co): PHS* Substrate: Steel	2.0×10^{-2}	1.0×10^{-2}	0.6×10^{-2}	0.2×10^{-2}
11	Cr_2O_3 Substrate: Steel	21.9×10^{-2}	13.6×10^{-2}	10.1×10^{-2}	8.3×10^{-2}
12	Substrate: Steel	10.4×10^{-2}	3.0×10^{-2}	3.6×10^{-2}	5.8×10^{-2}
13	Substrate: Al	9.5×10^{-2}	10.4×10^{-2}	10.6×10^{-2}	10.7×10^{-2}

Table 4.5. Relative wear of tested coatings

Sample	Coating designation	Load, N			
		2.5	5	7.5	10
		$\varepsilon = i_{sb}/i_r$			
1	602P Substrate: Steel	8.0	2.7	12	5.3
2	602P: PHS* Substrate: Steel	11.6	4.3	15	7.3
3	80M60 Substrate: Steel	3.2	1.2	1.3	2.1
4	80M60: PHS* Substrate: Steel	6.9	3.1	2.6	4.2
5	80M60: PHS* Substrate: Al-Cu	1.5	3.2	3.8	4.7
6	6P50W Substrate: Steel	13.0	3.8	4.7	8.9
7	6P50W: PHS* Substrate: Steel	16.0	6.1	8.2	15.7
8	WC–12Co Substrate: Steel	21.0	7.3	8.2	15.7
9	602P–6P50W–(WC–12Co) Substrate: Steel	6.5	3.1	6.0	12.9
10	602P–6P50W– (WC–12Co): PHS* Substrate: Steel	5.3	2.2	6.0	24.0
11	Cr_2O_3 Substrate: Steel	0.5	0.2	0.3	0.7
12	Substrate: Steel	1	1	1	1
13	Substrate: Al	1	1	1	1

Table 4.6. Influence of the thermal treatment of the substrate on the specific wear

Sample	Coating designation	Load, N			
		2.5	5	7.5	10
		$\varepsilon_{ij} = i_r^{PHS}/i_r$			
1	602P Substrate: Steel	1.5	1.6	1.3	1.4
2	602P: PHS* Substrate: Steel				
3	80M60 Substrate: Steel	2.2	2.6	2.0	2.0
4	80M60: PHS* Substrate: Steel				
5	80M60: PHS* Substrate: Al-Cu	-	-	-	--
6	6P50W Substrate: Steel	1.2	1.6	1.7	1.8
7	6P50W: PHS* Substrate: Steel				
8	WC–12Co Substrate: Steel	-	-	-	-
9	602P–6P50W–(WC–12Co) Substrate: Steel				
10	602P–6P50W– (WC–12Co): PHS* Substrate: Steel	0.8	0.7	1.0	1.9
11	Cr$_2$O$_3$ Substrate: Steel	-	-	-	-
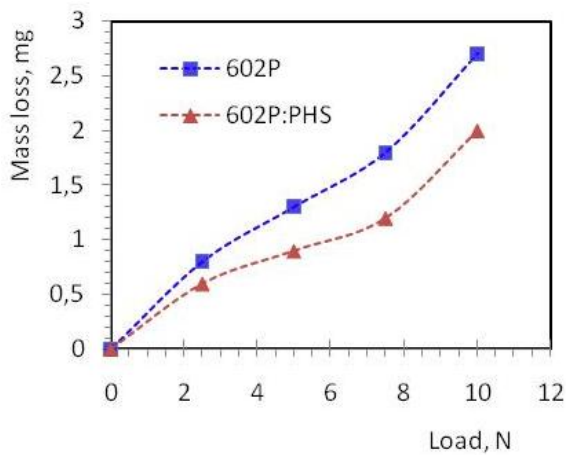
Fig. 4.2. Mass loss vs. load for coatings 602P and 602P: PHS*
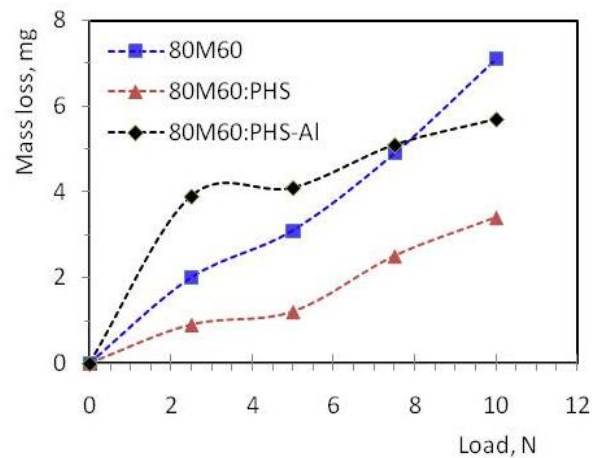
Fig. 4.3. Mass loss vs. load for coatings 80M60 (sub.Steel): PHS* and 80M60(su. Al): PHS*
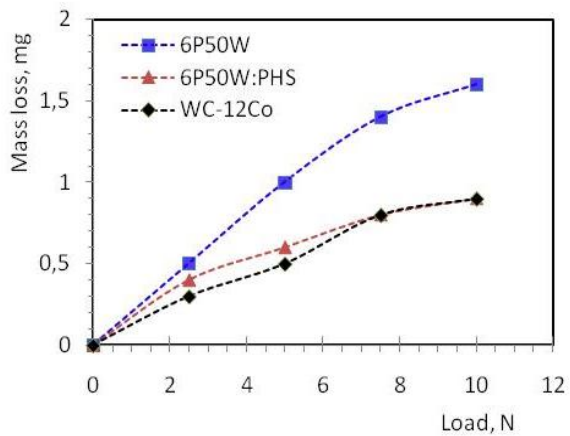
Fig. 4.4. Mass loss vs. load for coatings 6P50W and 6P50W: PHS* and WC-12Co
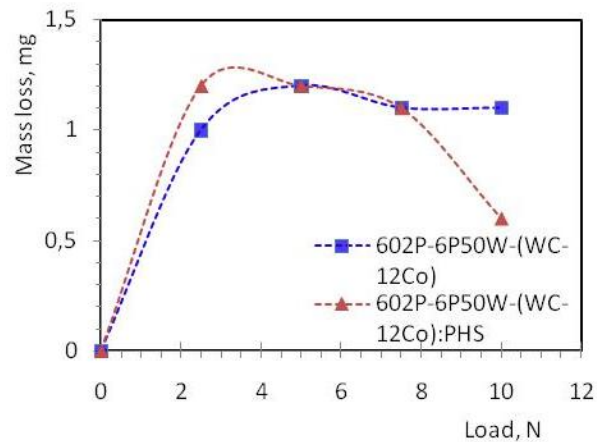
Fig. 4.5. Mass loss vs. load for coatings 602P-6P50W-WC-12Co and 602P-6P50W- (WC-12Co):PHS*

Wear of High-Technology Coatings, Deposited by High-Velocity Oxygen Flame (HVOF)
Abrasive Wear of HVOF Coatings with Metal, Ceramic and Metal-Ceramic Composites and Their
Mixtures
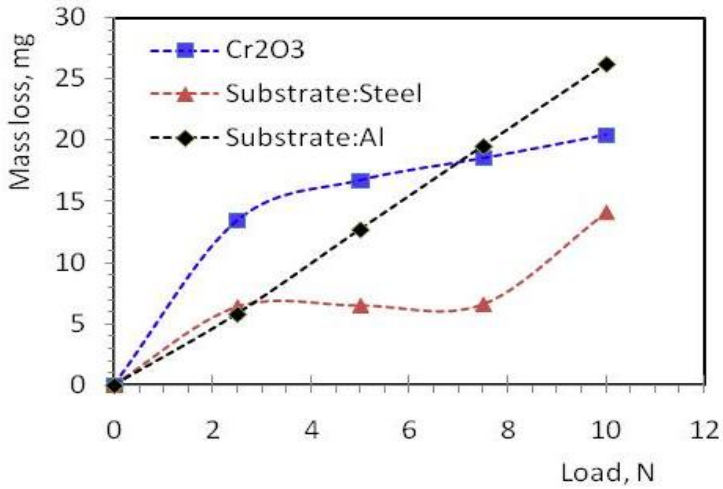
Fig. 4.6. Mass loss vs. load for coatings Cr2O3, substrate Steel and Substrate Al
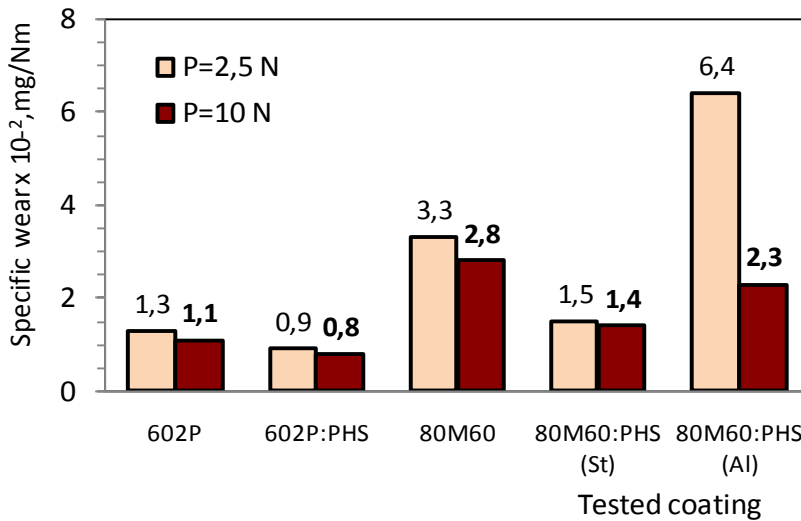
Fig. 4.7. Comparative specific wear values for coatings 602P, 602P:PHS*, 80M60 (Steel), 80M60(sub.Steel):PHS*, 80M60(sub.Al):PHS*

Wear of High-Technology Coatings, Deposited by High-Velocity Oxygen Flame (HVOF)
Abrasive Wear of HVOF Coatings with Metal, Ceramic and Metal-Ceramic Composites and Their
Mixtures
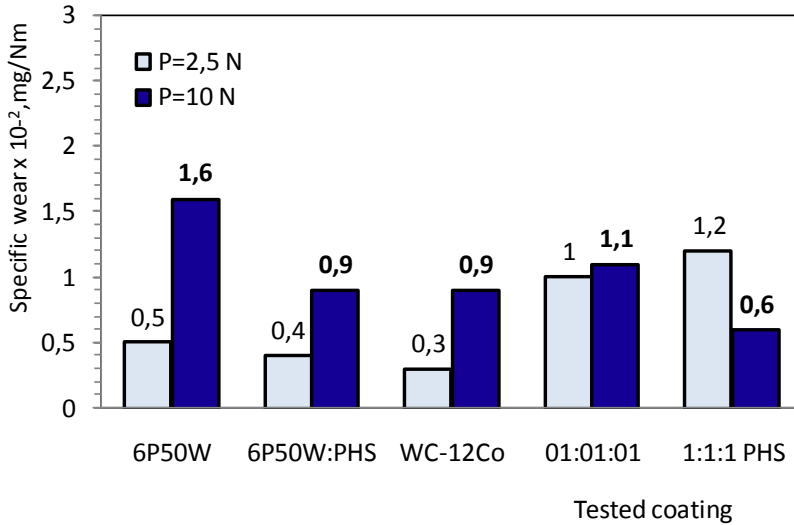
Fig. 4.8. Comparative specific wear values for coatings 6P50W, 6P50W:PHS*, C-12Co, 1:1:1, 1:1:1:PHS*
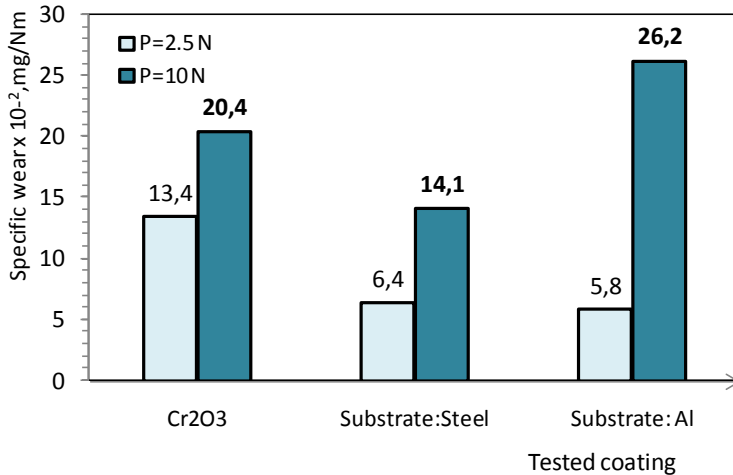
Fig. 4.9. Comparative specific wear values for coating Cr_2O_3 and substrate Steel and substrate Al

Among all the studied samples with and without preliminary heat treatment of the substrate, the lowest wear degree is shown by the sample with a coating of WC-12Co at all the values for the normal loading. Similar values of the wear are

Wear of High-Technology Coatings, Deposited by High-Velocity Oxygen Flame (HVOF)
Abrasive Wear of HVOF Coatings with Metal, Ceramic and Metal-Ceramic Composites and Their
*Mixtures*

shown by the coating based on tungsten 6P50W: PHS with thermal treatment of the substrate. The high abrasive wear resistance of the coating WC-12Co is not surprising. It is due to the combination of very hard carbides and hard, but still having some plasticity matrix of cobalt Co. The good wetting of the tungsten carbides in the cobalt matrix contributes to the high cohesion strength of the metal-ceramics WC-Co. In other words, in the bulk of the coating, an internal contact network is formed having high strength characteristics, which ensure high resistance of the coating against destruction caused by the scratching effect of the abrasive particles. The systematic investigations of some other authors [13-15] using WC-Co coatings having various percentages of the content of cobalt – 12, 17 and 25% show that the lowest wear is manifested by the coatings WC-12Co, i.e. containing 12% of cobalt.

A prerequisite for the high abrasive wear resistance of the coatings WC-12Co, deposited by the HVOF technology, is their low porosity – 1.3%, which is the lowest among the porosities of all the studied coatings. The low porosity, i.e. the high density of the coating is connected with the liberation of particles and gases from the substrate during the process of deposition of the coating. The liberation of the carbon can be induced on one side due to its oxidation to carbon dioxide ($2C + CO_2 \rightarrow 2CO$), while on the other side it is the result of diffusion processes.

In comparison to the other types of technologies using a thermal spray, the HVOF technology is one of the best methods for the preparation of metal-ceramic WC-Co coatings. The short time interval of staying of the particles inside the flame in the specific case of this technology using supersonic speed and comparatively low temperatures leads to a lower degree of degradation of the compound WC. This fact gives the reason to assume, that the degradation of the compound WC during the process of deposition of the coating is reduced to a minimum, which ensures its high abrasive wear resistance.

The preliminary heat treatment of the substrate leads to a decrease in the specific wear degree of all the studied coatings, but a different degree. The influence of the heat treatment is the strongest for the coating 80M60, however, this influence depends on the magnitude of the normal loading. In cases of loadings from P=2.5N up to P=5N the degree of influence is strongest and the specific wear degree drops down from 2.2 to 2.6 times. Upon loading pressure P=7.5N up to P=10N the specific wear degree decreases 2 times. For the coatings, deposited using three powder composites, at loading up to 7.5 N the preliminary thermal treatment does not influence positively – the specific wear grows up. At higher loading, however, the specific wear is diminished up to 2 times.

4.3 CONCLUSION

A comparative study of 11 types of coatings has been carried out, which were deposited by the High-Velocity Oxy-Fuel (HVOF) technology under conditions of dry friction along the surface having attached abrasive particles. The coatings

have been deposited using metal, metal-ceramic and ceramic powder composites based on nickel - 602P, 80M60; based on tungsten - 6P50W, WC-12Co, chromium trioxide - Cr_2O_3 and a combination of the three composites on nickel tungsten basis at ratio 1:1:1 - 602P–6P50W– (WC–12Co).

Results have been obtained about the influence of the normal loading, preliminary thermal treatment of the substrate and type of the substrate upon the characteristics of the abrasive wear.

It has been established, that the dependence of the abrasive wear on the magnitude of the normal loading gas has a different character for the different coatings. At small values of the loading, this dependence is straightly proportional, while at high values of the loading it passes over to non-linear dependence.

The degree of loading depends on the nature and the preliminary thermal treatment of the substrate. In cases of coatings, deposited on steel substrate the wear is lower than that for coatings, deposited on aluminium. The preliminary thermal treatment of the substrate leads to a decrease in the wear degree for all the coatings, but a different extent.

The lowest wear degree among all the studied coatings is shown by the coating, deposited using powder composite WC-12Co on a steel substrate. The coating WC-12Co is a combination of very hard carbides and a plastic matrix of cobalt. The high abrasive wear resistance of the coating is due to the high degree of wetting of the tungsten carbides in the cobalt matrix, as a result of which inside the bulk phase of the coating an internal contact network is formed having high cohesion strength of the metal-ceramics WC-Co. The homogeneity of this network is of exceptional importance for the high mechanical and tribological characteristics of the WC-12Co coating. The preliminary heat treatment of the steel substrate leads to an increase in the abrasive wear resistance of the coating 6P50W: PHS, which comes near to the wear resistance of the WC-12Co coating.

The greatest abrasive wear among all the studied coatings is manifested by the coating of Cr_2O_3, which is greater than the wear of steel and aluminium substrate under normal loadings up to 7.5 N. At high loading – 10N, the wear degree of this coating assumes values between the values of the two substrates. Based on this result one can conclude, that the coating of Cr_2O_3, deposited by the HVOF technology, is not suitable for surfaces and details, operating under conditions of abrasion.

_____

Vibro-Abrasive Wearing of HVOF Coatings

5.1 MATERIALS AND EXPERIMENTAL DETAILS

Four types of coatings have been studied, obtained by the HVOF process, which is deposited on the carrier (substrate) of steel having a chemical composition, represented in Table 5.1 [45].

Two types of powder composites with commercial notation 602P and WC-12Co have been used to prepare the coatings. The chemical composition and the physical and mechanical properties are listed in Table 5.1 and Table 5.2.

Table 5.1. Powder composite for the coating 602P

Chemical composition, wt.%	Temperature of melting, ^{o}C	Moos Hardness
Cr: 13.2	1907	8.5
Si: 3.98	1414	7
B: 2.79	2076	9.5
Fe: 4.6	1538	4
Co: 0.03	1495	5
C: 0.63	3550	-
Ni: balance	1455	4

The temperature on the surface during the deposition of the coating at nozzle distance 120 mm: 263° C; Adhesion strength of the coating: 42 - 43 MPa

Table 5.2. Powder composite for the coating WC-12Co

Chemical composition, wt.%	Temperature of melting, ^{o}C	Moos Hardness
Co: 12	1495	5
C: 2.4	3550	-
Fe < 0.1	1538	4
Ni < 0.1	1455	4
W: balance	3422	7.5

The temperature on the surface during the deposition of the coating at nozzle distance 120 mm: 95°C; Adhesion strength of the coating: 63 – 69 MPa

The particles have an average size of $45 \pm 2,5$ μm and they have been prepared by an agglomeration process involving a stage of sintering. The coatings have been deposited using the system model MICROJET+Hybrid GMA.

The following coatings have been deposited: № 1 – with powder composite 602P on the substrate without preliminary heat treatment (cold process); № 2 – with powder composite 602P on a substrate with preliminary heat treatment up to temperature 650° C in a chamber having a duration of 5 minutes; № 3 – with powder composite WC-12Co without preliminary heat treatment of the substrate; № 4 – with powder composite, obtained by mixing of the two composites - 602P and WC-12Co at a ratio 1:1, without preliminary heat treatment of the substrate. All the coatings after their mechanical treatment have an identical thickness of 680 μm.

Each sample with the deposited coating is studied at various vibration rates within the range from 3.03 mm/s up to 21.08 mm/s under identical conditions of friction. The samples have a cylindrical form of diameter d=9 mm, a height of 30 mm, and identical roughness of the contact surface Ra=0.425 μm.

The testing has been carried out at constant parameters of friction: loading 3,92 N (0.4kg), nominal contact area $A_a=0,64.10^{-4}m^2$, nominal contact pressure $p_a=6,12N/cm^2$, sliding velocity v=0.31 m/s and friction path lenth S= 49,01 m.

Results have been obtained for the mass wearing, the relative wear resistance and vibration factor of the wearing of the studied coatings are different values of the vibration rate.

5.2 EXPERIMENTAL RESULTS

Table 5.3 represents the results for the mass wearing of the four types of coatings and that of the base surface as a result of abrasive friction without any vibration and at five values of the vibration rate within the range from 3.03 mm/s up to 21.08 mm/s.

Table 5.4 represents the range of changes and the average value of the hardness of the coatings before the wearing process, after abrasive friction without vibration, and after vibrational friction at a rate of vibration of 21.08 mm/s.

Figs. 5.1, 5.2, 5.3 and 5.4 represent graphically the dependences of mass wear versus the magnitude of the vibration rate for all the studied coatings and the substrate.

Fig. 5.5 represents the diagram of the relative wear resistance of the coatings for cases without vibration for both values of the vibration velocity.

Fig. 5.6 represents the diagram of the vibrational factor upon abrasion for all the coatings, while 5.7. – the interconnection between the relative wear resistance and the hardness of the coatings before friction, friction without and with vibration, and the hardness of the coatings, measured before the process of friction.

Table 5.3. Abrasive wear of the studied coatings

№	Coating	Vibration rate, mm/s	0	3.03	6.04	9.08	16.88	21.08
1	602 P	wear, mg	7.2	5.8	4.9	7.2	9.6	11.5
2	602P+HT 650°C	wear, mg	4.6	3.5	2.5	4.8	6.2	7.4
3	WC-12Co	wear, mg	0.5	0.4	0.4	0.5	0.6	0.6
4	602P+WC-12Co 1:1	wear, mg	5.5	4.1	3.2	5.6	7.3	8.2
5	coated material	wear, mg	20.6	16.5	12.4	18.5	20.6	25.4

Table 5.4. Range of changing an average value of the hardness of the coatings before and after the abrasive friction without and with vibration

№	Coating	Hardness before friction, HV	Hardness, HV w=0 mm/s	Hardness, HV w=21.08 mm/s
1	602P	168÷196 182	165÷193 179	141÷163 152
2	602P+HT650^{o}C	310÷328 319	301÷325 313	290÷309 300
3	WC-12Co	405÷441 423	398÷432 415	381÷409 395
4	602P+WC-12Co 1:1	480÷508 494	460÷498 479	449÷490 470
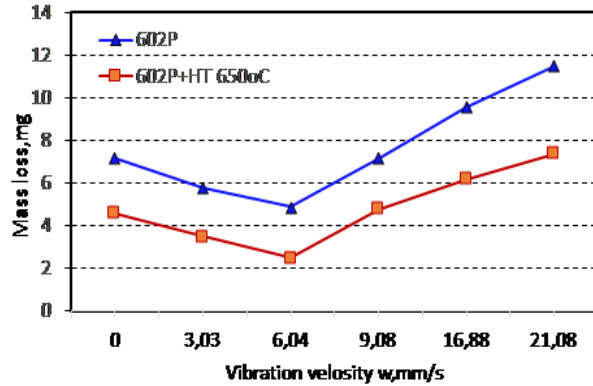
Fig. 5.1. Change in the wear versus vibration velocity for coatings 602P without and with preliminary heating of the substrate
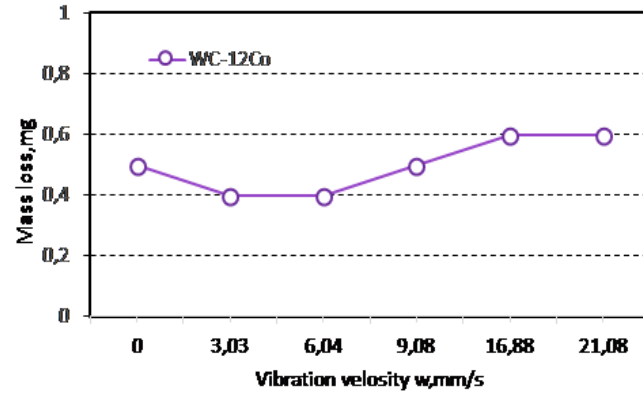
Fig. 5.2. Change in the wear versus vibration velocity for coating WC-12Co without preliminary heating of the substrate
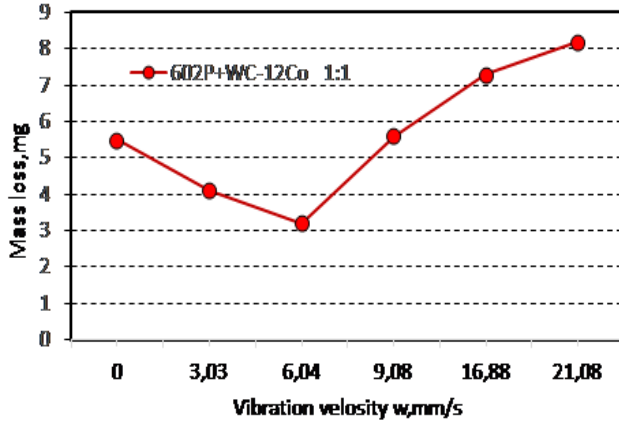
Fig. 5.3. Change in the wear versus vibration velocity for coating 602P+WC-12Co 1:1 without preliminary heating of the substrate
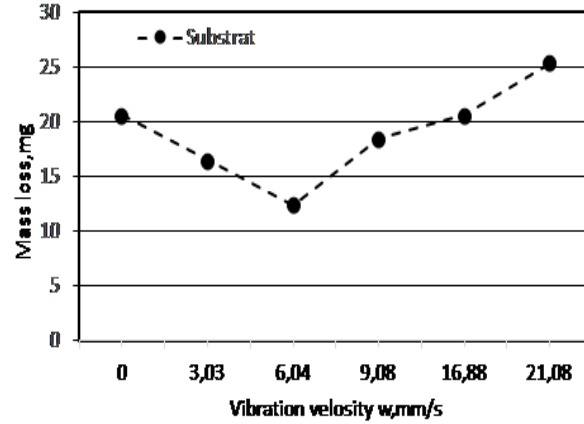
Fig. 5.4. Change in the wear versus vibration velocity of the substrate
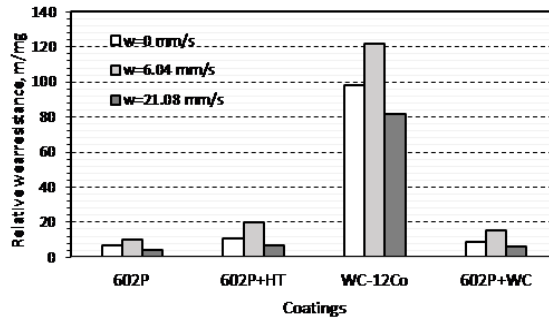
Fig. 5.5. Diagram of the relative wear resistance of the coatings with and without vibrational loading
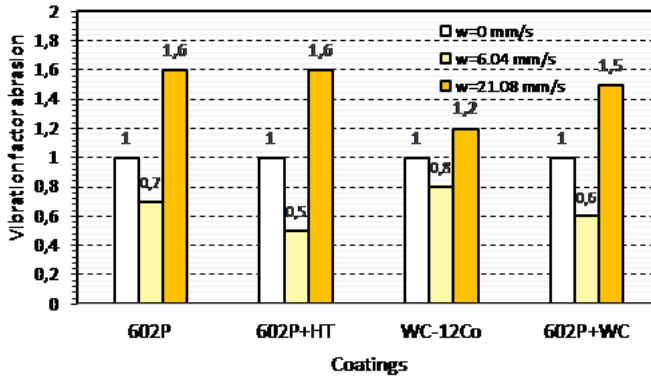
Fig. 5.6. Diagram of the vibrational factor of the abrasion
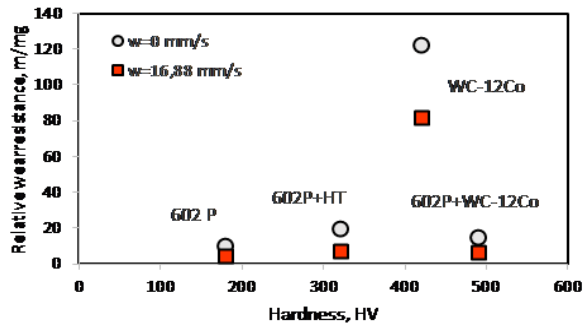
Fig. 5.7. Dependence of the relative wear resistance of the hardness of the coatings during friction without and with vibration velocity w=16,88mm/s
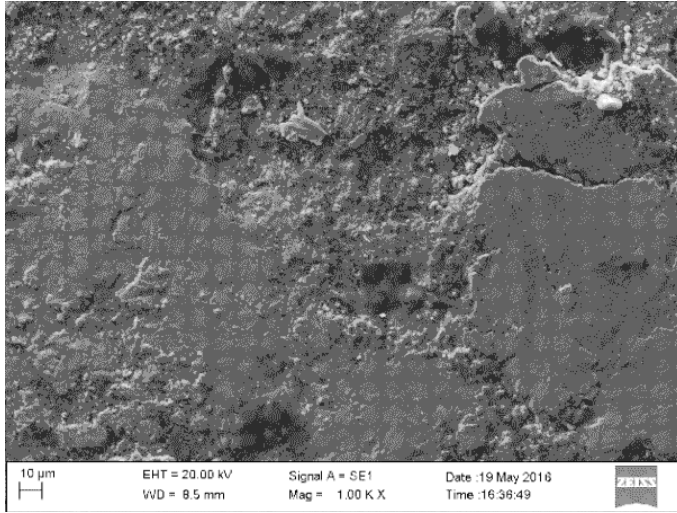
Fig. 5.8. Microstructure of the coating 602P on steel
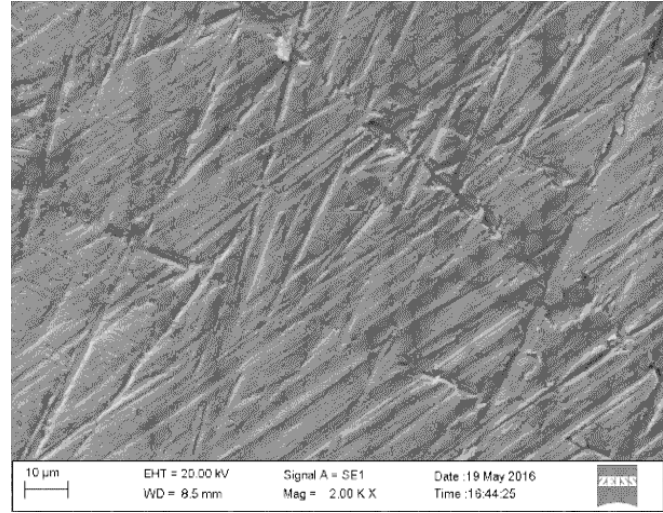
Fig. 5.9. Microstructure of the coating 602P+HT 650°C on steel
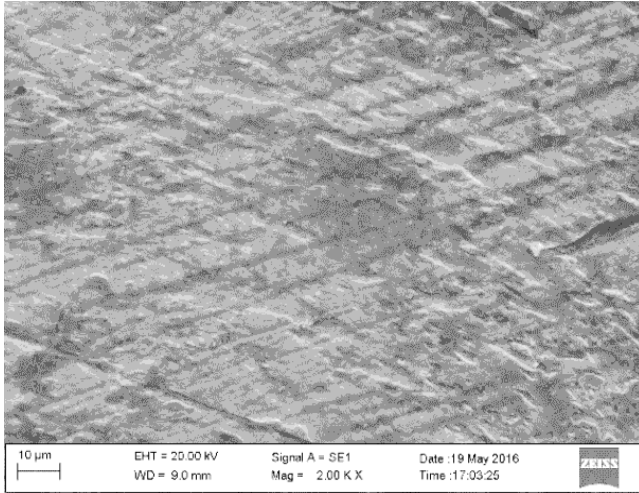
Fig. 5.10. Microstructure of the coating WC-12Co on steel
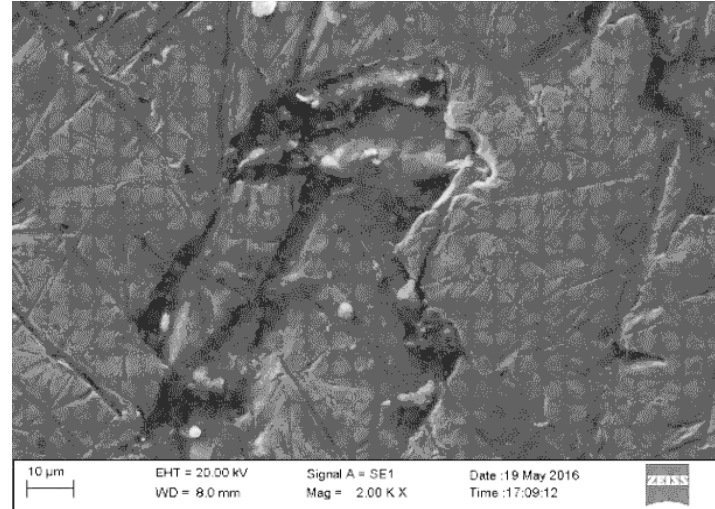
Fig. 5.11. Microstructure of the coating 602P+WC-12Co on steel

The Figs. 5.8, 5.9, 5.10 and 5.11 represent the microstructure of the coatings after abrasive friction at a vibrational velocity of 21.08 mm/s.

5.3 CONCLUSION

The basic interpretations and conclusions from this investigation are the following:

- The magnitude of the vibration velocity influences the magnitude and the character of the changes in the mass wear of the coatings. Up to a certain value of the vibration velocity, the wearing degree diminishes, and thereafter it grows up and at velocity w>16,88 mm/s the wearing degree reaches greater values than that in the absence of vibrations.
- The dependence between the wearing degree and the vibration velocity has a non-linear character with a minimum, which for all the samples is observed at a vibration velocity of 6,04 mm/s.
- The lowest wear degree among all the studied samples for the entire range of the vibration velocity is displayed by the coating WC-12Co, which is an order of magnitude lower than that of the rest of the coatings. The dependence of the wear on the vibration velocity also has a minimum at w=6,04 mm/s, but at high velocities w>16,88 mm/s the wear degree has a constant value, which is near to its value under conditions without vibration.
- The preliminary heating of the substrate up to temperature 650°C for 5 minutes during deposition of the coating 602P leads to a decrease in the wear degree with 55% for the entire range of variation of the vibration velocity. Upon changing the vibration velocity the relative wear resistance is changing within small limits in comparison to the rest of the coatings and it is near to that in the case without vibration.
- The wear degree and the relative wear resistance of the combined coating 602P+WC-12Co (1:1) do not differ substantially from those of the coatings 602P and 602P+HT650^{o}C.
- The highest hardness among all the studied coatings is displayed by the coating 602P+WC-12Co (1:1) before friction, during friction without, and with vibration velocity 21,08 mm/s. However, this coating does not have the highest relative wear resistance. This confirms the fact, that in the cases of composite coatings and materials there is not always a correlation between the hardness and the wear resistance.
- Analyzing the microstructure of the coatings after abrasive wearing at a vibration velocity of 21.08 mm/s, it is seen that for the coating WC-12Co the basic mechanism of wearing is the mechanical scratching by the abrasive particles during relative movement. It is seen in Fig.5.10, that the worn-out coating has the homogeneous texture of the type of flat plain network of scratches, obtained during the planar movement of the sample. The high wear resistance of the coating is owing to strictly differentiated functions, which are fulfilled by the components in its structure: the particles WC ensure great resistance of the coating against the cutting tangential action of the abrasive particles and the fatigue vibration strength of the coating; The cobalt (Co) fulfills contact role in the structure of the

coating – it builds internal boundary network between the particles of WC and it guarantees the completeness of the coating. The wear resistance of the composite coatings to a great extent is determined by the thickness and the physical-mechanical properties of this network. The internal contact network in many cases determines the damping properties of the coating in cases of impulse and periodical actions.

- In the cases of coatings 602P and 602P+WC-12Co (1:1), the basic mechanism of wearing is the fatigue destruction of the surface, as a consequence of the periodical loading with high vibration velocities (Figs.5.8 and 5.9).

In conclusion, we can summarize, that during the exploitation of details and machines under extreme conditions of vibrational loading and abrasive friction the most appropriate coatings, deposited by the HVOF process, are the coatings WC-12Co. The preliminary heating of the substrate in the case of deposition of the coating 602P leads to enhancement of the wear resistabywith 50%.

Influence of the Concentration of Chromium upon the Abrasive Wearing of the HVOF Coatings

6.1 MATERIALS

Samples have been prepared of 10 types of HVOF-coatings, combined in five groups having chromium concentration in the powder mixture - 9,9%, 13,2%, 14%, 16%, 20%, and approximately identical composition of the remaining chemical elements. Two types of coatings have been obtained from each group of coatings with definite chromium concentration – without thermal treatment of the substrate (cold HVOF process) and with preliminary heating of the substrate in the thermal chamber at temperature 650^oC in 60 minutes. The coatings having thermal treatment of the substrate are denoted by PHS. The group of coatings №9 and №10 contain in their composition 20% Cr and 80% Ni without including other elements, present in the rest of the coatings [46].

Table 6.1 represents the designation, description, chemical composition, hardness and thickness of the studied coatings.

6.2 EXPERIMENTAL RESULTS

The abrasive wearing of the coatings has been studied under conditions of dry friction during sliding along the surface with firmly attached abrasive particles.

Results have been obtained on the mass wearing degree, the reduced intensiveness, the absolute and the relative wear resistance for all the studied coatings, described in Table 6.1.

The results are represented in Tables 6.2, 6.3, and 6.4.

By the data in Table 6.2 kinetic curves have been plotted for the mass wearing of all the coatings without and with thermal treatment of the substrate, represented in Figs. 6.1, 6.2, 6.3, 6.4, and 6.5. Each graphics contains the regression equations for the wearing versus the friction path length $m=m(L)$ and the value of the intensity of wearing in the case of friction path length $L=80\ m$. It is seen, that in the case of dry abrasive friction the dependence of the mass wearing on the sliding distance has a linear character for coatings without and with thermal treatment of the substrate.

Table 6.1. Description, chemical composition, hardness, and thickness of the tested coatings

Sample	Coating designation	Description	Chemical composition, wt. %	Hard ness HRC	Thickness µm
1	72M40	Coatings without heat treatment of the substrate	**Cr: 9,9**; Si:3.1; B:1.7; Fe:3.2; C: 0.35; Mo: 3;	55-56 HRC	410-415
2	72M40:PHS	Coatings with heat treatment of the substrate	Cu:3; **Ni Balance**	58-59 HRC	400-412
3	602P	Coatings without heat treatment of the substrate	**Cr: 13.2**; Si: 3.98; B: 2.79; Fe: 4.6; Co: 0.03;	56-57 HRC	395-400
4	602P:PHS	Coatings with heat treatment of the substrate	C: 0.63; **Ni: Balance**	59-60 HRC	408-414
5	80M60	Coatings without heat treatment of the substrate	**Cr: 14**; Si:4.2; B:2,9; Fe:4,6; C:0.6; Mo:2,5;	57-58 HRC	395-406
6	80M60:PHS	Coatings with heat treatment of the substrate	Cu:2,4; **Ni: Balance**	59-60 HRC	400-405
7	1355	Coatings without heat treatment of the substrate	**Cr:16;** Si:4; B:3.4; Fe:2.7; C:0.6; Mo:3;	58-59 HRC	394-405
8	1355:PHS	Coatings with heat treatment of the substrate	Cu:3; **Ni: Balance**	61-62 HRC	404-410
9	HN40	Coatings without heat treatment of the substrate	**Cr**: 20; **Ni**: 80	54-55 HRC	400-408
10	HN40:PHS	Coatings with heat treatment of the substrate		57-60 HRC	393-403

Table 6.2. Abrasive wear of tested coatings

Sample	Coating designation	Number of cycles (N)			
		100	200	300	400
		Sliding distance, m			
		20	40	60	80
		Mass wear, mg			
1	72M40	4.7	8.5	12.7	15.3
2	72M40:PHS	3.2	5.8	11.2	12.6
3	602P	4.4	7.9	10.6	12.3
4	602P:PHS	3.5	7.1	9.8	10.4
5	80M60	4.0	6.0	7.6	10.5
6	80M60:PHS	3.1	4.2	5.8	7.6
7	1355	1.5	2.2	2.8	3.3
8	1355:PHS	0.9	1.2	1.6	1.8
9	HN40	2.9	5.6	7.6	10.4
10	HN40:PHS	1.8	4.1	6.3	9.1

Table 6.3. Wear intensity of the tested coatings

Sample	Coating designation	Number of cycles (N)			
		100 Sliding distance, m 20 Wear intensity, mg/N.m	200 40	300 60	400 80
1	72M40	5.22×10^{-2}	4.71×10^{-2}	4.71×10^{-2}	4.24×10^{-2}
2	72M40:PHS	3.56×10^{-2}	3.22×10^{-2}	4.15×10^{-2}	3.51×10^{-2}
3	602P	4.89×10^{-2}	4.4×10^{-2}	3.93×10^{-2}	3.42×10^{-2}
4	602P:PHS	3.89×10^{-2}	3.96×10^{-2}	3.62×10^{-2}	2.89×10^{-2}
5	80M60	4.44×10^{-2}	3.33×10^{-2}	2.82×10^{-2}	2.91×10^{-2}
6	80M60:PHS	3.44×10^{-2}	2.33×10^{-2}	2.16×10^{-2}	2.11×10^{-2}
7	1355	1.67×10^{-2}	1.22×10^{-2}	1.04×10^{-2}	0.91×10^{-2}
8	1355:PHS	1.0×10^{-2}	0.67×10^{-2}	0.58×10^{-2}	0.49×10^{-2}
9	HN40	3.22×10^{-2}	3.11×10^{-2}	2.82×10^{-2}	2.89×10^{-2}
10	HN40:PHS	2.0×10^{-2}	2.22×10^{-2}	2.33×10^{-2}	2.51×10^{-2}

Table 6.4. Wear resistance of the tested coatings

Sample	Coating designation	Number of cycles (N)			
		100	200	300	400
		Sliding distance, m			
		20	40	60	80
		Wear resistance, m.N/mg			
1	72M40	0.19×10^2	0.21×10^2	0.21×10^2	0.24×10^2
2	72M40:PHS	0.28×10^2	0.31×10^2	0.24×10^2	0.28×10^2
3	602P	0.20×10^2	0.23×10^2	0.25×10^2	0.29×10^2
4	602P:PHS	0.26×10^2	0.25×10^2	0.28×10^2	0.35×10^2
5	80M60	0.23×10^2	0.30×10^2	0.35×10^2	0.34×10^2
6	80M60:PHS	0.29×10^2	0.42×10^2	0.46×10^2	0.47×10^2
7	1355	0.60×10^2	0.82×10^2	0.96×10^2	1.10×10^2
8	1355:PHS	1.00×10^2	1.49×10^2	1.72×10^2	2.04×10^2
9	HN40	0.31×10^2	0.32×10^2	0.35×10^2	0.35×10^2
10	HN40:PHS	0.50×10^2	0.45×10^2	0.43×10^2	0.40×10^2

The second observation from the analysis of these curves refers to the fact, that the wearing of all the coatings with thermal treatment of the substrate is lower than the wear of the coatings without thermal treatment of the substrate.
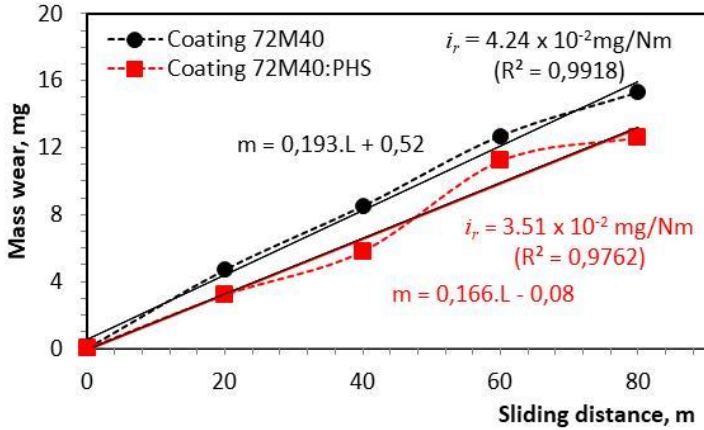
Fig. 6.1. Mass wear vs. sliding distance for 72M40 and 72M40: PHS coatings
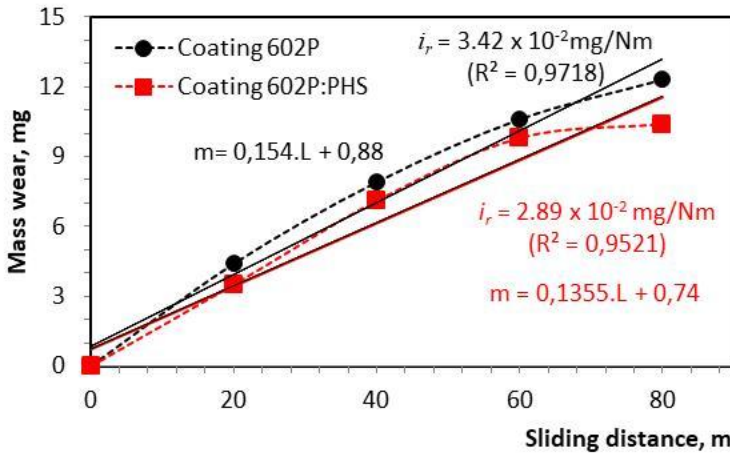
Fig. 6.2. Mass wear vs. sliding distance for 602P and 602P: PHS coatings
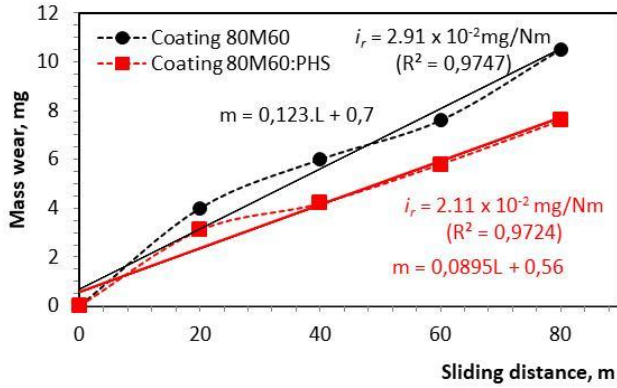
Fig. 6.3. Mass wear vs. sliding distance for 80M60 and 80M60: PHS coatings
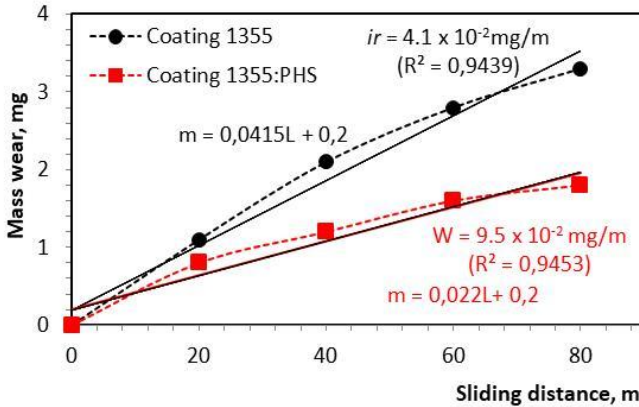
Fig. 6.4. Mass wear vs. sliding distance for 1355 and 1355: PHS coatings

Fig. 6.6 represents graphically the dependence of the intensity of wearing versus the chromium concentration for the coatings without thermal treatment of the substrate and for the coatings with thermal treatment of the substrate for the same friction path length $L = 80\ m$.

The curves have a non-linear character with a clearly expressed minimum of the intensity of wearing at 16% concentration of Cr for the coatings without and with thermal treatment. In the first section, in which the concentration of chromium is changing within the range from 9.9% up to 16% with the increase in the concentration of chromium the wearing intensity decreases until reaching a minimum value at the concentration of chromium of 16% respectively: for

coatings without thermal treatment of the substrate i_r = 0.91 x 10^{-2} mg/Nm and

for coatings with thermal treatment of the substrate - i_r = 0.49 x 10^{-2} mg/Nm. In the second section at a higher concentration of chromium 20% (the coatings HN40 and HN40: PHS), the wearing intensity is sharply increased. Despite the increased content of chromium, the increase in the wearing is due to the absence of the elements B, Si, Cu, and others, which are contained in the other coatings. These elements in the process of contact interaction of the flame jet with the substrate at the high temperature are forming inter-metallic compounds of chromium, which lead to a diminishing of the intensity of wearing.
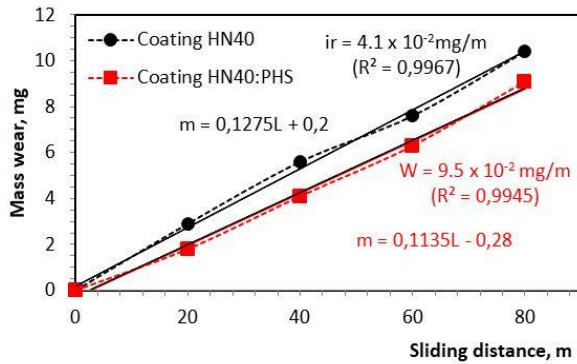
Fig. 6.5. Mass wear vs. sliding distance for HN40 and HN40: PHS coatings

The curve of the dependence of the wear resistance on the concentration of chromium in the coatings without thermal treatment and with thermal treatment of the substrate is reciprocal to the curve of the intensity of wearing (Fig. 6.7).
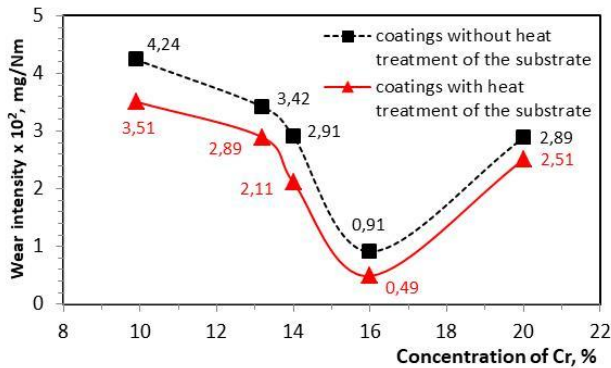
**Fig. 6.6. Dependence of wear intensity on the concentration of chromium
in the tested HVOF coatings**
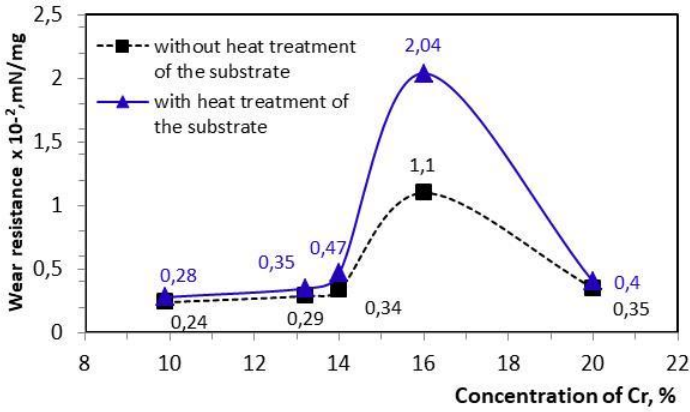
Fig. 6.7. Dependence of wear resistance on the concentration of chromium in the tested HVOF coatings
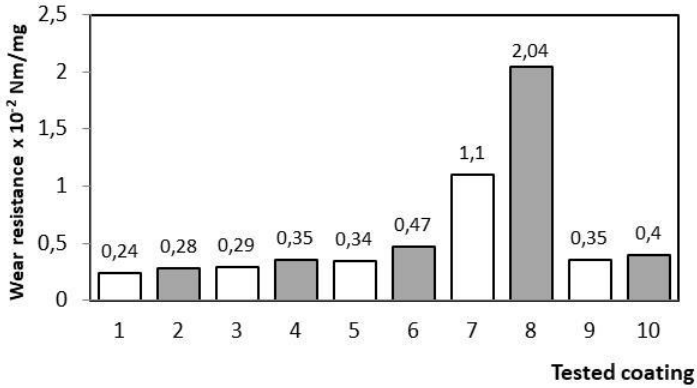
Fig. 6.8. Diagram of the abrasive wear resistance of the tested coatings

Fig. 6.8 illustrates the diagram of the wear resistance of all the tested coatings, where it is seen, that the lowest wear resistance is displayed by coatings having the smallest concentration of chromium without heat treatment of the substrate - $I_r = 0.24 \times 10^2$ Nm/mg, while the highest wear resistance is shown by the coatings having 16% chromium content after heat treatment of the substrate - $I_r = 2.04 \times 10^2$ Nm/mg.

Table 6.5 represents the results of the relative wear resistance, calculated using the formula (4). The last two columns reflect the results respectively for the influence of the heat treatment of the substrate and the influence of chromium concentration in the powder composites. These results are represented in the form of diagrams in Figs. 6.9 and 6.10.

Table 6.5. The relative abrasive wear resistance of the tested coatings

Sample	Coating designation	Wear resistance, mN/mg in the sliding distance of 80 m	Relative abrasive wear resistance	
			Influence of heat treatment on the substrate	Influence of the concentration of Cr, %
1	72M40	0.24×10^2	$R_{1,1} = 1$	$R_{1,1} = 1$
2	72M40:PHS	0.28×10^2	$R_{2,1} = 1.17$	$R_{2,2} = 1$
3	602P	0.29×10^2	$R_{3,3} = 1$	$R_{3,1} = 1.21$
4	602P:PHS	0.35×10^2	$R_{4,3} = 1.21$	$R_{4,2} = 1.25$
5	80M60	0.34×10^2	$R_{5,5} = 1$	$R_{5,1} = 1.42$
6	80M60:PHS	0.47×10^2	$R_{6,5} = 1.38$	$R_{6,2} = 1.68$
7	1355	1.10×10^2	$R_{7,7} = 1$	$R_{7,1} = 4.58$
8	1355:PHS	2.04×10^2	$R_{8,7} = 1.84$	$R_{8,2} = 7.29$
9	HN40	0.35×10^2	$R_{9,9} = 1$	$R_{9,1} = 1.46$
10	HN40:PHS	0.40×10^2	$R_{10,9} = 1.14$	$R_{10.2} = 1.67$
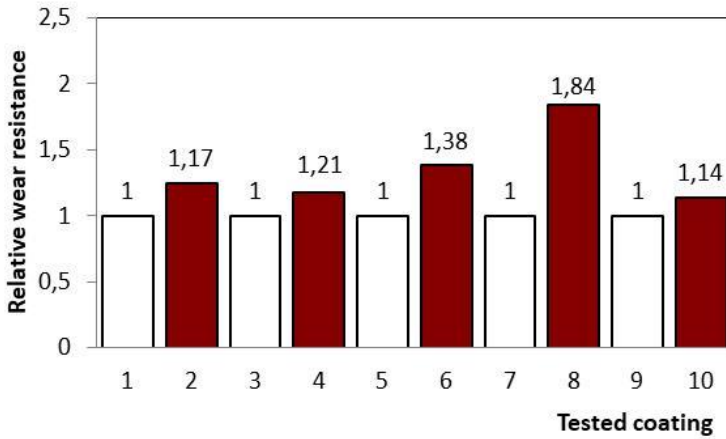
Fig. 6.9. Diagram of the influence of the heat treatment of the substrate on the wear resistance of the tested coatings

The strongest influence on the wear resistance is exerted by the heat treatment of the substrate in the case of coating 1355:PHS having a chromium concentration of 16%, where the wear resistance is 1.84 times higher than that of the same coating without heat treatment of the substrate. After it there follows the coating 80M60:PHS having a chromium concentration of 14%. For the rest of the coatings, the influence of the heat treatment is almost the same from 1,14 to 1,21.
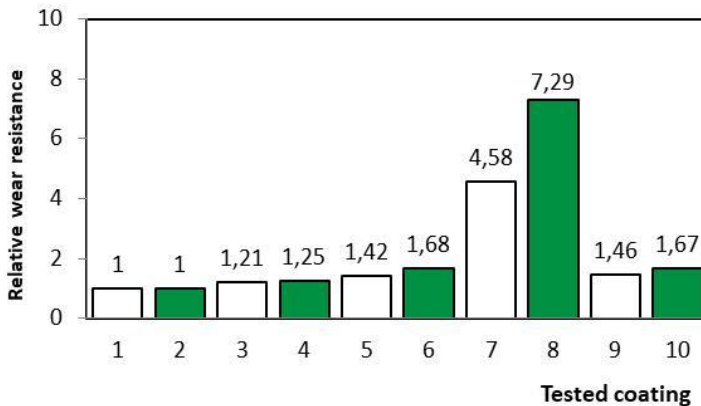
Fig. 6.10. Diagram of the influence of Cr concentration on the wear resistance of the tested coatings

The influence of the chromium concentration on the abrasive wear resistance of the coatings is greatest for the coatings 1355:PHS and 1355 (16% Cr). In the case of coating with heat treatment (the coating 1355:PHS), the wear resistance grows up 7,29 times, while for the same coating without heat treatment (the coating 1355) it is increased 4,58 times, which is an exceptional result. Another good result is the enhancement of the wear resistance of the coatings 80M60:PHS and HN40:PHS, which is increased almost to the same degree - respectively 1.68 and 1.67 times. The results on the wear resistance are correlating with the hardness of the coatings at different concentrations of Cr (Fig. 6.11).
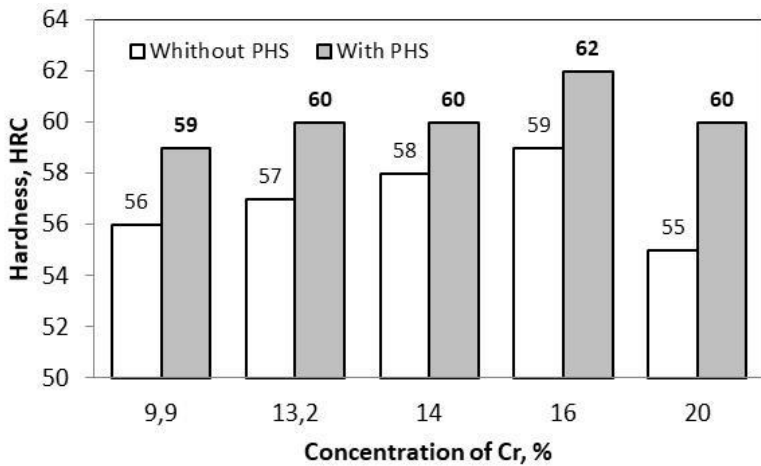
Fig. 6.11. Diagram of the influence of Cr concentration on the hardness of the tested coatings

Fig. 6.12 illustrates the diagram of the interconnection between the abrasive wear resistance and the hardness of the tested coatings.

6.3 REGRESSION MODELS

The experimental curve is considered for the dependence of the wearing intensity on the chromium concentration within the interval $9,9\% \leq w \leq 16\%$ (Fig. 6.6).

The section of the curve is not considered, because it includes the coatings №9 and №10 (HN40 and HN40:PHS) having chemical compositions differing from that of the other coatings. These coatings contain only nickel (80%) and chromium (20%), which fact does not give us any reason to analyze them in parallel with the rest of the coatings.

Experimental results about the intensity of wearing in more points of the curve in Fig. 6.6 are represented in Table 6.6.
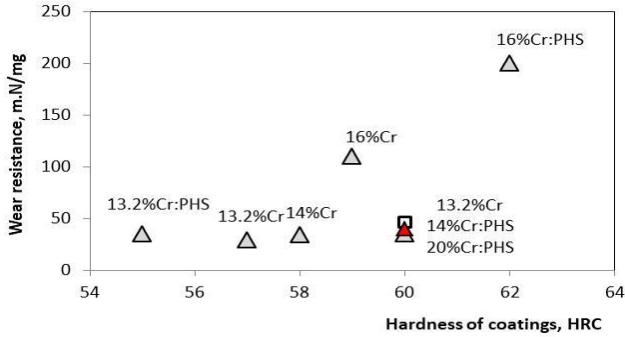
Fig. 6.12. Diagram of abrasive wear resistance and hardness of the tested coatings

Table 6.6. Wear intensity at different chromium concentrations, %

w, Concentration of Cr, (%)	9.9	11.8	13.2	14.0	15.2	16.0
i_r, the intensity of wear, mg/Nm, without heat treatment of the substrate	4.24	3.82	3.42	2.91	2.1	0.91
i_r, the intensity of wear, mg/Nm, with heat treatment of the substrate	3.51	3.35	2.89	2.11	1.35	0.49

The graphical dependence of the wear intensity on the percentage of the chromium content based on the data in Table 6.6 is shown in Fig. 6.13.
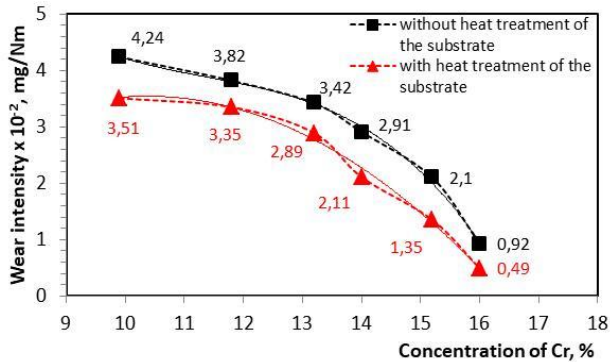
Fig. 6.13. Dependence of wear intensity on chromium concentration range from 9.9% to 16%

Based on the regression analysis analytical dependences have been obtained about the wear intensity versus the concentration of chromium, represented as polynomials of second the and third order.

For coatings without heat treatment of the substrate, the dependence acquires

the fo$i_r(w) = a_3w^3 + a_2w^2.$ (6.1)

The results are represented in the Fig. 6.14.
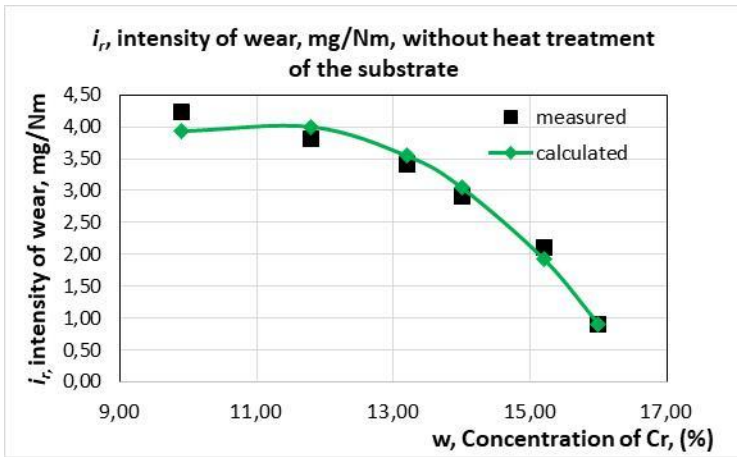
Fig. 6.14. Analytical dependence of the intensity of wear on the chromium concentration for coatings without heat treatment,
$$i_r(w) = -0,00599819w^3 + 0,099501902w^2.$$

The corrected coefficient of determination *Adjusted R Square* is 0,745894827, which shows, that 74,58% of the total variation of the concentration is explained by the chosen factors (w^3, w^2), i.e. they are adequately included in the model. The value of the significance of F is 0.00012<0.05 (0.012%<5%), i.e. the results are reliable (statistically significant) and the model is adequate. The P-values of the coefficients of the regression equation are less than 0.000032, i.e. they are less than 0.05, which means, that the coefficients are statistically significant and this fact confirms the adequacyof the model.

For coatings with heat treatment of the substrate the dependence acquires the form:

$$i_r(w) = b_3w^3 + b_2w^2.$$ (6.2)

The results are represented in Fig. 6.15.
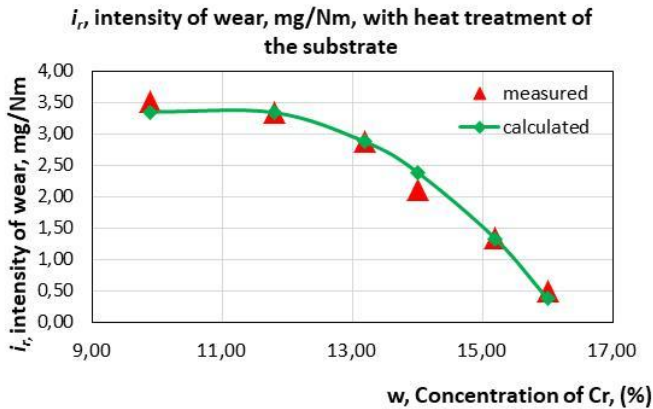
Fig. 6.15. Analytical dependence of the intensity of wear on the concentration of chromium for coatings with heat treatment, $i_r(w) = -0,005371987w^3 + 0,087400503w^2$

The corrected coefficient of determination *Adjusted R Square* is 0,74616892, which shows, that 74,62% of the total variation of the concentration is explained by the chosen factors (w^3, w^2), i.e. they are adequately included in the model. The value of the F statistics is 0.00011<0.05 (0.011%<5%), i.e. the results are reliable (statistically significant) and the model is adequate. The P-values of the coefficients of the regression equation are less than 0.000019, i.e. they are less than 0.05, which means, that the coefficients are statistically significant and this fact confirms the adequacy of the model.

6.4 CONCLUSION

This chapter represents comparative results about the wear characteristics and the wear resistance of the composite powder coatings, deposited by high velocity oxygen flame jet (HVOF), which contain composite mixtures Ni-Cr-B-Si with different concentrations of chromium – 9.9%; 13.2%; 14%; 16% and 20%, at one and the same size of the particles 45 µm and identical content of the rest of the elements boron and silicon. The coating, obtained with 20% Cr does not contain the elements B and Si. Coatings have been obtained out of each powder composite without preliminary heat treatment of the substrate and with preliminary heat treatment of the substrate up to 650°C. The coatings have been tested under identical conditions of dry friction along the surface with firmly fixed abrasive particles using tribo-tester „Pin-disk".

Results have been obtained about the dependence of the mass wearing on the friction path length, the variation of the intensity of wear as a function of the chromium concentration for coatings without heat treatment of the substrate and with heat treatment of the substrate.

It has been established, that for all the coatings the preliminary heat treatment of the substrate leads to a decrease in the intensity of wear.

It has been shown, that upon increasing the concentration of chromium the intensity of wear is decreasing non-linearly, whereupon it reaches minimal values at 16% Cr. For coatings with a 20% concentration of Cr the intensity of wear grows up, which is owing to the absence of the components B and Si in the composite mixture, whereupon no new intermetallic structures are formed having high hardness and wear resistance. A diagram is represented for the interconnection between the hardness of the coatings and the abrasive wear resistance.

Based on regression analysis analytical dependences have been obtained for the intensity of wear versus the concentration of chromium for coatings without heat treatment and with heat treatment of the substrate, represented as polynomials of the second and third order.

_____

Influence of the Concentration of Chromium on the Erosion Wear of HVOF Coatings

7.1 MATERIALS

Ten types of HVOF-coatings have been studied, divided in five groups having different concentrations of chromium in the powder composites - 9,9%, 13,2 %, 14%, 16%, 20% and approximately identical composition of the remaining chemical elements. Two types of coatings have been obtained for each group with definite concentration of chromium – without thermal treatment of the substrate (cold HVOF process) and with preliminary thermal treatment of the substrate in thermal chamber at temperature 650°C in the course of 60 minutes. The coatings with heat treatment of the substrate are denoted as PHS. The groups of coatings №9 and №10 contain in their composition 20% Cr and 80% Ni without including other elements, present in the rest of the coatings. The Table 7.1 represents the description, the chemical composition, the hardness and the thickness of the studied coatings [47].

All the coatings have been deposited on substrate of one and the same material – steel with chemical composition: C – 0.15%; S - 0.025%; Mn – 0.8%; P – 0.011%; Si – 0.21%; Cr – 0.3%; Ni – 0.3% and hardness 193.6 - 219.5 HV. The particles in all the powder composites have one and the same size - $45\pm2,5$ μm.

7.2 EXPERIMENTAL RESULTS

Results have been obtained for the mass erosion wear m_e, the rate of the erosion wear $\dot{m}_e$, the intensity i_e of the erosion, the absolute I_e and the realtive $R_{i,j}$ erosion wear resistance at two values of the angle of interaction of the jet with the surface α – 90° and 60°. The results are represented in Tables 7.2, 7.3 and 7.4.

The Fig. 7.1 represents the diagram of the intensity of wearing of all the tested coatings at the two angles of the jet. It is seen, that all the coatings at angle 90°, i.e. in the case of perpendicular disposition of the axis of the jet with respect to the surface, have greater intensity of the erosion. In this case the velocity of the separate particles has great value of its normal component and the destruction is

under the action of many strikes onto the surface. The mechanism of fatigue is prevailing, in which at the initial moment submicrocracks are appearing, which gradually grow up into microcrackings and at certain moment there occurs removal of particles from the surface. The intensity of wearing in this case depends on the chemical composition of the coating and on the strength of the cohesion bonds between the particles of coating. The greatest intensity of wear at angle of the jet 90° is shown by the coatings №9 and 10, which contain in their composition only the elements nickel and chromium, without having the other elements– boron, silicon and others. The lack of these elements reduces the plastic properties of the coatings and then the prevailing mechanism is that of brittle destruction. At jet angle 60° the intensity of wearing is lower and it is explained by the appearance of tangential component in the velocity of the particles, which has smaller value and for the time interval of erosion is not sufficient for the particle to cause effect of micro-splitting on the surface.
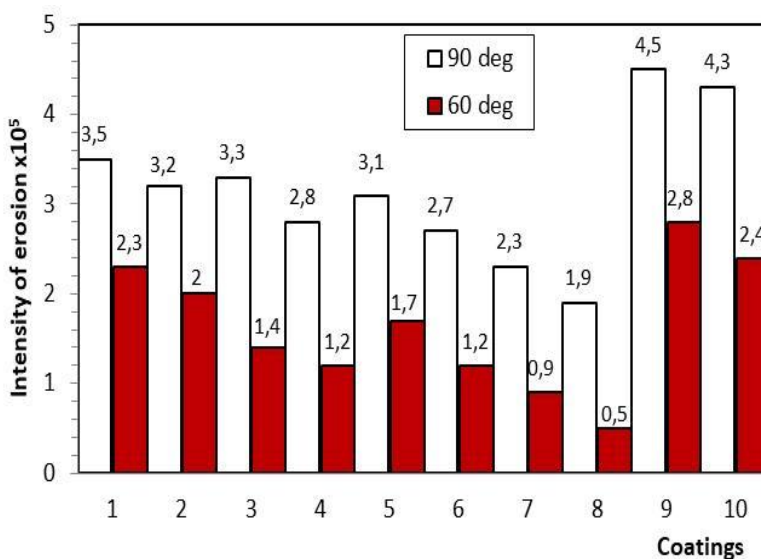
Fig. 7.1. A diagram of the intensity of erosion of the test coatings at an angle of interaction of the jet 90° and 60°

The Fig. 7.2 illustrates the influence of the angle of erosion upon the erosive wear resistance of the coatings in accordance with the results in Table 7.6. At jet angle 60° the wear resistance grows up within the range from 1.5 up to 2.6 times for coatings without heat treatment of the substrate and within the interval from 1.6 up to 3.5 times for coatings with heat treatment of the substrate. This effect is the strongest - 3.5 times for coating №8 having 16% Cr and with preliminary heat treatment of the substrate, while it is the lowest -1.5 times in the case of coating №1 – having 9.9% Cr without heat treatment of the substrate.

Table 7.1. Description, chemical composition, hardness and thickness of the tested coatings

Sample	Coating designation	Description	Chemical composition, wt. %	Hard ness HRC	Thickness µm
1	72M40	Coatings without heat treatment	**Cr: 9,9**; Si:3.1; B:1.7; Fe:3.2; C: 0.35;	55-56 HRC	410-415
2	72M40:PHS	Coatings with heat treatment	Mo: 3; Cu**:**3;	58-59 HRC	400-412
			Ni Balance		
3	602P	Coatings without heat treatment	**Cr: 13.2**; Si: 3.98; B: 2.79; Fe: 4.6; Co:	56-57HRC	395-400
4	602P:PHS	Coatings with heat treatment	0.03; C: 0.63;	59-60 HRC	408-414
			Ni: Balance		
5	80M60	Coatings without heat treatment	**Cr: 14**; Si:4.2; B:2,9; Fe:4,6; C:0.6;	57-58HRC	395-406
6	80M60:PHS	Coatings with heat treatment	Mo:2,5; Cu:2,4;	59-60 HRC	400-405
			Ni: Balance		
7	1355	Coatings without heat treatment	**Cr:16;** Si:4; B:3.4; Fe:2.7; C:0.6; Mo:3;	58-59 HRC	394-405
8	1355:PHS	Coatings with heat treatment	Cu:3;	61-62 HRC	404-410
			Ni: Balance		
9	HN40	Coatings without heat treatment	**Cr**: 20; **Ni**: 80	54-55 HRC	400-408
10	HN40:PHS	Coatings with heat treatment		57-60 HRC	393-403

Table 7.2. Erosive wear of the test coatings at the jet angle of contact with the α=90°

Sample	Coating designation	Mass wear, mg	Wear rate, mg/min	Intensity of erosion	Erosion wear resistance
1	72M40	29.1	5.82	3.49×10^{-5}	2.8×10^{4}
2	72M40:PHS	26.4	5.28	3.17×10^{-5}	3.2×10^{4}
3	602P	27.3	5.46	3.27×10^{-5}	3.1×10^{4}
4	602P:PHS	23.5	4.7	2.8×10^{-5}	3.6×10^{4}
5	80M60	26.1	5.22	3.13×10^{-5}	3.2×10^{4}
6	80M60:PHS	22.8	4.56	2.7×10^{-5}	3.7×10^{4}
7	1355	19.3	3.86	2.31×10^{-5}	4.3×10^{4}
8	1355:PHS	15.7	3.14	1.88×10^{-5}	5.3×10^{4}
9	HN40	37.8	7.56	4.54×10^{-5}	2.2×10^{4}
10	HN40:PHS	35.5	7.1	4.3×10^{-5}	2.3×10^{4}

Table 7.3. Erosive wear of the test coatings at the jet angle of contact with the α=60°

Sample	Coating designation	Mass wear, mg	Wear rate, mg/min	Intensity of erosion	Erosion wear resistance
1	72M40	19.4	3.88	2.33×10^{-5}	4.3×10^{4}
2	72M40:PHS	17.0	3.4	2.0×10^{-5}	5.0×10^{4}
3	602P	11.4	2.28	1.36×10^{-5}	7.4×10^{4}
4	602P:PHS	9.9	1.98	1.2×10^{-5}	8.3×10^{4}
5	80M60	13.9	2.78	1.67×10^{-5}	6.0×10^{4}
6	80M60:PHS	9.8	1.96	1.2×10^{-5}	8.3×10^{4}
7	1355	7.7	1.54	0.9×10^{-5}	11.1×10^{4}
8	1355:PHS	4.5	0.9	0.54×10^{-5}	18.5×10^{4}
9	HN40	23.3	4.66	2.79×10^{-5}	3.6×10^{4}
10	HN40:PHS	19.6	3.92	2.4×10^{-5}	4.1×10^{4}

Table 7.4. Relative wear rate and the influences of angle and both influences of erosive wear rate of tested coatings

Sample	Coating designation	Wear resistance, min/mg		Relative wear resistance (R)		
				Influence of angle	Influence of substrate heating	
		$\alpha = 90^o$	$\alpha = 60^o$	α	$\alpha = 90^o$	$\alpha = 60^o$
1	72M40	2.8×10^4	4.3×10^4	$R_{60/90} = 1.5$	$R_{1,1} = 1$	$R_{1,1} = 1$
2	72M40:PHS	3.2×10^4	5.0×10^4	$R_{60/90} = 1.6$	$R_{2,1} = 1.1$	$R_{2,1} = 1.2$
3	602P	3.1×10^4	7.4×10^4	$R_{60/90} = 2.4$	$R_{3,3} = 1$	$R_{3,3} = 1$
4	602P:PHS	3.6×10^4	8.3×10^4	$R_{60/90} = 2.3$	$R_{4,3} = 1.2$	$R_{4,3} = 1.1$
5	80M60	3.2×10^4	6.0×10^4	$R_{60/90} = 1.9$	$R_{5,5} = 1$	$R_{5,5} = 1$
6	80M60:PHS	3.7×10^4	8.3×10^4	$R_{60/90} = 2.2$	$R_{6,5} = 1.2$	$R_{6,5} = 1.4$
7	1355	4.3×10^4	11.1×10^4	$R_{60/90} = 2.6$	$R_{7,7} = 1$	$R_{7,7} = 1$
8	1355:PHS	5.3×10^4	18.5×10^4	$R_{60/90} = 3.5$	$R_{8,7} = 1.2$	$R_{8,7} = 1.7$
9	HN40	2.2×10^4	3.6×10^4	$R_{60/90} = 1.6$	$R_{9,9} = 1$	$R_{9,9} = 1$
10	HN40:PHS	2.3×10^4	4.1×10^4	$R_{60/90} = 1.8$	$R_{10,9} = 1,1$	$R_{10,9} = 1,2$
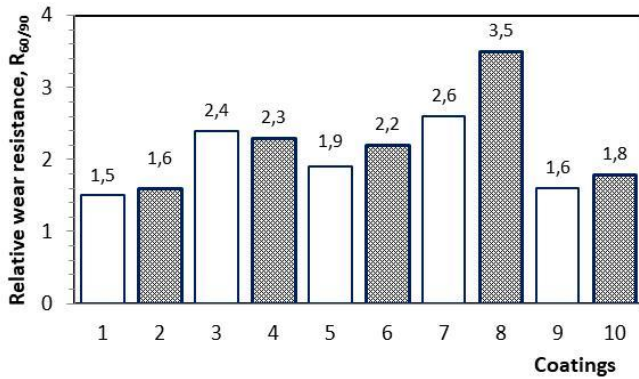
Fig. 7.2. Diagram of the influence of the jet angle on the wear resistance erosion of the tested coatings

The Figs. 7.3 and 7.4 illustrate the diagrams for the influence of the heat treatment of the substrate upon the erosion wear resistance at the two angles of the jet.

For the two angles of the jet all the tested coatings with heat treatment of the substrate have higher wear resistance than that of coatings without heat treatment. The effect of the heat treatment of the substrate on the wear resistance is greater at jet angle 60° and it is changing within the limits from 1.2 up to 1.7 times (Fig. 7.4). At jet angle of 90° the increase in the erosion wear resistance is insignificant – from 1.1 up to 1.2 times and it is almost one and the same for all the tested coatings (Fig. 7.3).
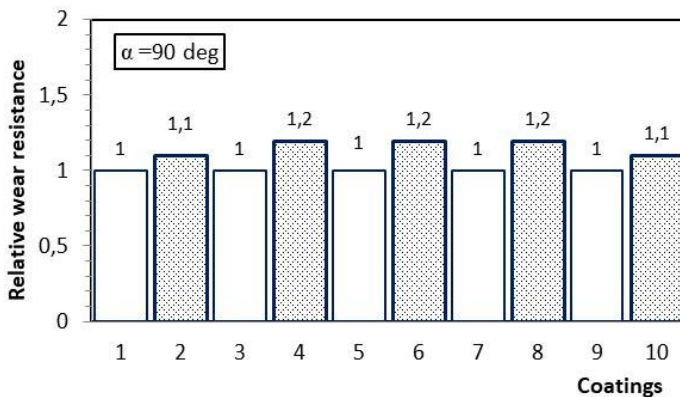
Fig. 7.3. Diagram of the influence of the heating of the substrate on the erosion wear resistance at a contact angle of the jet 90⁰
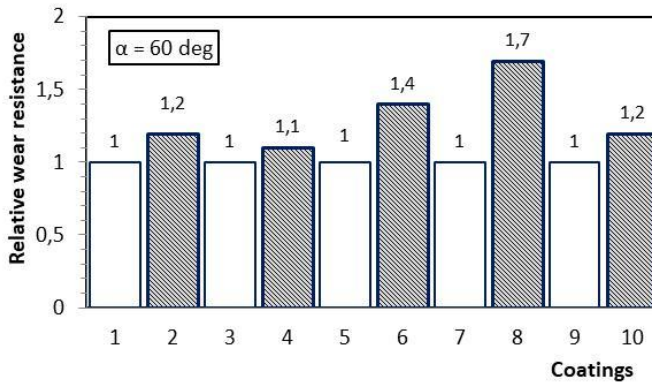
Fig. 7.4. Diagram of the influence of the heating of the substrate on the erosion wear resistance at a contact angle of the jet 60°

The Figs. 7.5 and 7.6 plot the dependence of the intensity of wearing on the concentration of chromium at the two contact angles of the jet respectively for the coatings without heat treatment of the substrate and with heat treatment of the substrate. It is seen, that the dependence has non-linear character. Upon increasing the concentration of chromium the intensity of the erosion is decreasing, reaching minimal value for the coatings with 16% Cr, and thereafter it sharply grows up in the case of the coatings with 20% Cr, which do not contain the elements boron and silicon. At jet angle 60° the curve has wave-like character, which is more clearly expressed for the coatings without heat treatment of the substrate and containing 14% Cr, where one observes slight increase of the intensity of erosion (the broken line).
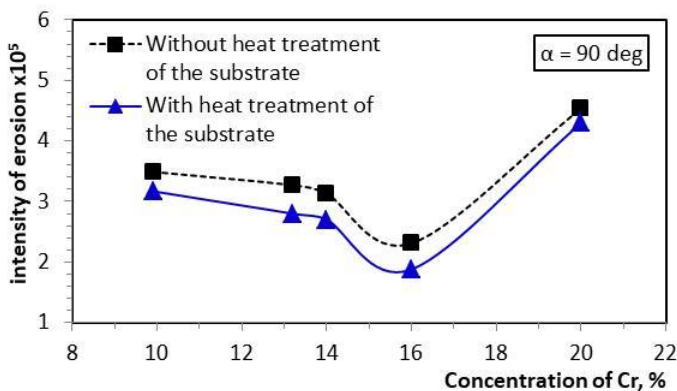
Fig. 7.5. Dependence of the erosion intensity on the chromium concentration at a jet angle of 90°
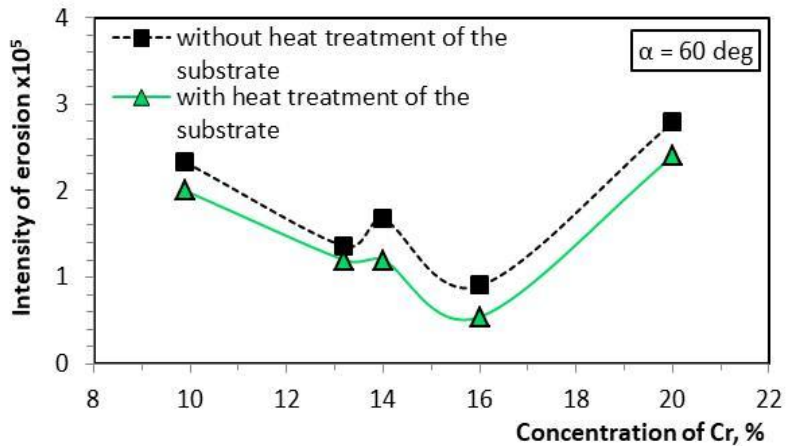
Fig. 7.6. Dependence of the erosion intensity on the chromium concentration at a jet angle of 60°

The dependence of the erosion wear resistance on the concentration of chromium is reciprocal with respect to the curve of the intensity of the erosion. For the two jet angles of 90° and 60° it is illustrated in the Fig. 7.7 and Fig. 7.8 for all the tested coatings.
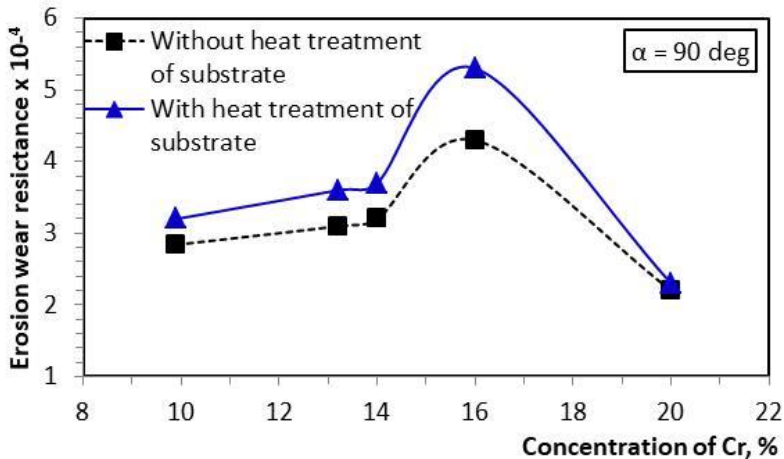
Fig. 7.7. Dependence of the erosion wear resistance on the chromium concentration at a jet angle of 90°
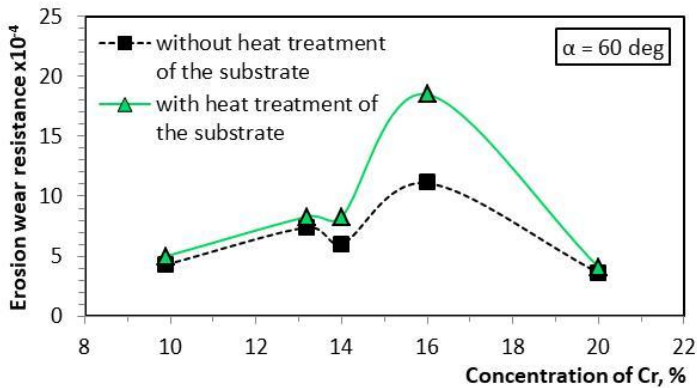
Fig. 7.8. Dependence of the erosion wear resistance on the chromium concentration at a jet angle of 60°

In the cases of coatings, containing the highest concentration of chromium the erosion wear resistance is decreased. At jet angle α=90° the wear resistance reaches values equal to the wear resistance of the coatings having the lowest content of chromium – 9.9% (Fig. 7.7), while at angle α=60° – it has lower values (Fig. 7.8).

7.3 REGRESSION MODELS

The experimental curve of the dependence of the intensity of erosion i_e on the chromium concentration in the range $9.9\,\% \leq w \leq 16\,\%$ for two angles of interaction of the jet with the surface is considered (Fig. 7.5 and Fig. 7.6).

The section of the curve where $w > 16\,\%$ is not considered because it includes coatings No. 9 and No. 10 (HN40 and HN40: PHS) with different chemical composition from the other coatings. These coatings contain only nickel (80%) and chromium (20%), which does not give us reason to analyze them in parallel with the other coatings.

Experimental results for the erosion intensity at more points on the curve in Fig. 7.9 and Fig. 7.10 are presented in Table 7.5 and Table 7.6, respectively.

Based on the regression analysis, analytical dependences of the intensity of erosion on the chromium concentration were obtained, presented as second- and third-degree polynomials.

For coatings without heat treatment of the substrate at jet angle 90° the dependence has the following form:

$$i_e(w) = a_3 w^3 + a_2 w^2. \tag{7.1}$$

Table 7.5. Intensity of erosion at different chromium concentration, % at a jet angle of 90°

w, Concentration of Cr, (%)	9.9	11.8	13.2	14.0	15.2	16.0
i_e, intensity of erosion without heat treatment of the substrate	3.49×10^{-5}	3.4×10^{-5}	3.27×10^{-5}	3.13×10^{-5}	2.4×10^{-5}	2.31×10^{-5}
i_e, intensity of erosion with heat treatment of the substrate	3.17×10^{-5}	3.0×10^{-5}	2.8×10^{-5}	2.7×10^{-5}	1.8×10^{-5}	1.88×10^{-5}

Table 7.6. Intensity of erosion at different chromium concentration, % at a jet angle of 60°

w, Concentration of Cr, (%)	9.9	11.8	13.2	14.0	15.2	16.0
i_e, intensity of erosion without heat treatment of the substrate	2.33×10^{-5}	1.8×10^{-5}	1.36×10^{-5}	1.67×10^{-5}	1.2×10^{-5}	0.9×10^{-5}
i_e, intensity of erosion with heat treatment of the substrate	2.0×10^{-5}	1.6×10^{-5}	1.2×10^{-5}	1.2×10^{-5}	0.6×10^{-5}	0.54×10^{-5}

Fig. 7.9. Dependence of Intensity of erosion on chromium concentration range from 9.9% to 16% at a jet angle 90°
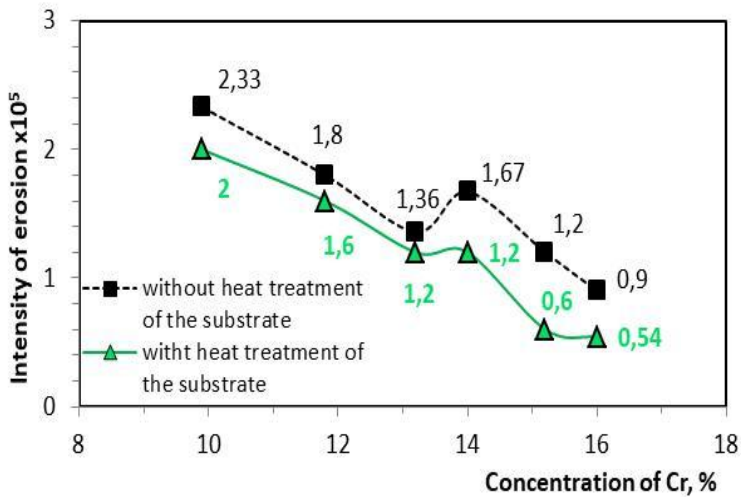
Fig. 7.10. Dependence of intensity of erosion on chromium concentration range from 9.9% to 16% at a jet angle 60°

The results are represented in the next Fig. 7.11.
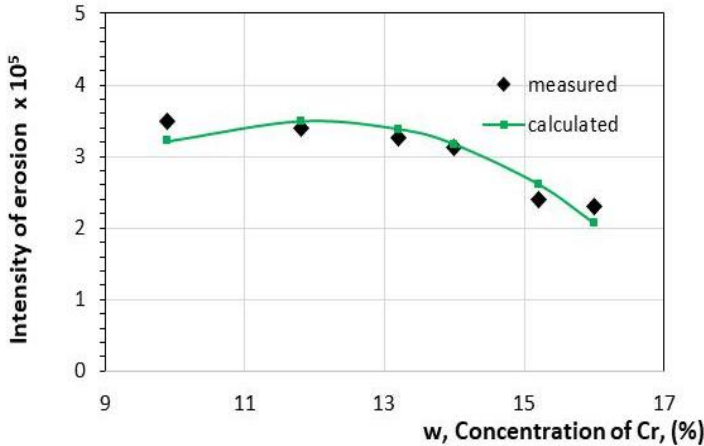
Fig. 7.11. Analytical dependences of the intensity of erosion on the chromium concentration for coatings without heat treatment at jet angle 90°, $i_e(w) = -0.00000004053535w^3 + 0.000000729229w^2$

The Adjusted R Square is 0.7454 and it shows that 74.54% of the variance of the intensity of erosion is predictable from chosen factors (w^3, w^2) which are adequately included in the model. The value of the significance F with significance level 0.05 is 0.000146 < 0.05 (0.0146% < 5%), i.e., the results are reliable (statistically significant) and the model is adequate. P-values of the coefficients of the regression equations with level of significance 0.05 are smaller than 0.00017, i.e., they are smaller than 0.05, which means that the coefficients are statistically significant, and the adequacy of the model is confirmed.

For coatings with heat treatment of the substrate at jet angle 90° the dependence has the following form:

$$i_e(w) = b_2 w^2 + b_1 w. \qquad (7.2)$$

The results are represented in the next Fig. 7.12.

The Adjusted R Square is 0.7457 and it shows that 74.57% of the variance of the intensity of erosion is predictable based on chosen factors (w^2, w), which are adequately included in the model. The value of the significance F with significance level 0.05 is 0.0001306 < 0.05 (0.01306% < 5%), i.e., the results are reliable (statistically significant) and the model is adequate. The P-values of the coefficients of the regression equations with level of significance 0.05 are smaller than 0.00033, i.e., they are smaller than 0.05, which means that the coefficients are statistically significant, and the adequacy of the model is confirmed.
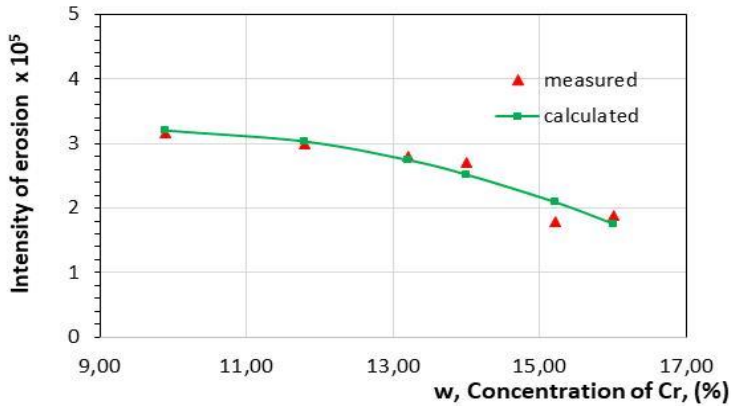
Fig. 7.12. Analytical dependences of the intensity of erosion on the chromium concentration for coatings with heat treatment at jet angle 90°,
$$i_e(w) = -0.000000349986w^2 + 0.000006699146w$$

For coatings without heat treatment of the substrate at jet angle 60° the dependence has the following form:

$$i_e(w) = c_3 w^3 + c_0. \tag{7.3}$$

The results are represented in the next Fig. 7.13.
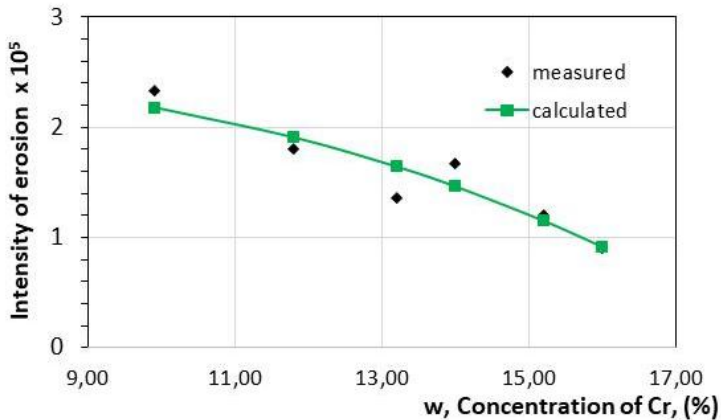
Fig. 7.13. Analytical dependences of the intensity of erosion on the chromium concentration for coatings without heat treatment at jet angle 60°, $i_e(w) = -0.000000004054378w^3 + 0.0000257484$

The Adjusted R Square is 0.8426 and it shows that 84.26% of the variance of the intensity of erosion is predictable using chosen factor (w^3), which is adequately included in the model. The value of the significance F with significance level 0.05 is 0.0062 < 0.05 (0.62% < 5%), i.e., the results are reliable (statistically significant) and the model is adequate. The P-values of the coefficients of the regression equations with level of significance 0.05 are smaller than 0.0063, i.e., they are smaller than 0.05, which means that the coefficients are statistically significant, and the adequacy of the model is confirmed.

For coatings with heat treatment of the substrate at jet angle 60° the dependence has the following form:

$$i_e(w) = d_2 w^2 + d_1 w. \tag{7.4}$$

The results are represented in the next Fig. 7.14.
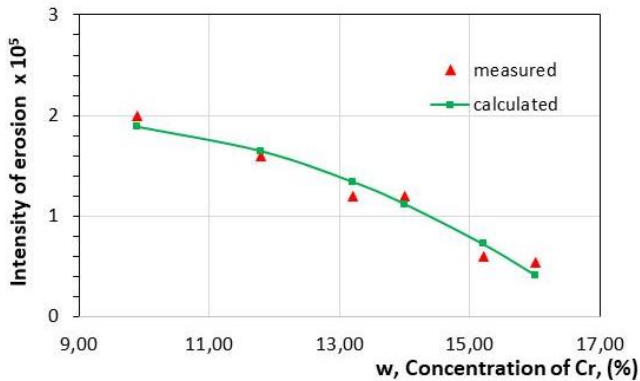
Fig. 7.14. Analytical dependences of the intensity of erosion on the chromium concentration for coatings with heat treatment at jet angle 60°,
$$i_e(w) = -0.000000270476968w^2 + 0.0000045861326w$$

The Adjusted R Square is 0.7411 and it shows that 74.11% of the variance of the intensity of erosion is predictable based on chosen factors (w^2, w), which are adequately included in the model. The value of the significance F with significance level 0.05 is 0.0003885< 0.05 (0.03885% < 5%), i.e., the results are reliable (statistically significant) and the model is adequate. P-values of the coefficients of the regression equations with level of significance 0.05 are smaller than 0.00024, i.e., they are smaller than 0.05, which means that the coefficients are statistically significant, and the adequacy of the model is confirmed.

7.4 CONCLUSION

Comparative results are represented for the erosion wear and for the erosion wear resistance of coatings, deposited by supersonic high velocity oxy-flame jet

(HVOF), which contain composites Ni-Cr-B-Si having different concentration of chromium – 9.9%; 13.2%; 14%; 16% and 20%, at identical size of the particles 45 μm and the same contents of the remaining elements boron and silicon. The coating, prepared to have 20% Cr does not contain the elements B and Si. Coatings have been obtained from each powder composition without preliminary heat treatment of the substrate and with preliminary heat treatment of the substrate at 650°C. The coatings have been tested uder identical conditions of erosion with air stream, carrying abrasive particles under identical conditions – nature, sizes and flow rate of the particles, time interval of erosion, air pressure, distance between the nozzle and the surface, angle between the axis of the jet stream and the surface.

Results have been obtained for the dependences of the mass wear, the intensity of erosion and erosion wear resistance on the concentration of chromium in coatings without and with heat treatment of the substrate at two angles of the jet 60° and 90°.

It has been established that:

- For all the coatings the preliminary heat treatment of the substrate leads to decrease in the intensity of wearing, i.e. increase in the erosion wear resistance.
- The angle of the jet influences the wear resistance of all the coatings. At jet angle 60° the wear resistance grows up within the interval from 1.5 to 2.6 times for coatings without heat treatment of the substrate and within the interval from 1.6 to 3.5 times for coatings with heat treatment of the substrate in comparison to the wear resistance at angle 90°. This effect is the greatest - 3.5 times for the coating №8 having 16% Cr. At jet angle 90° the wear resistance is increased up to 10% and this increase is one and the same for all the coatings.
- The dependence of the erosion wear resistanceon the concentration of chromium has strongly expressed non-linear character. The wear resistance grows up with the increase in the chromium concentration and it reaches a maximum in the case of coatings having 16% Cr with heat treatment of the substrate at jet angle 60°.
- The wear resistance of the coatings, containing the highest concentration of chromium – 20%, but not containing the elements boron and silicon, is lower or almost equal to the wear resistance of the coatings having the lowest concentration of chromium – 9.9%.

Regression models have been developed for the intensity of the erosion at the two angles of the jet 60° and 90° for the coatings without heat treatment and for the coatings with heat treatment of the substrate.

Influence of the Size of the Microparticles in Super-Alloys on the Abrasive Wearing of HVOF Coatings

8.1 MATERIALS

Twelve types of coatings have been studied, which had been prepared using six types of powder composites, divided into six series – I, II, III, IV, Vand, VI. All the composites have identical chemicompositionstion, ho, wever they contain particles of different sizes – 5 µm, 11 µm, 22 µm, 35 µm, 45 µm, and 55 µm. Two types of coatings have been deposited from each series of powder composites – upon substrate without preliminary heat treatment (cold HVOF process) and upon substrate with preliminary heat treatment up to temperature 650°C of 60 minutes. The designation of each coating NiCrSiB contains Arabic numeral (5, 11, 22, 35, 45, 55), which shows the size of the particles in micrometers, while the coatings with heat treatment of the substrate are denoted by PHS (Table 8.1) [27].

Tables 8.2 and 8.3 represent the chemical composition and some of the properties of the powder particles and those of the substrate.

8.2 EXPERIMENTAL RESULTS

Tests have been carried out using tribo-tester „pin-disc" and results have been obtained for the parameters of the abrasive wearing – the mass wear and linear wear, the intensity of wear, the absolute and the relative wear resistance at different friction path lengths: 40 m, 80 m, 120 m, 160 m, 200 m and several values of the normal loading 5 N, 10 N, 15 N, 20 N, 25 N for all the studied coatings, described in Table 8.1.

Influence of the friction path length on the wear and the wear resistance

Tables 8.4, 8.5, 8.6 and 8.7 represent the results for the mass wear, the linear wear, the wear intensity, y, and the wear resistance of the tested coatings at friction path lengths (sliding distances) 40 m, 80 m, 120 m, 16,0, m and 200 m. The experiments have been carried out anduand that sometimesameame normal loading pressure P = 4.5 N.

Table 8.1. Description, chemical composition, hardness, and thickness of the tested coatings

Series	Sample	Coating designation	Description	Hardness HRC	Thickness µm
I	1	NiCrSiB-5	Coatings with a particle size of 5 µm without heat treatment of the substrate	55-56	410-415
	2	NiCrSiB-5:PHS	Coatings with a particle size of 5 µm with heat treatment of the substrate	62-64	400-412
II	3	NiCrSiB-11	Coatings with a particle size of 11 µm without heat treatment of the substrate	53-54	395-400
	4	NiCrSiB-11:PHS	Coatings with a particle size of 11 µm with heat treatment of the substrate	57-58	408-414
III	5	NiCrSiB-22	Coatings with a particle size of 22 µm without heat treatment of the substrate	51-52	395-406
	6	NiCrSiB-22:PHS	Coatings with a particle size of 22 µm with heat treatment of the substrate	54-56	400-405
IV	7	NiCrSiB-35	Coatings with a particle size of 35 µm without heat treatment of the substrate	51-52	394-405
	8	NiCrSiB-35:PHS	Coatings with a particle size of 35 µm with heat treatment of the substrate	54-55	404-410
V	9	NiCrSiB-45	Coatings with a particle size of 45 µm without heat treatment of the substrate	50-51	400-408
	10	NiCrSiB-45:PHS	Coatings with a particle size of 45 µm with heat treatment of the substrate	54-55	393-403
VI	11	NiCrSiB-55	Coatings with a particle size of 55 µm without heat treatment of the substrate	51-52	380-390
	12	NiCrSiB-55:PHS	Coatings with a particle size of 55 µm with heat treatment of the substrate	52-53	390-400

Table 8.2. Particle properties

Chemical composition, wt. %	Melting point, ^{o}C	Mohs hardness
Cr: 16.0	1907	8.5
Si: 4.2	1414	7
B: 3.4	2076	9.5
Fe: 2.7	1538	4
C: 0.6	3550	-
Mo: 3	2623	5.5
Cu: 3	1085	5
Ni: Balance	1455	4

Table 8.3. Substrate properties

Chemical composition, wt. %	Melting point, ^{o}C	Mohs hardness
Cr: 0.30	1907	8.5
Si: 0.21	1414	7
Ni:0.30	1455	4
P: 0.011	44.1	-
C: 0.15	3550	-
Mn: 0.8	1246	6
S: 0.02	115.2	2
Fe: Balance	1455	4

By the data in Table 8.4, dependences have been plotted for the mass wear of all the coatings without and with heat treatment of the substrate, which are represented in Figs. 8.1, 8.2, 8.3, 8.4, 8.5 and 8.6. Each figure contains the regression equations of the mass wear as a function of the sliding distance (friction pathlength= $m(L)$.

Fig. 8.1. Mass wear vs. sliding distance for coatings with a particle size of 5 μm without and with heat treatment of the substrate

Table 8.4. Mass wear of the tested coatings at different sliding distances

Sample	Designation	Number of cycles (N)				
		200	400	600	800	1000
		Sliding distance, m				
		40	80	120	160	200
		Mass loss, mg				
1	NiCrSiB-5	2.5	4.8	6.5	8.3	8.6
2	NiCrSiB-5:PHS	0.9	2.6	3.4	4.1	5.1
3	NiCrSiB-11	3.8	7.8	10.5	11.1	12.5
4	NiCrSiB-11:PHS	1.8	2.6	5.2	7.1	8.3
5	NiCrSiB-22	4.2	8.5	12.8	16.9	18.4
6	NiCrSiB-22:PHS	3.5	4.5	7.4	10.2	11.9
7	NiCrSiB-35	4.6	10.2	16.4	22.3	24.5
8	NiCrSiB-35:PHS	3.8	6.3	11.6	14.5	15.8
9	NiCrSiB-45	6.8	12.5	18.9	24.5	26.4
10	NiCrSiB-45:PHS	4.2	7.8	12.3	17.2	20.1
11	NiCrSiB-55	7.2	14.1	20.0	25.3	27.4
12	NiCrSiB-55:PHS	4.9	10.2	15.4	20.8	22.3

Table 8.5. Linear wear of the tested coatings at different sliding distances

Sample	Designation	Number of cycles (N)				
		200	400	600	800	1000
		Sliding distance, m				
		40	80	120	160	200
		linear wear, μm				
1	NiCrSiB-5	35	67	90	117	120
2	NiCrSiB-5:PHS	12	37	48	58	72
3	NiCrSiB-11	52	109	144	155	176
4	NiCrSiB-11:PHS	24	37	73	100	116
5	NiCrSiB-22	59	120	179	237	258
6	NiCrSiB-22:PHS	48	63	103	142	166
7	NiCrSiB-35	64	142	228	312	344
8	NiCrSiB-35:PHS	52	88	168	203	220
9	NiCrSiB-45	95	175	264	336	360
10	NiCrSiB-45:PHS	59	110	173	240	282
11	NiCrSiB-55	100	198	280	354	384
12	NiCrSiB-55:PHS	69	143	216	291	312

Table 8.6. Wear intensity of the tested coatings at different sliding distances

Sample	Designation	Number of cycles (N)				
		200	400	600	800	1000
		Sliding distance, m				
		40	80	120	160	200
		Wear intensity, m/m				
1	NiCrSiB-5	0.88×10^{-6}	0.84×10^{-6}	0.75×10^{-6}	0.73×10^{-6}	0.6×10^{-6}
2	NiCrSiB-5:PHS	0.3×10^{-6}	0.46×10^{-6}	0.4×10^{-6}	0.36×10^{-6}	0.36×10^{-6}
3	NiCrSiB-11	1.3×10^{-6}	1.36×10^{-6}	1.2×10^{-6}	0.97×10^{-6}	0.88×10^{-6}
4	NiCrSiB-11:PHS	0.6×10^{-6}	0.46×10^{-6}	0.61×10^{-6}	0.62×10^{-6}	0.58×10^{-6}
5	NiCrSiB-22	1.5×10^{-6}	1.49×10^{-6}	1.49×10^{-6}	1.48×10^{-6}	1.29×10^{-6}
6	NiCrSiB-22:PHS	1.2×10^{-6}	0.79×10^{-6}	0.86×10^{-6}	0.89×10^{-6}	0.83×10^{-6}
7	NiCrSiB-35	1.6×10^{-6}	1.78×10^{-6}	1.9×10^{-6}	1.95×10^{-6}	1.72×10^{-6}
8	NiCrSiB-35:PHS	1.3×10^{-6}	1.1×10^{-6}	1.4×10^{-6}	1.27×10^{-6}	1.1×10^{-6}
9	NiCrSiB-45	2.38×10^{-6}	2.19×10^{-6}	2.2×10^{-6}	2.1×10^{-6}	1.8×10^{-6}
10	NiCrSiB-45:PHS	1.47×10^{-6}	1.37×10^{-6}	1.44×10^{-6}	1.5×10^{-6}	1.41×10^{-6}
11	NiCrSiB-55	2.52×10^{-6}	2.47×10^{-6}	2.33×10^{-6}	2.21×10^{-6}	1.92×10^{-6}
12	NiCrSiB-55:PHS	1.72×10^{-6}	1.79×10^{-6}	1.8×10^{-6}	1.82×10^{-6}	1.56×10^{-6}

Table 8.7. Wear resistance of the tested coatings at different sliding distances

Sample	Designation	Number of cycles (N)				
		200	400	600	800	1000
		Sliding distance, m				
		40	80	120	160	200
		Wear resistance, m/m				
1	NiCrSiB-5	1.1×10^6	1.2×10^6	1.3×10^6	1.4×10^6	1.7×10^6
2	NiCrSiB-5:PHS	3.3×10^6	2.2×10^6	2.5×10^6	2.8×10^6	2.8×10^6
3	NiCrSiB-11	0.77×10^6	0.74×10^6	0.83×10^6	1.03×10^6	1.14×10^6
4	NiCrSiB-11:PHS	1.67×10^6	2.17×10^6	1.64×10^6	1.61×10^6	1.72×10^6
5	NiCrSiB-22	0.68×10^6	0.67×10^6	0.67×10^6	0.68×10^6	0.78×10^6
6	NiCrSiB-22:PHS	0.83×10^6	1.27×10^6	1.16×10^6	1.12×10^6	1.2×10^6
7	NiCrSiB-35	0.62×10^6	0.56×10^6	0.53×10^6	0.51×10^6	0.58×10^6
8	NiCrSiB-35:PHS	0.77×10^6	0.91×10^6	0.71×10^6	0.79×10^6	0.9×10^6
9	NiCrSiB-45	0.42×10^6	0.46×10^6	0.45×10^6	0.48×10^6	0.56×10^6
10	NiCrSiB-45:PHS	0.68×10^6	0.73×10^6	0.69×10^6	0.67×10^6	0.71×10^6
11	NiCrSiB-55	0.4×10^6	0.4×10^6	0.43×10^6	0.45×10^6	0.52×10^6
12	NiCrSiB-55:PHS	0.58×10^6	0.56×10^6	0.56×10^6	0.55×10^6	0.64×10^6
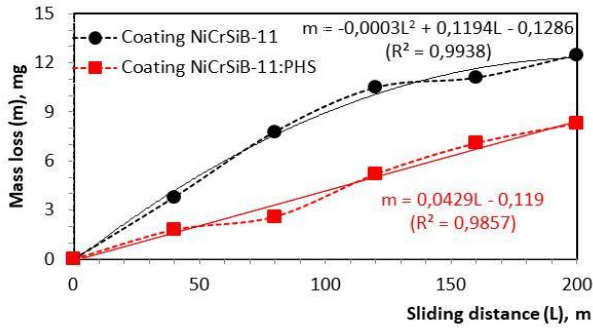
Fig. 8.2. Mass wear vs. sliding distance for coatings with a particle size of 11 μm without and with heat treatment of the substrate
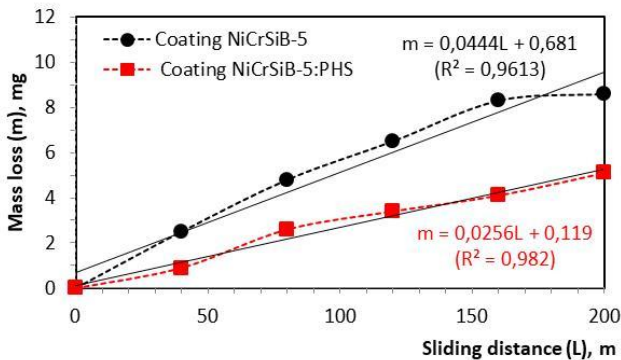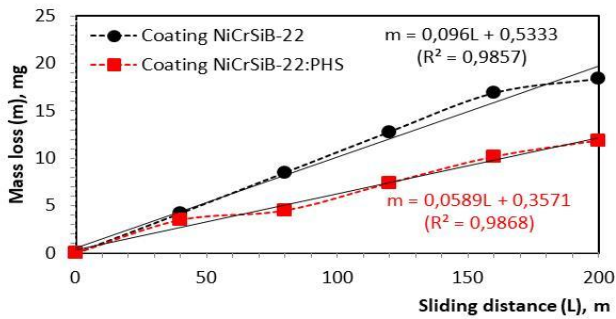

Fig. 8.3. Mass wear vs. sliding distance for coatings with a particle size of 22 μm without and with heat treatment of the substrate
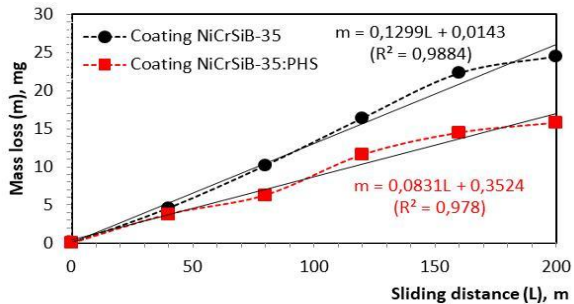
Fig. 8.4. Mass wear vs. sliding distance for coatings with a particle size of 35 μm without and with heat treatment of the substrate
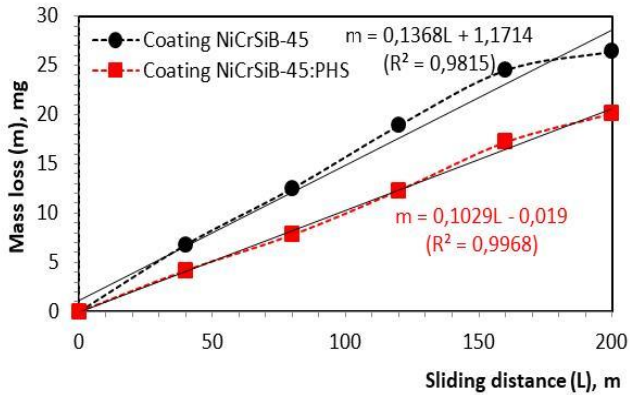
Fig. 8.5. Mass wear vs. sliding distance for coatings with a particle size of 45 μm without and with heat treatment of the substrate
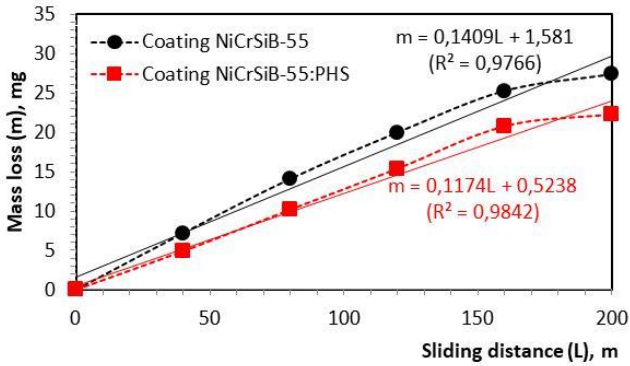
Fig. 8.6. Mass wear vs. sliding distance for coatings with a particle size of 55 μm without and with heat treatment of the substrate

It can be seen in the figures, that in the case of dry abrasive friction the dependence of the mass wear is increasing directly proportional to the sliding distance, i.e. the dependence has clearly expressed linear character for coatings without and with heat treatment of the substrate. The only exception is observed for coatings with particles of size 11 μm, deposited on the substrate without preliminary heat treatment.

Fig. 8.7 illustrates the diagram of the wear resistance for all the coatings at one the sanding distance 200 m in accof Nordby listed in Table 8.7.
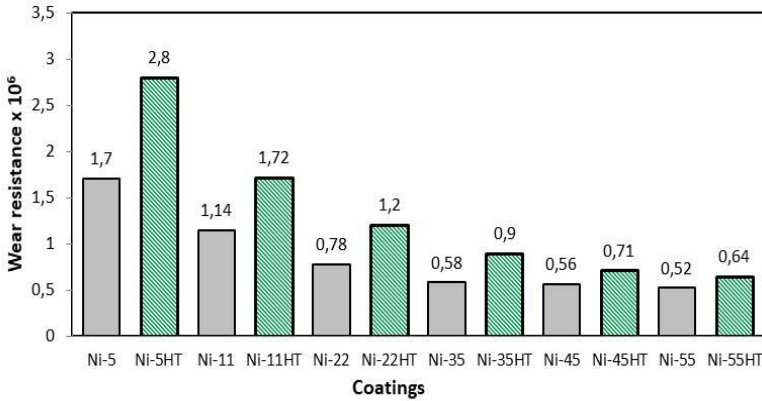
Fig. 8.7. Diagram of the wear resistance of the tested coatings in case of sliding distance 200 m and normal loading pressure P = 4.5 N

It is seen in the diagram, that the greatest wear resistance $I_r = 2sixties.8x10^6$ is shown by the coating NiCrSiB-5:PHS having a size of the powder particles 5 μm and with preliminary heat treatment of the substrate.

The lowest wear resistance $I_r = 0.sixth is52x10^6$ is that of the coating NiCrSiB-55, i.e. the coating obtained with the greatest size of the powder particles of the composite mixture without preliminary heat treatment of the substrate.

Table 8.8 represents the results for the relative wear resistance of the coatings based on two indices: heat treatment of the substrate and the size of the powder particles [41,42].

It is seen, that all the coatings having heat treatment of the substrate possess higher wear resistance than the same coatings without heat treatment of the substrate. The influence is the strongest in the case of coatings having the smallest size of the particles - NiCrSiB-5:PHS. For these coatings the, wear resistance grows up 1.65 times. The smallest increase in the wear resistance - 1.23 times is observed for two types of coatings NiCrSiB-11:PHS and NiCrSiB-55:PHS, i.e. deposited using particles of sizes 11 and 55 μm. It is not possible to claim, that there exists a direct correlation between the increase in the wear resistance as a consequence of the heat treatment of the substrate and the size of the particles.

Figs. 8.8 and 8.9 illustrate the diagrams of the relative wear resistance respectively for the influence of the heat treatment of the substrate (Fig. 8.11) and the influence of the size of the particles (Fig. 8.12). The influence of the size of the particles (Fig. 8.12) has been determined as relative wear resistance concerning the wear resistance of coatings having particles size of 5 μm respectively for coatings with and without heat treatment of the substrate.

Table 8.8. The relative wear resistance of the tested coatings

Sample	Designation	Wear resistance to a sliding distance of 300 m	Relative wear resistance	
			Influence of the heat treatment	Influence of particle size
1	NiCrSiB-5	1.7×10^6	$R_{1,1} = 1$	$R_{1,1} = 1$
2	NiCrSiB-5:PHS	2.8×10^6	$R_{2,1} = 1.65$	$R_{2,2} = 1$
3	NiCrSiB-11	1.4×10^6	$R_{3,3} = 1$	$R_{1,3} = 1.2$
4	NiCrSiB-11:PHS	1.72×10^6	$R_{4,3} = 1.23$	$R_{2,4} = 1.63$
5	NiCrSiB-22	0.78×10^6	$R_{5,5} = 1$	$R_{1,5} = 2.18$
6	NiCrSiB-22:PHS	1.2×10^6	$R_{6,5} = 1.54$	$R_{2,6} = 2.33$
7	NiCrSiB-35	0.58×10^6	$R_{7,7} = 1$	$R_{1,7} = 2.93$
8	NiCrSiB-35:PHS	0.9×10^6	$R_{8,7} = 1.55$	$R_{2,8} = 3.11$
9	NiCrSiB-45	0.56×10^6	$R_{9,9} = 1$	$R_{1,9} = 3.04$
10	NiCrSiB-45:PHS	0.71×10^6	$R_{10,9} = 1.27$	$R_{2,10} = 3.94$
11	NiCrSiB-55	0.52×10^6	$R_{11,11} = 1$	$R_{1,11} = 3.27$
12	NiCrSiB-55:PHS	0.64×10^6	$R_{12,11} = 1.23$	$R_{2,12} = 4.38$
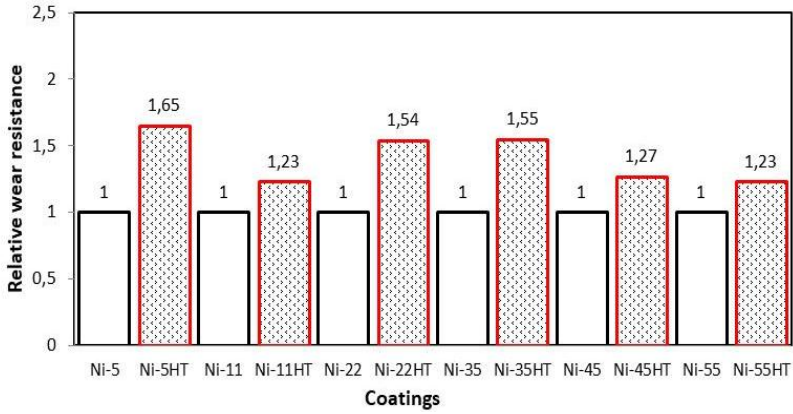
Fig. 8.8. Diagram of the influence of the heat treatment of the substrate on the relative wear resistance of the coatings
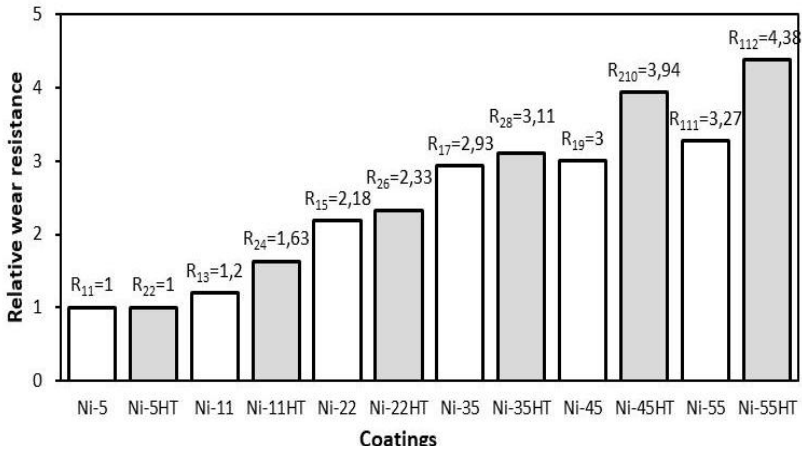
Fig. 8.9. Diagram of the influence of particle sizes on the relative wear resistance of coatings

Influence of the normal loading on the wear and the wear resistance

Results have been obtained for the parameters of the wearing process – mass and linear wear, wear intensity and wear resistance of the tested coatings at several values of the normal loading – 5 N, 10 N, 15 N, 20 N, and 25 N, which are listed in Tables 8.9, 8.10, 8.11 and 8.12.

Table 8.9. Mass wear of the tested coatings at different normal loads

Sample	Designation	Normal load, N				
		5	10	15	20	25
		Mass loss, mg				
1	NiCrSiB-5	7.9	10.1	12.3	14.1	16.4
2	NiCrSiB-5:PHS	3.8	5.9	8.0	10.4	12.6
3	NiCrSiB-11	11.2	14.2	16.9	20.5	24.2
4	NiCrSiB-11:PHS	8.3	10.9	13.3	16.5	20.5
5	NiCrSiB-22	16.6	19.8	21.9	24.6	28.1
6	NiCrSiB-22:PHS	10.1	12.5	15.1	17.9	21.5
7	NiCrSiB-35	22,5	26.1	29.5	33.8	37.6
8	NiCrSiB-35:PHS	14.3	18.5	22.7	27.0	31.9
9	NiCrSiB-45	23.8	27.9	32.0	35.5	40.8
10	NiCrSiB-45:PHS	16.4	19.8	24.4	29.2	33.6
11	NiCrSiB-55	25.2	28.9	33.8	36.9	42.1
12	NiCrSiB-**55**:PHS	17.9	21.6	25.8	31.0	34.8

Table 8.10. Linear wear of the tested coatings at different normal loads

Sample	Designation	Normal loads, N; Sliding distance 200 m = const				
		5 N	10 N	15 N	20 N	25 N
		Linear wear, µm				
1	NiCrSiB-5	110	142	172	198	230
2	NiCrSiB-5:PHS	54	82	112	146	176
3	NiCrSiB-11	156	200	236	286	338
4	NiCrSiB-11:PHS	116	152	186	230	286
5	NiCrSiB-22	232	278	306	344	394
6	NiCrSiB-22:PHS	142	176	212	250	300
7	NiCrSiB-35	316	366	420	474	526
8	NiCrSiB-35:PHS	200	260	318	378	446
9	NiCrSiB-45	334	390	448	498	572
10	NiCrSiB-45:PHS	230	278	342	408	470
11	NiCrSiB-55	352	404	474	516	590
12	NiCrSiB-55:PHS	250	302	362	434	488

Table 8.11. Wear intensity of the tested coatings at different normal loads

Sample	Designation	Normal loads, N; Sliding distance 200 m = const				
		5 N	10 N	15 N	20 N	25 N
		Wear intensity, m/m				
1	NiCrSiB-5	0.55×10^{-6}	0.71×10^{-6}	0.86×10^{-6}	0.99×10^{-6}	1.15×10^{-6}
2	NiCrSiB-5:PHS	0.27×10^{-6}	0.41×10^{-6}	0.56×10^{-6}	0.73×10^{-6}	0.88×10^{-6}
3	NiCrSiB-11	0.78×10^{-6}	0.99×10^{-6}	1.18×10^{-6}	1.43×10^{-6}	1.69×10^{-6}
4	NiCrSiB-11:PHS	0.58×10^{-6}	0.76×10^{-6}	0.93×10^{-6}	1.15×10^{-6}	1.43×10^{-6}
5	NiCrSiB-22	1.16×10^{-6}	1.39×10^{-6}	1.53×10^{-6}	1.72×10^{-6}	1.97×10^{-6}
6	NiCrSiB-22:PHS	0.71×10^{-6}	0.88×10^{-6}	1.06×10^{-6}	1.25×10^{-6}	1.5×10^{-6}
7	NiCrSiB-35	1.58×10^{-6}	1.83×10^{-6}	2.1×10^{-6}	2.37×10^{-6}	2.63×10^{-6}
8	NiCrSiB-35:PHS	1.0×10^{-6}	1.3×10^{-6}	1.59×10^{-6}	1.89×10^{-6}	2.23×10^{-6}
9	NiCrSiB-45	1.67×10^{-6}	1.95×10^{-6}	2.24×10^{-6}	2.49×10^{-6}	2.86×10^{-6}
10	NiCrSiB-45:PHS	1.15×10^{-6}	1.39×10^{-6}	1.71×10^{-6}	2.04×10^{-6}	2.35×10^{-6}
11	NiCrSiB-55	1.76×10^{-6}	2.02×10^{-6}	2.37×10^{-6}	2.58×10^{-6}	2.95×10^{-6}
12	NiCrSiB-55:PHS	1.25×10^{-6}	1.51×10^{-6}	1.81×10^{-6}	2.17×10^{-6}	2.44×10^{-6}

Table 8.12. Wear resistance of the tested coatings at different normal loads

Sample	Designation	Normal loads, N; Sliding distance 200 m = const				
		5 N	10 N	15 N	20 N	25 N
		Wear resistance, m/m				
1	NiCrSiB-5	1.82×10^6	1.41×10^6	1.16×10^6	1.01×10^6	0.87×10^6
2	NiCrSiB-5:PHS	3.7×10^6	2.44×10^6	1.79×10^6	1.37×10^6	1.14×10^6
3	NiCrSiB-11	1.28×10^6	1.0×10^6	0.85×10^6	0.7×10^6	0.59×10^6
4	NiCrSiB-11:PHS	1.72×10^6	1.32×10^6	1.08×10^6	0.86×10^6	0.7×10^6
5	NiCrSiB-22	0.86×10^6	0.72×10^6	0.65×10^6	0.58×10^6	0.51×10^6
6	NiCrSiB-22:PHS	1.41×10^6	1.14×10^6	0.94×10^6	0.8×10^6	0.67×10^6
7	NiCrSiB-35	0.63×10^6	0.55×10^6	0.48×10^6	0.42×10^6	0.38×10^6
8	NiCrSiB-35:PHS	1.0×10^6	0.77×10^6	0.63×10^6	0.53×10^6	0.45×10^6
9	NiCrSiB-45	0.6×10^6	0.51×10^6	0.45×10^6	0.4×10^6	0.35×10^6
10	NiCrSiB-45:PHS	0.87×10^6	0.72×10^6	0.58×10^6	0.49×10^6	0.42×10^6
11	NiCrSiB-55	0.57×10^6	0.5×10^6	0.42×10^6	0.39×10^6	0.34×10^6
12	NiCrSiB-55:PHS	0.8×10^6	0.66×10^6	0.55×10^6	0.46×10^6	0.41×10^6

For each studied coating the dependence is plotted of the mass wear as a function of the normal loading $mbyce$ with the results in Table 8.10, which are illustrated in Figs. 8.10, 8.11, 8.12, 8.13, 8.14 and 8.15. It is seen in the figures, that the increase in the wear upon increasing the loading has clearly expressed linear character for all the coating except the coating NiCrSiB-11:PHS.

Fig. 8.10. Change in mass wear from the normal load for coatings with a particle size of 5 μm without and with heat treatment of the substrate

Fig. 8.11. Change in mass wear from the normal load for coatings with a particle size of 11 μm without and with heat treatment of the substrate

The diagrams of the wear resistance for each of the tested coatings at the same friction path length of 200 m for values of the normal loading 5 N, 10 N, 15 N, 20 N, and 25 N are represented in Figs. 8.16, 8.17, 8.18, 8.19, and 8.20.

Among all the tested coatings the coating with the smallest size of the powder particles - NiCrSiB-5:PHS is characterized by the greatest wear resistance at each value of the normal loading. It is the highest $I_r = 3.7 \times 10^6$ at the lowest loading ppressurecapressure $P = 5\,N$, w ccaseoffiveimes higher loading ppressurecapressure $P = 25\,N$ the wear resistance is decreased down to $I_r = 1.14 \times 10^6$, i.e. more than three times.
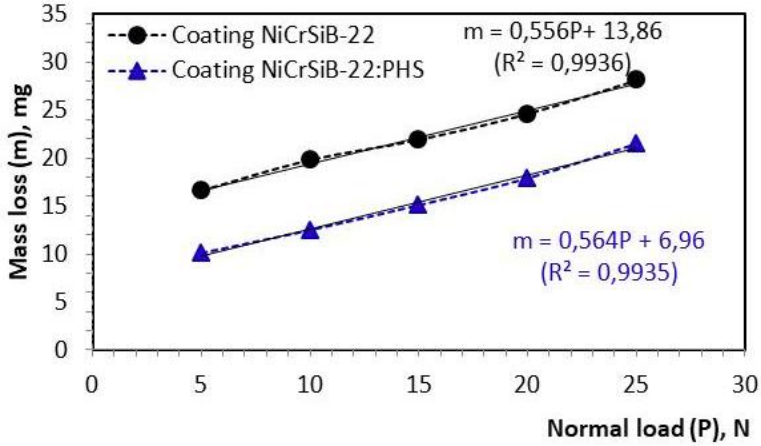
Fig. 8.12. Change in mass wear from the normal load for coatings with a particle size of 22 μm without and with heat treatment of the substrate
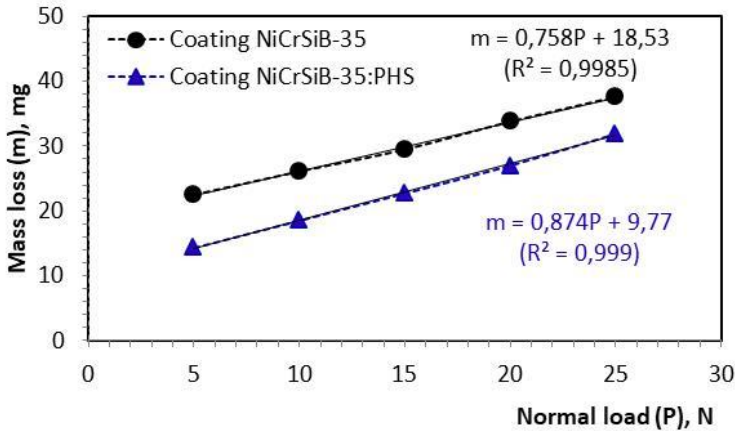
Fig. 8.13. Change in mass wear from the normal load for coatings with a particle size of 35 μm without and with heat treatment of the substrate
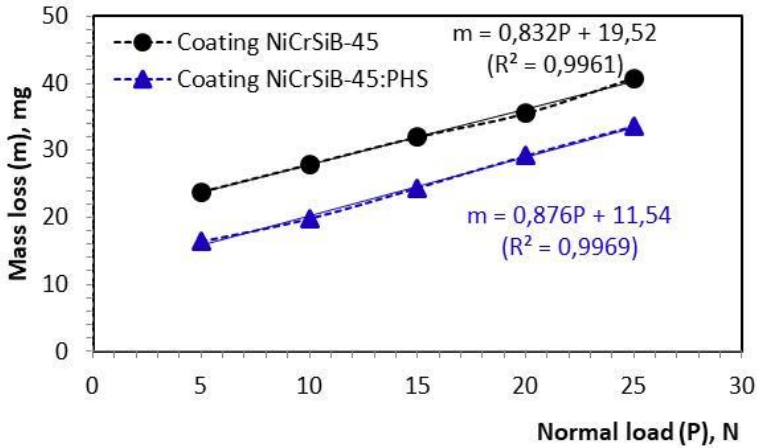
Fig. 8.14. Change in mass wear from the normal load for coatings with a particle size of 45 μm without and with heat treatment of the substrate
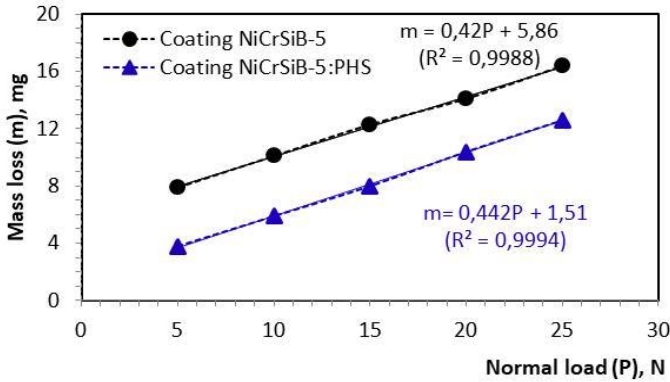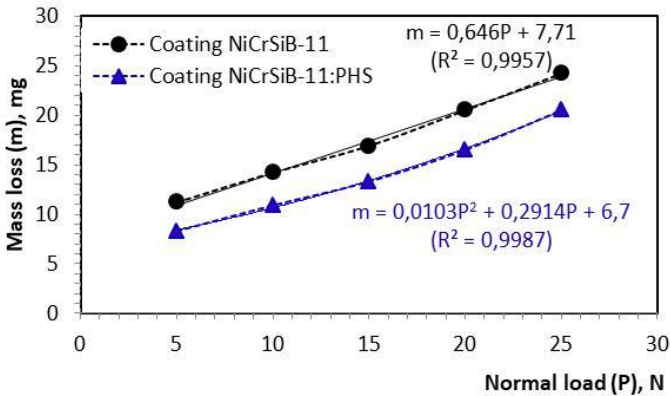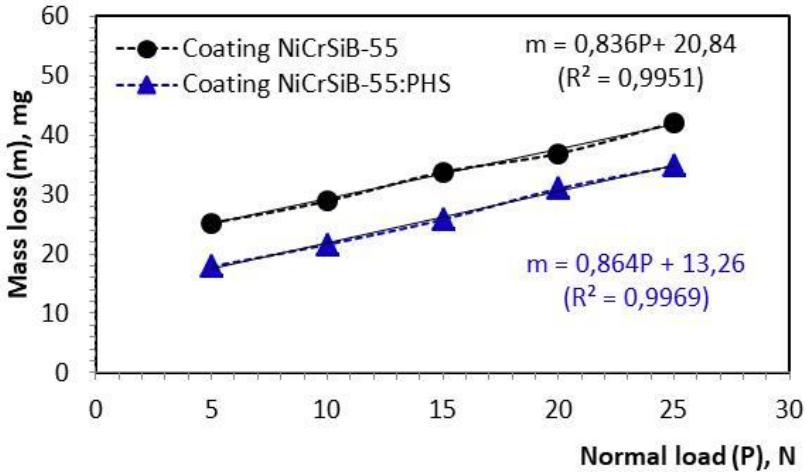

Fig. 8.15. Change in mass wear from the normal load for coatings with a particle size of 55 μm without and with heat treatment of the substrate

The data for the relative wear resistance of all coatings at different values of the normal loading is represented in Table 8.13.

Table 8.13. The relative wear resistance of the tested coatings at different normal loads

Sample	Designation	Normal loads				
		$P_1 = 5$ N	$P_2 = 10$ N	$P_3 = 15$ N	$P_4 = 20$ N	$P_5 = 25$ N
		Relative wear resistance				
1	NiCrSiB-5	$R_{P1} = 1$	$R_{P2,1} = 0.77$	$R_{P3,1} = 0.64$	$R_{P4,1} = 0.55$	$R_{P5,1} = 0.48$
2	NiCrSiB-5:PHS	$R_{P1} = 1$	$R_{P2,1} = 0.66$	$R_{P3,1} = 0.48$	$R^P_{1,4} = 0.37$	$R_{P5,1} = 0.31$
3	NiCrSiB-11	$R_{P1} = 1$	$R_{P2,1} = 0.78$	$R_{P3,1} = 0.66$	$R_{P4,1} = 0.55$	$R_{P5,1} = 0.46$
4	NiCrSiB-11:PHS	$R_{P1} = 1$	$R_{P2,1} = 0.77$	$R_{P3,1} = 0.63$	$R_{P4,1} = 0.5$	$R_{P5,1} = 0.41$
5	NiCrSiB-22	$R_{P1} = 1$	$R_{P2,1} = 0.84$	$R_{P3,1} = 0.75$	$R_{P4,1} = 0.67$	$R_{P5,1} = 0.59$
6	NiCrSiB-22:PHS	$R_{P1} = 1$	$R_{P2,1} = 0.81$	$R_{P3,1} = 0.67$	$R_{P4,1} = 0.57$	$R_{P5,1} = 0.48$
7	NiCrSiB-35	$R_{P1} = 1$	$R_{P2,1} = 0.87$	$R_{P3,1} = 0.76$	$R_{P4,1} = 0.67$	$R_{P5,1} = 0.6$
8	NiCrSiB-35:PHS	$R_{P1} = 1$	$R_{P2,1} = 0.77$	$R_{P3,1} = 0.63$	$R_{P4,1} = 0.53$	$R_{P5,1} = 0.45$
9	NiCrSiB-45	$R_{P1} = 1$	$R_{P2,1} = 0.85$	$R_{P3,1} = 0.75$	$R_{P4,1} = 0.67$	$R_{P5,1} = 0.58$
10	NiCrSiB-45:PHS	$R_{P1} = 1$	$R_{P2,1} = 0.83$	$R_{P3,1} = 0.67$	$R_{P4,1} = 0.56$	$R_{P5,1} = 0.48$
11	NiCrSiB-55	$R_{P1} = 1$	$R_{P2,1} = 0.88$	$R_{P3,1} = 0.74$	$R_{P4,1} = 0.68$	$R_{P5,1} = 0.6$
12	NiCrSiB-55:PHS	$R_{P1} = 1$	$R_{P2,1} = 0.83$	$R_{P3,1} = 0.69$	$R_{P4,1} = 0.58$	$R_{P5,1} = 0.51$
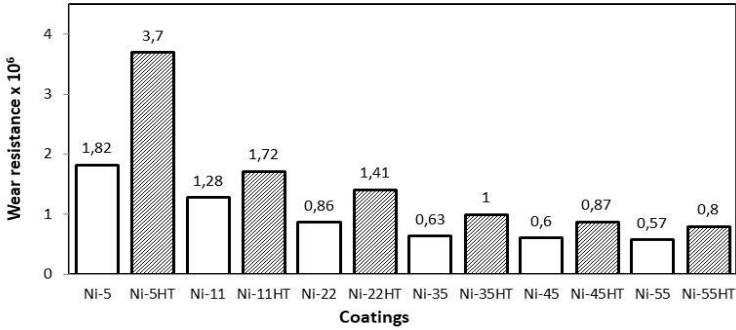
Fig. 8.16. Diagram of the wear resistance of the tested coatings at a normal load of 5 N
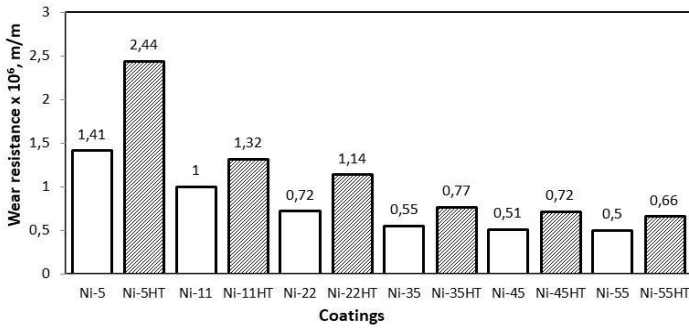
Fig. 8.17. Diagram of the wear resistance of the tested coatings at a normal load of 10 N
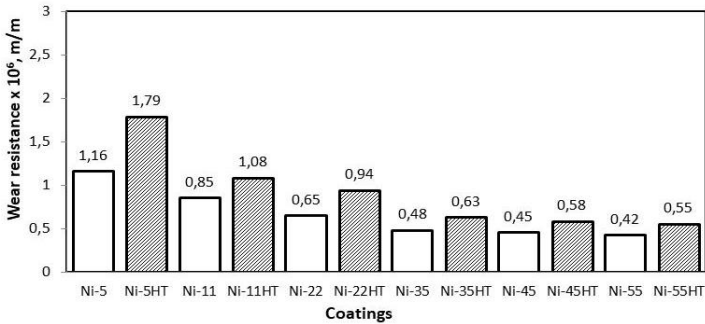
Fig. 8.18. Diagram of the wear resistance of the tested coatings at a normal load of 15 N
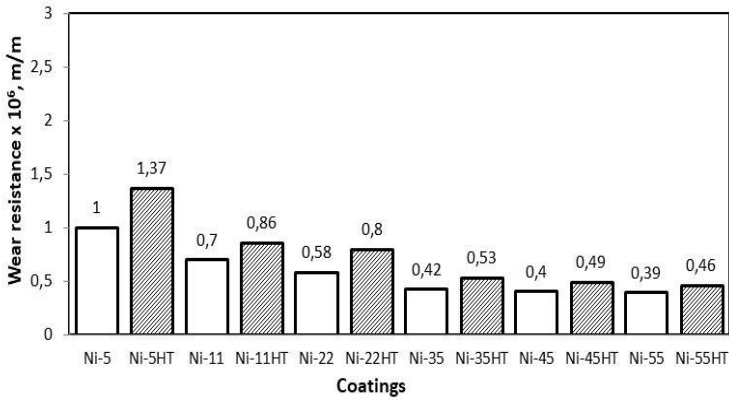
Fig. 8.19. Diagram of the wear resistance of the tested coatings at a normal load of 20 N
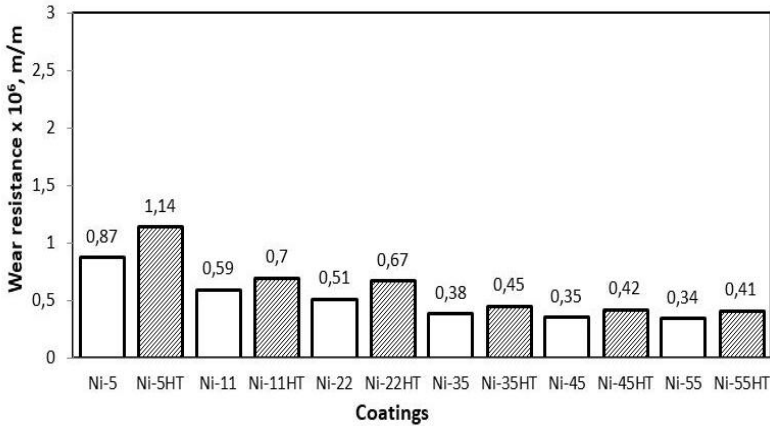
Fig. 8.20. Diagram of the wear resistance of the tested coatings at a normal load of 25 N

Influence of the size of the particles on the mass wear at different loads

The results for the mass wear at the same sliding distance for all tested coatings at different values of the normal load are summarized in Table 8.14.

Based on these results, graphical dependences have been plotted for the mass wear as a function of the size of the particles at each value of the normal load. These graphics combined with the regression models are illustrated in Figs. 8.21, 8.22, 8.23, and 8.24.

Table 8.14. Mass wear of coatings with different dust particle sizes at different loads

Particle size		5 μm	11 μm	22 μm	35 μm	45 μm	55 μm
P_1 5 N	Wear of coatings without heat treatment of the substrate, mg	7.9	11.2	16.6	22.5	23.8	25.2
	Wear of coatings with heat treatment of the substrate, mg	3.8	8.3	10.1	14.3	16.4	17.9
P_2 10 N	Wear of coatings without heat treatment of the substrate, mg	10.1	14.2	19.8	26.1	27.9	28.9
	Wear of coatings with heat treatment of the substrate, mg	5.9	10.9	12.5	18.5	19.8	21.6
P_3 15 N	Wear of coatings without heat treatment of the substrate	12.3	16.9	21.9	29.5	32.0	33.8
	Wear of coatings with heat treatment of the substrate, mg	8.0	13.3	15.1	22.7	24.4	25.8
P_4 20 N	Wear of coatings without heat treatment of the substrate, mg	14.1	20.5	24.6	33.8	35.5	36.9
	Wear of coatings with heat treatment of the substrate, mg	10.4	16.5	17.9	27.0	29.2	31
P_5 25 N	Wear of coatings without heat treatment of the substrate, mg	16.4	24.2	28.1	37.6	40.8	42.1
	Wear of coatings with heat treatment of the substrate, mg	12.6	20.5	21.5	31.9	33.6	34.8
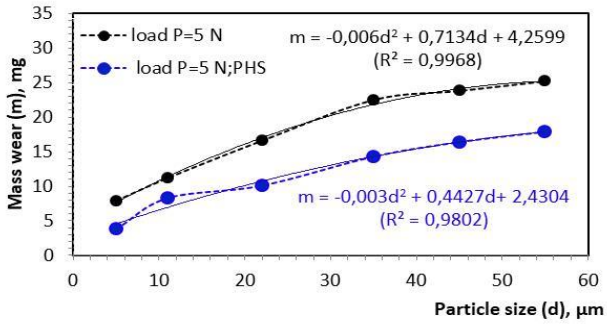
Fig. 8.21. Dependence of mass wear on particle size for coatings without and with heat treatment of the substrate at a load of 5 N
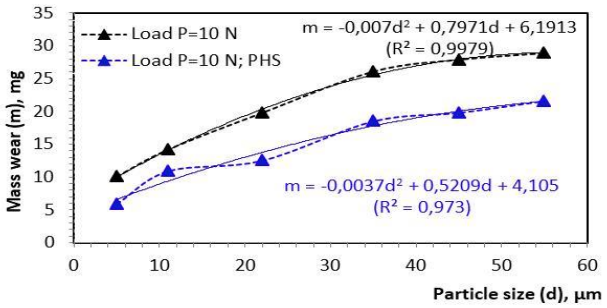
Fig. 8.22. Dependence of mass wear on particle size for coatings without and with heat treatment of the substrate at a load of 10 N
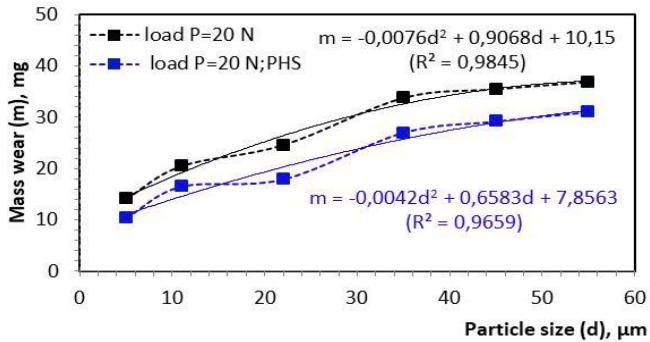
Fig. 8.23. Dependence of mass wear on particle size for coatings without and with heat treatment of the substrate at a load of 20 N
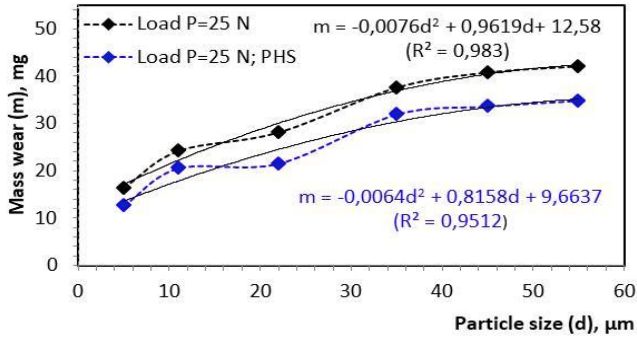
Fig. 8.24. Dependence of mass wear on particle size for coatings without and with heat treatment of the substrate at a load of 25 N

It can be seen in the shown curves, that the dependence of the mass abrasive wear on the size of the powder particles has a non-linear character for all the tested coatings – both with and without heat treatment of the substrate and at all values of the normal load. It can be observed, that at higher values of the loading pressure P = 20N and P = 25N within the range of the particles sizes from 5 µm up to 35 µm the dependence has a wave-like character, while at sizes larger than 35 µm the wear is very little and it remains almost constant.

The decrease in the wearing degree, i.e. the increase in the wear resistance of the coatings upon diminishing the size of the powder particles can be explained by enhancement of the mechanical properties of the coatings at smaller sizes of the particles. During the interaction of the powder particles with the substrate and between themselves some contact compounds are being formed between the particles in the coating, which are forming internal contact network /cohesion network/. The decrease in the size of the particles has two aspects regarding the contact network: first – upon decreasing the size of the particles the contact network has a larger area, which contains a larger number of internal contact compounds; second - in the case of smaller particles the contact area of the particle grows up, i.e. the ratio between the surface and the volume of the particles is greater, the surface energy of the particles is larger, which leads to the formation of higher adhesion strength of the internal contact network of inter-metallic compounds of the separate chemical elements. This is confirmed by the data for the higher hardness of the coatings having smaller sizes of the particles. As it can be seen from Table 8.1, the hardness of the coatings decreases with the increase in their size. In the case of particles of size 5 µm, the hardness of the coatings having heat treatment reaches 64 HRC, while for the coatings with powder particles 55 µm the hardness of the coating with heat treatment is 53 HRC.

The size of the powder particles in the coating exerts influence on the mechanisms of the wearing process. In the cases of coatings having smaller

sizes of the particles from 5 µm and up to 35 µm and loading of 5 up to 15 N, the prevailing mechanism is that of micro-cutting without visible traces of plastic deformation. At higher loading of 20 N and 25 N for these coatings, one can observe traces of micro-cutting and small volumes of pushed-away material from the furrows of wearing. In the cases of coatings having larger sizes of the particles from 35 µm up to 55 µm at greater loadings the prevailing mechanism to a great extent is that of plastic deformation, while at small and medium loadings one observes a mixed mechanism of abrasive wearing – the presence of furrows of micro-cutting and plastic deformation.

8.3 CONCLUSION

The present chapter represents comparative results for the characteristics of the wearing process and the wear resistance of 12 types of composite powder coatings, combined in six series – I, II, III, IV, V, VI. All the composites have identical chemical compositions, but they contain particles of different sizes – 5 µm, 11 µm, 22 µm, 35 µm, 45 µm, and 55 µm. From each series of powder composites two types of coatings have been deposited – on the substrate without preliminary heat treatment (cold HVOF process) and on a substrate with preliminary heat treatment up to a temperature of 650°C in 60 minutes.

Results have been obtained and the respective dependences of the mass wear and the linear wear, the wear intensity, the absolute and the relative wear resistance on the friction path length, the normal loading, and the size of the powder particles for all the tested coatings - without and with preliminary heat treatment of the substrate.

It has been established, that:

- The preliminary heat treatment of the substrate influences the magnitude and the mechanisms of the abrasive wear, whereupon it leads to a lowering of the intensity of wear for all the tested coatings, which is due to enhancement of the hardness of the coatings;
- The increase in the abrasive wearing upon increasing the friction path length has linear character for all the tested coatings;
- Upon increasing the normal loading the abrasive wearing is increasing linearly for all the tested coatings;
- The sizes of the composite particles exert an effect upon the magnitude of the abrasive wear. Upon increasing the size of the particles the wear grows up and the dependence has a wave-like character. The degree of non-linearity depends on the magnitude of the normal loading.
- The sizes of the composite particles influence the mechanisms of the abrasive wearing process unified with the normal loading: in cases of coatings having small sizes of the particles from 5 µm and up to 35 µm and small loadings of up to 15 N the prevailing mechanism of wearing is micro-cutting, while at the higher loading of 20 N and 25 N for these coatings one observes traces of micro-cutting and plastic deformation. In cases of coatings having larger sizes of the particles from 35 µm up to 55 µm at high

loadings the mechanism of plastic deformation is prevailing, while at small and medium loadings there occurs mixed mechanism of the abrasive wearing process – micro-cutting and plastic deformation.

_____

Comparative Studies of HVOF-coatings of WC/Co and Chromium Galvanic Coatings, Modified with Nano-diamond Particles

9.1 GENERAL EVIDENCE

It is now more than 70 years since the galvanic chromium coatings played the role of „golden standard" for achieving на high wear resistance of details, operating under extreme conditions – abrasion, erosion, cavitation, corrosion, impact, and vibration loadings.

The modification of chromium galvanic coatings by nanosized particles promotes their mechanical and tribological characteristics. This fact explains the great interest and the numerous studies in the field of nano-technologies and nano-tribology [48-50].

The specific conditions during the preparation of chromium galvanic coatings, containing sixth-valency chromium, require extraordinary highly strict measures for the safety of human labour and protection of the environment from waste toxic chromium electrolytes.

The basic disadvantages of galvanic chromium coatings consist of the following:

- Non-uniform distribution of the thickness of the chromium coating over the underlayer basic surface;
- Considerable porosity and high internal tension, which deteriorates the resistance against fatigue wearing and corrosion;
- High sensitivity of the structure, the mechanical and the tribological characteristics concerning the composition of the electrolyte and the parameters and the kinetics of the regime of electrolysis;
- Impossibility to restore significantly worn-out details due to the great brittleness of the thicker chromium coatings;
- Impossibility to deposit galvanic chromium coatings on special steels having a high content of tungsten and cobalt, and also on cast iron of great hardness.

A promising alternative to replace the galvanic chromium coatings is represented by the composite tungsten carbide coatings WC/Co, deposited by the high velocity oxy-flame process (HVOF). The HVOF-technology belongs to the superior contemporary technologies due to its ecological aspect, economy of the

Wear of High-Technology Coatings, Deposited by High-Velocity Oxygen Flame (HVOF)
Comparative Studies of HVOF-coatings of WC/Co and Chromium Galvanic Coatings, Modified with
Nano-diamond Particles

expenses and much greater productivity in comparison to the galvanic chromating process.

The tungsten carbide coatings, deposited by the HVOF-technology, are a new generation of powder composite coatings, which find application in important details and nodes of the aviation technics, the space industry, energy production, in the petroleum and chemical industry and some others.

The Table 9.1 represents some comparative characteristics of tungsten carbide coating WC/Co and those of galvanic chromium coating based on data from current literature sources [5].

Table 9.1. Comparative values of some parameters of galvanic chromium coating and of the HVOF coating WC/Co

Parameter	Galvanic chromium coating	HVOF coating WC/Co
Hardness, HRc	60-70	>70
Micro-hardness, DPH 300	750-850	>1050
Adhesion strength, MPa(psi)	41 (60 00)	> 80 (10 000)
Porosity, %	Submicro-cracks	< 1
Thickness, mm	< 0.13	> 1
Oxides, %	> 1	<1

The subject of the present chapter is a comparative investigation of the abrasive wear and the coefficient of friction of galvanic chromium coatings without any nano-particles, galvanic chromium coatings, modified with different concentration of nano-diamond particles, and tungsten carbide coating WC/Co (88/12) under identical conditions of friction [51].

9.2 EXPERIMENTAL PROCEDURES

The composite galvanic chromium-nanodiamond coatings have been deposited on cylindrical samples of diameter 30 mm and height 10 mm of steel, which has chemical composition, represented in Table 9.2.

Table 9.2. Chemical composition (wt. %) based on steel, upon which galvanic chromium-nanodiamond coatings have been deposited

Chemical element	C	S	Mn	P	Si	Cr	Ni	Fe
%	0.4	0.045	0.55	0.45	0.20	0.30	0.30	Balance

The chromium-containing electrolyte for obtaining chromium-diamond coatings has the following composition: CrO_3 – 220 g/l, H_2SO_4 – 2,2 g/l. Chromium-nanodiamond coatings have been obtained by three different technological regimes through variation of the density of the current: 45 A/dm^2 and 60 A/dm^2 and duration of the process – 35 and 45 minutes (Table 9.3).

Wear of High-Technology Coatings, Deposited by High-Velocity Oxygen Flame (HVOF)
Comparative Studies of HVOF-coatings of WC/Co and Chromium Galvanic Coatings, Modified with
Nano-diamond Particles

Table 9.3. Technological regimes for deposition of galvanic chromium coatings having different concentrations of nano-diamond particles

Regimes	R1	R2	R3
Current density, A/dm^2	45	45	60
Duration, min	35	45	35

The three regimes R1, R2 and R3 make use of nano-diamond particles having one and the same size 25 nm and variation of the concentration of the nano-particles – 0,6 g/l, 10 g/l, 15 g/l and 20 g/l. The nano-diamond particles are added to the electrolyte as aqueous suspension. The process of deposition of the coatings is occurring during intensive stirring of the electrolyte. The temperature in the electrolyte bath is constant within the range 52-55°C.

The composite coating WC/Co(88/12) has been deposited by the HVOF-technology upon the flat surface of cylindrical samples having the same sizes and the same chemical composition of the steel (Table 9.2). The coating is deposited using the system MICROGET+Hibrid at parameters of the technological regime, indicated in Table 9.4. The average size of the particles of the powder composite alloy WC/Co(88/12) is 35 μm.

Table 9.4. Parameters of the technological regime for the deposition of HVOF coatings

№	Parameter	Technological regime
1.	Propylene/oxygen ratio, %	55/100
2.	Jet velocity, m/s	1000
3.	Distance „nozzle-coating" L, mm	120
4.	Angle between nozzle and coating, α , grad	90
5.	Air pressure from compressor, bar	5
6.	N$_2$ pressure in the proportioning device, bar	4
7.	Velocity of powder material feeding, tr/min	1,5
8.	Mass flow rate of the powder material, g/min	22

The obtained galvanic chromium-nanodiamond coatings and the coating WC/Co have not been subjected to additional heat treatment.

The thickness of the obtained coatings has been measured by the device Pocket LEPTOSKOP 2021Fe in eight points on the contact surface. The hardness of the coatings has been measured by the device Equotip Bambino 2.

The abrasive wear of the galvanic chromium, chromium-nanodiamond coatings and WC/Co (88/12) HVOF-coating has been studied under conditions of dry friction over surface with solid fixed abrasive particles using the tribo-tester „Pin disc". All the tests have been carried out under identical conditions of the contact interaction – loading, sliding velocity, friction path length and type and parameters of the abrasive material (Table 9.5).

Wear of High-Technology Coatings, Deposited by High-Velocity Oxygen Flame (HVOF)
Comparative Studies of HVOF-coatings of WC/Co and Chromium Galvanic Coatings, Modified with
Nano-diamond Particles

Table 9.5. Parameters of testing the abrasive wear

Normal loading pressure	P = 10,3 N
Nominal contact area	$A_a = 706,5.10^{-6}$ m^2
Nominal contact pressure	$P_a = 1,46$ N/cm^2
Average rate of sliding	V = 0,82 m/s
Friction path length	L=630 m
Abrasive surface	Corrundum P 320

The coefficient of friction for each experiment is calculated by the Law of Leonardo-Amonton according to the formula:

$$\mu = T \ / \ P \tag{9.1}$$

where T is the force of friction, while P – the normal loading in the center of the sample.

For comparing the coatings two relative criteria have been introduced – K_{ND} and K_{WC}. The first criterion K_{ND} characterizes the influence of the concentration of the nao-diamond particles on the wear resistance of chromium-nanodiamond coatings:

$$K_{ND} = \frac{I(Cr - ND)}{I(Cr)} \tag{9.2}$$

And it represents dimensionless ratio between the wear resistance of the chromium coating, containing nano-diamond particles $I(Cr - ND)$ and the wear resistance of the chromium coating without nano-diamond particles $I(Cr)$ for identical conditions of friction.

The second comparative criterion $K_{WC/Co}$ illustrates how many times the coating WC/Co (88/12), deposited by the HVOF-technology, has greater wear resistance than the chromium-nano-diamond coating. It represents the ratio between the wear resstance of coating WC/Co (88/12) - $I(WC/Co)$ and the wear resstance of the electrolytic chromium coating with nano-diamond particles - $I(Cr - ND)$, i.e.

$$K_{WC \ / \ Co} = \frac{I(WC / Co)}{I(Cr - ND)} \tag{9.3}$$

9.3 EXPERIMENTAL RESULTS

The Fig. 9.1 represents the microstructure of galvanic chromium coating, deposited by technological regime R1 in the case a) without nano-diamond particles and in the case b) with nano-diamond particles of concentration 10 g/l.

Wear of High-Technology Coatings, Deposited by High-Velocity Oxygen Flame (HVOF)
Comparative Studies of HVOF-coatings of WC/Co and Chromium Galvanic Coatings, Modified with
Nano-diamond Particles
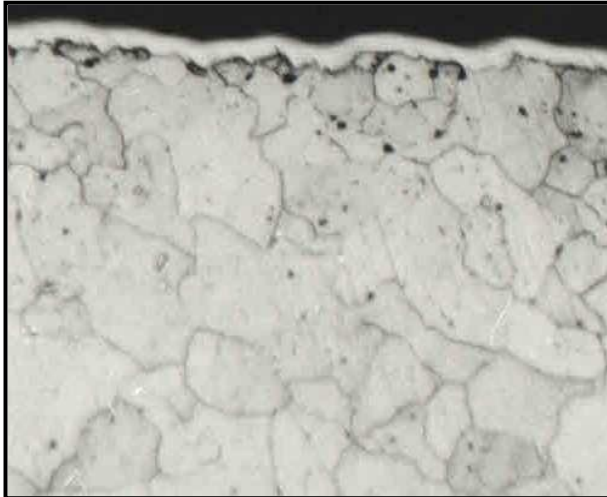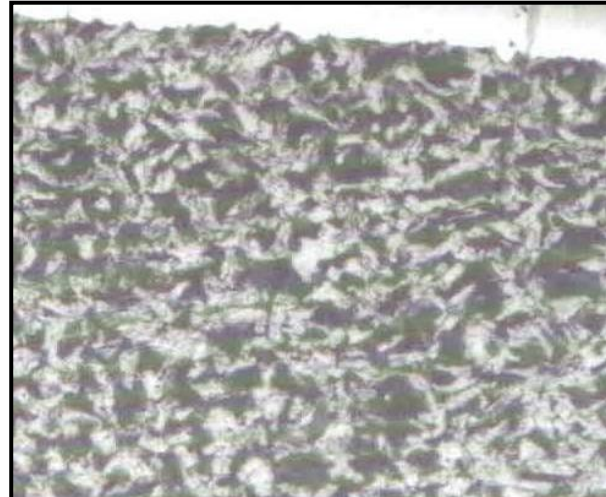
| a) Coating without nanodiamond particles | b) Coating with nanodiamond particles 25 nm and concentration 10 g/l |

Fig. 9.1. Microstructure of galvanic chromium coating on steel, current density – 45 A/dm^2, time of the process – 35 min, x200

Wear of High-Technology Coatings, Deposited by High-Velocity Oxygen Flame (HVOF)
Comparative Studies of HVOF-coatings of WC/Co and Chromium Galvanic Coatings, Modified with
Nano-diamond Particles
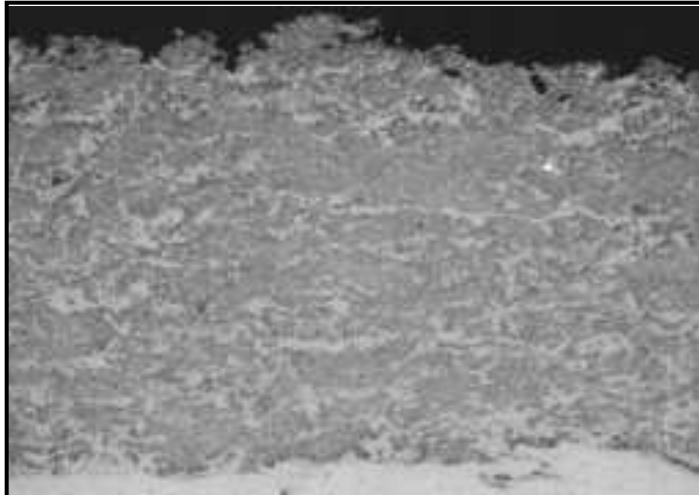
a) Texture

b) Microstructure x200

Fig. 9.2. Microstructure of WC/Co (88/12) HVOF- coating on steel

Wear of High-Technology Coatings, Deposited by High-Velocity Oxygen Flame (HVOF)
Comparative Studies of HVOF-coatings of WC/Co and Chromium Galvanic Coatings, Modified with
Nano-diamond Particles

Table 9.6. Data for the thickness, microhardness, mass wear, wear resistance and the coefficient of friction of the studied galvanic coatings and coating WC/Co (88/12)

№	Sample	Coating	Concentration NDDS	Thickness µm	Micro Hardness MPa	Mass Wear g	Wear resistance m/kg	COF
1	0-R1	Cr	0	20-35	5906	42.2×10^{-3}	1.5×10^{7}	0.35
2	1-R1	Cr-(0.6)ND	0,6 g/l	12-16	8170	89×10^{-3}	0.7×10^{7}	0.46
3	2-R1	Cr-(10)ND	10 g/l	6-23	7907	32.4×10^{-3}	2×10^{7}	0.24
4	3-R1	Cr-(15)ND	15 g/l	10-20	8260	34.3×10^{-3}	1.8×10^{7}	0.26
5	4-R1	Cr-(20)ND	20 g/l	13-17	8401	$40. \times 10^{-3}$	1.6×10^{7}	0.32
6	0-R2	Cr	0	7-11	6010	40.4×10^{-3}	1.6×10^{7}	0.31
7	1-R2	Cr-(0.6)ND	0.6 g/l	33-40	8172	72.10^{-3}	0.9×10^{7}	0.42
8	2-R2	Cr-(10)ND	10 g/l	23-38	8196	68.4×10^{-3}	0.9×10^{7}	0.40
9	3-R2	Cr-(15)ND	15 g/l	22-25	8455	53.5×10^{-3}	1.2×10^{7}	0.38
10	4-R2	Cr-(20)ND	20 g/l	22-26	8613	44.4×10^{-3}	1.4×10^{7}	0.36
11	0-R3	Cr	0	18-32	6890	80.2×10^{-3}	0.8×10^{7}	0.42
12	1-R3	Cr-(0.6)ND	0.6 g/l	29-34	8075	49.1×10^{-3}	1.3×10^{7}	0.37
13	2-R3	Cr-(10)ND	10 g/l	26-29	7618	51.2×10^{-3}	1.2×10^{7}	0.38
14	3-R3	Cr-(15)ND	15 g/l	20-25	8520	66.4×10^{-3}	0.9×10^{7}	0.40
15	4-R3	Cr-(20)ND	20 g/l	18-24	9820	96.8×10^{-3}	0.6×10^{7}	0.58
16	WC/Co	WC/Co (88/12)		220	72 HRc	5.8×10^{-3}	10.8×10^{7}	0.14

Wear of High-Technology Coatings, Deposited by High-Velocity Oxygen Flame (HVOF)
Comparative Studies of HVOF-coatings of WC/Co and Chromium Galvanic Coatings, Modified with
Nano-diamond Particles
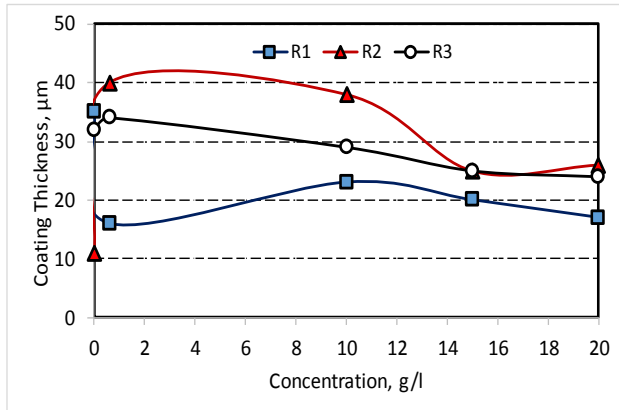
Fig. 9.3. Influence of the concentration of NDDS on the thickness of the coating

Fig. 9.4. Influence of the concentration of NDDS on the microhardness of the coating

Wear of High-Technology Coatings, Deposited by High-Velocity Oxygen Flame (HVOF)
Comparative Studies of HVOF-coatings of WC/Co and Chromium Galvanic Coatings, Modified with
Nano-diamond Particles
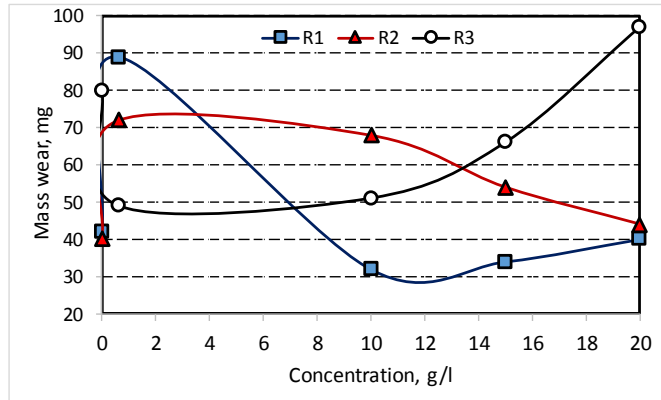
Fig. 9.5. Influence of the concentration of NDDS on the mass wear
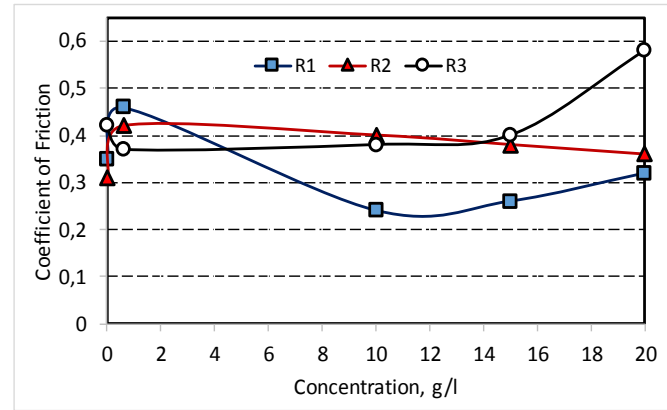
Fig. 9.6. Influence of the concentration of NDDS on the coefficient of friction

Wear of High-Technology Coatings, Deposited by High-Velocity Oxygen Flame (HVOF)
Comparative Studies of HVOF-coatings of WC/Co and Chromium Galvanic Coatings, Modified with
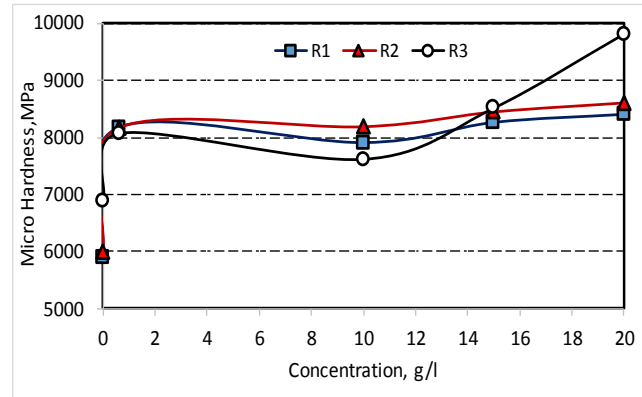*Nano-diamond Particles*

Fig. 9.7. Diagram of criterion

Fig. 9.8. Diagram of criterion

Wear of High-Technology Coatings, Deposited by High-Velocity Oxygen Flame (HVOF)
Comparative Studies of HVOF-coatings of WC/Co and Chromium Galvanic Coatings, Modified with
Nano-diamond Particles
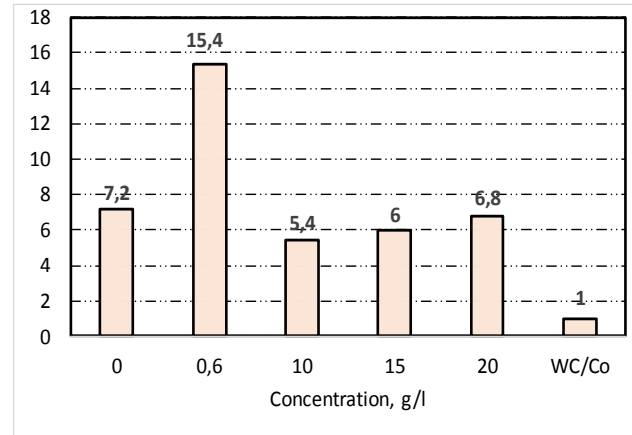
The Fig. 9.2 illustrates the microstructure of the coating WC/Co (88/12), deposited by the HVOF – process using the regime, described in Table 9.4.

The obtained results for the thickness, hardness, mass wear, wear resistance and coefficient of friction for all the coatings, are represented in Table 9.6.

Fig. 9.3 and Fig. 9.4 illustrate graphically the variation of the thickness and the microhardness of the galvanic chromium-nanodiamond coatings depending on the concentration of the nano-diamond particles in the electrolyte for the three regimes of deposition R1, R2 and R3.

Fig. 9.5 and Fig. 9.6 represent graphically the variation of the mass wear and the coefficient of friction of the galvanic chromium-nanodiamond coatings versus the concentration of the nano-diamond particles in the electrolyte for the three regimes of deposition R1, R2 and R3.

Fig. 9.7 and Fig. 9.8 represent the diagrams of the two criteria at different concentrations of the nano-diamonf particles of the chromium coatings in the case of regime R1 and the coating WC/Co (88/12).

9.4 ANALYSIS OF THE RESULTS AND OBSERVATIONS

On the basis of the comparative results for galvanic chromium and chromium-nanodiamond coatings the following interpretations are derived and conclusions can be drawn:

- The addition of nano-diamond particles (NDDS) in the electrolytic chromium coating exerts effects on the thickness, the hardness, the wearing process and on the coefficient of friction. The character and the absolute value of this influence depend on the technological regime for deposition of the coatings – density of the current, duration of the process and concentration of the nano-diamond particles.
- At small concentration of NDDS – 0,6 g/l in the cases of the three technological regimes R1, R2, R3 the wearing degree grows up in comparison with the wearing of chromium coating without NDDS (Fig. 9.5) The wear resistance of these coatings decreases with 50% in comparison with the wear resistance of the chromium coating without NDDS.
- The dependence of the mass wear on the concentration of NDDS has non-linear character and the type of the curve depends on the regime of deposition of the coating – Fig. 9.5.
- The lowest wear degree is shown by the chromium-diamond coating, deposited upon applying the regime R1 at concentration of NDDS 10-15 g/l (Fig. 9.5). The wear resistance of these coatings increases with 30% with respect to the wear resistance of chromium coating without NDDS.
- The curve of variation of the coefficient of friction on the concentration of NDDS (Fig. 9.6) for the same regime R1 has analogous character with that of the curve of variation of the wear (Fig. 9.5). Upon increasing the concentration of NDDS COF grows up from 0.35 up to 0.46, while

Wear of High-Technology Coatings, Deposited by High-Velocity Oxygen Flame (HVOF)
Comparative Studies of HVOF-coatings of WC/Co and Chromium Galvanic Coatings, Modified with
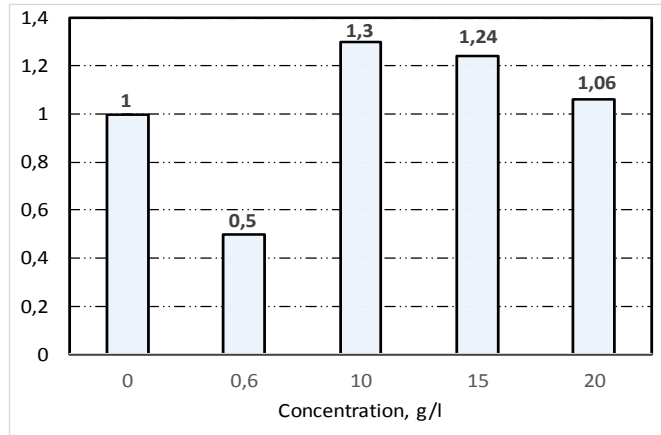*Nano-diamond Particles*

thereafter it is decreasing, passing through a minimum of 0,24 at concentration 10 g/l of NDDS and then gradually it is increasing up to 0.32 at concentration 20 g/l (Fig. 9.6). In the cases of technological regimes R2 and R3 COF preserves constant value, whereupon at concentration 20g/l applying regime R3 a sharp increase in COF is observed having maximal value of 0,58 for all the studied coatings. This corresponds to the greatest wear of the same coating – Fig. 9.5, curve R3.

- The electrolytic chromium and chromium-nanodiamond coatings have non-uniform distribution of the thickness and its absolute value depends on the technological regime and on the concentration of NDDS (Fig. 9.3). Upon increasing the concentration of NDDS the thickness of the coating grows up to a certain value and thereafter it decreases and reaches minimal values at concentration 20 g/l. The lowest thickness is shown by chromium-nanodiamond coatings, deposited by the technological regime R1, which have the lowest wear among all the studied galvanic coatings (Fig. 9.5).

- The presence of NDDS leads to enhancement of the hardness of the chromium coatings (Fig. 9.4). At small concentration 0,6 g/l the hardness of all the coatings is increased with 42% in comparison with the chromium coating without NDDS. The following increase in the concentration of NDDS does not influence the hardness applying the different regimes. An exception is observed in the case of coating, obtained applying the regime R3 and concentration 20 g/l, whereupon the hardness sharply increases with 20% with respect to the hardness of the rest of the coatings. The increased hardness, however, does not lead to increase in the wear resistance of this coating. To the contrary – its wear resistance ($I=0.6.10^7$) is lower than that of the wear resistance of the coatings, obtained by regimes R1 and R2. This once again confirms the fact, that between the wear resistance and the hardness of the surface layer there is not always a direct proportional dependence.

Summarizing the obtained results about galvanic chromium, chromium-nanodiamond coatings and composite coating WC/Co 988/12), deposited by the HVOF technology, we can observe the following:

- ➢ The coating WC/Co (88/12) has the greatest wear resistance compared to all the electrolytic chromium coatings without and with NDDS, obtained by the three regimes R1, R2 and R3.
- ➢ The wear resistance of WC/Co coating is 7,2 times higher than that of the chromium coating without NDDS for the regime R1 and from 5,4 up to 15,4 times higher than the wear resistance of chromium coatings with NDDS within the entire range of variation of their concentration (Figs. 9.3-9.6).
- ➢ The high wear resistance of the WC/Co coating is due to its high density and homogeneous fine-grain structure, built up of grains of WC, bonded with one another with internal contact network of cobalt (Co). The properties and the thickness of this network play an exceptionally

Wear of High-Technology Coatings, Deposited by High-Velocity Oxygen Flame (HVOF)
Comparative Studies of HVOF-coatings of WC/Co and Chromium Galvanic Coatings, Modified with
Nano-diamond Particles

important role in the contact interaction of the coating during friction – small tangential resistance and respectively low degree of wearing.

The results of the carried out comparative investigation give us the reason to draw the main conclusion, that the composite coating WC/Co (88/12), deposited by the HVOF technology, can replace the existing non-ecological chromium and chromium-nanodiamons coatings in the tribological systems.

Determining the Influence of Chromium Concentration on the Erosive Wear of Ni-Cr-B-Si Coatings Applied by Supersonic Flame Jet (HVOF)

ABSTRACT

The object of the present research work is to study the influence of chromium concentration in powder composites on the erosion wear of Ni-Cr-B-Si coatings, deposited by supersonic flame jet upon the substrate without thermal treatment and on substrate with thermal treatment. Without any prior heat treatment of the sub-strate and with some preliminary thermal treatment of the substrate up to 650 C, coatings were produced from each powder composite. The coatings were tested under identical circumstances of abrasive particle erosion in an air stream. The work also represents comparative results for erosion wear and erosion wear resistance of coatings, deposited by supersonic flame jet (HVOF), which contain composites Ni-Cr-B-Si having various chromium concentrations 9.9%; 13.2%; 14%; 16% and 20%, at identical size of the particles 45μm and the same content of the remaining elements boron and silicon. The coatings have been tested in identical regime of erosion using air stream, carrying abrasive particles under the same conditions - nature, sizes and velocity of the particles, duration of erosion, air pressure, distance between the nozzle and the surface, angle of the jet axis with respect to the surface. It has been shown that the angle of the jet stream influences the wear resistance of all the coatings: at jet angle $60°$ the wear resistance grows up within the in-terval from 1.5 up to 2.6 times for the coatings without thermal treatment of the substrate and within the interval from 1.6 up to 3.5 times for the coatings under-going thermal treatment of the substrate in comparison with the wear resistance at angle $90°$. This effect is strongest -3.5 times for the coating No 8 of $16\% Cr$. At jet angle $90°$ the wear resistance increases up to 10% and this increase is one and the same for all the coatings. The found relationship between erosive wear resistance and Cr concentration exhibits a considerable non-linear character. Wear resistance increases as the Cr concentration increases, reaching a maximum for 16 percent Cr coatings with thermal treatment of the substrate at jet angle of 60°. It has been found out that the wear resistance of the coatings, having the highest Cr content -20%, but not containing the elements boron and silicon, is lower or almost equal to the wear resistance of the coatings having the lowest Cr concentration -9.9%.

Keywords: HVOF coatings; chromium; tribology; erosion wear.

Wear of High-Technology Coatings, Deposited by High-Velocity Oxygen Flame (HVOF)
Determining the Influence of Chromium Concentration on the Erosive Wear of Ni-Cr-B-Si Coatings
Applied by Supersonic Flame Jet (HVOF)

10.1 BACKGROUND

The erosion wear of machine parts is caused by the impact of solid or liquid particles carried by a fluid jet stream such as air, water, or oil. It looks to be one of the most harmful types of wear, since it causes rapid disruption of a machine's overall functioning qualities and a reduction in its resource. This, on one side, is connected with large expenses for materials, spare parts, consumables and human resources for maintenance during the process of exploitation. On the other side the problem is associated with pollution of the environment, requiring increase in extraction of raw materials from the natural environment, which is directly connected with the equilibrium in the eco-systems [1-7].

The basic factors, on which the erosion wear rate depends are the nature, the dimensions and the form, the amount of solid particles, the direction of the stream and the velocity of the stream, the chemical composition and the mechanical properties of the surface layers, the chemical composition of the working environment [8-16].

The mechanical aspect of abrasion and erosion wear processes is a common trait. The distinction is that abrasion is dominated by varied intensities of plastic deformation and microsplitting of the surface layer, whereas erosion is caused by numerous impact actions of solid or liquid particles, with exhaustion wear as the main process of degradation. Both modes of degradation may be present in combination depending on the stream direction and particle flow rate.

One of the methods for promotion of the erosion wear resistance of the surface layers is the deposition of composite powder coatings of super alloys. The deposition of such coatings is accomplished using High Velocity Oxy-Fuel (HVOF), which represents great interest for the practice during the last two decades. The variation of the chemical composition of the powder composites and the concentrations of the separate chemical elements enables achieving within a wide range the desired combination of mechanical and tribological characteristics - high adhesion strength, density, hardness, wear resistance [17-22]. The spraying methods, counter materials, and normal loads were ranked based on the wear loss and coefficient of friction. The main wear mechanisms on the coating's wear track are abrasive and adhesive. The HVOF spraying method revealed enhanced wear resistance property as compared to the plasma-sprayed coating [23]. Recent publications have shown that the HVOF technique can be used both for the manufacture of new coatings and for the recovery of rods that have already been used. An advantage of the HVOF process is that is produces a coating with high density, low oxide content and good adhesion [24,25]. The powder particles in the supersonic flame jet at high temperature and high velocity, passing over to semi-plastic and plastic state, upon their collision with the substrate become involved in contact interaction with the substrate and between each other, forming inter-metallic phases of great hardness and plasticity. The specialized literature and practice report data on wide-scope of application of two groups of powder composites: based on nickel - chromium -

Wear of High-Technology Coatings, Deposited by High-Velocity Oxygen Flame (HVOF)
Determining the Influence of Chromium Concentration on the Erosive Wear of Ni-Cr-B-Si Coatings
Applied by Supersonic Flame Jet (HVOF)

boron - silicon (Ni-Cr-B-Si) and powder composites based on cobalt: tungsten - cobalt - chromium alloys. The chromium at high temperatures enters into contact interactions with carbon, silicon and boron forming new inter-metallic structures. It interacts with carbon to form solid high-melting structure (Cr_3C_2) of green colour, which is not soluble in acids and it attributes high corrosion stability to the coating. Chromium forms with oxygen some oxides (CrO_3, Cr_2O_3) , which are characterized by great hardness and fragility y [4,26-31]. In papers [32-33].

interesting results concerning ceramic coatings are represented, obtained on a matrix of alumina Al_2O_3 with the addition of 3% titanium oxide TiO_2, and also of zirconium oxide (ZrO_2) matrix with 30% calcium oxide (CaO) on the base of non-alloy structural steel of class S235JR. The buffer layer was obtained from a metal powder based on Ni-Al-Mo. Comprehensive studies with metallographic tests, phase composition, microhardness, adhesion of the coating to the substrate, resistance to abrasion and heat shock show that the coatings are characterized by high adhesion to the substrate, high abrasion and erosion resistance, as well as cyclic resistance load. In a paper [34] the same authors present the results of studies on the mechanical properties of aluminum coatings reinforced with carbon materials of nanoscale: carbon nanotubes Nanocyl NC $7000(0.5 \text{wt}.\%$ and $1 \text{wt}.\%$) and carburite ($0.5 \text{wt}.\%$). It has been proven that the obtained coatings with nanocarbon particles can be an effective alternative to coatings applied with laser technology and they can be successfully applied in the automotive, aerospace and aerospace industries through further refinement. In Ref [35], it has been shown that tungsten matrix (WC-Co) coatings containing NiCr-Si-B particles, obtained by detonation spraying have significantly higher wear resistance under extreme erosion conditions compared to a conventional cobalt matrix. In this article interesting results are presented for increasing the economic efficiency of coatings applied by thermal injection in the restoration of parts in abrasion and erosion resistance of thermo-sprayed coatings applied to WC-Co abrasion and erosion resistance of thermo-sprayed coatings applied to WC-Co obtained concerning the influence of the abrasive particle velocity and the particle impact angle on tungsten carbide (WC) - coated with inclusive nanosized particles of $Cr_3C_2 - NiCr75 - 25$ and $NiCrWSiFeB$ powder compositions. It has been found out that with the decrease of the size of the powder particles in the WC-CoCr coating, its erosion resistance increases. This is a result of improving the physical and mechanical properties of the coating: low porosity, high microhardness and toughness. The increase in the velocity of the particles during erosion flow leads to an increase in wear rate due to their high kinetic energy. It was found out that the maximal erosion wear is observed at large angles of impact $-90°$, which is due to the tired mechanism of destruction of the surface. The increase in wear resistance against cavitation erosion has also been confirmed in WC-CoCr metalceramic coatings applied by HVOF process with nanosized particles of powder particles compared to the wear resistance of WC-CoCr coatings with micron particle sizes [36].

Wear of High-Technology Coatings, Deposited by High-Velocity Oxygen Flame (HVOF)
Determining the Influence of Chromium Concentration on the Erosive Wear of Ni-Cr-B-Si Coatings
Applied by Supersonic Flame Jet (HVOF)

The object of the present research work is to study the influence of chromium concentration in powder composites on the erosion wear of Ni-Cr-B-Si coatings, deposited by supersonic flame jet upon the substrate without thermal treatment and on substrate with thermal treatment. The erosion wear is accomplished by the impact of air stream upon the coating, carrying solid abrasive particles at two angles of interaction of the stream with the surface $-60°$ and $90°$.

The current paper is a continuation of the paper [37].

10.2 EXPERIMENTAL

Ten types of coatings were prepared, obtained from five composite powder mixtures with nickel matrix, united in five series A, B, C, D, E (Table 10.1). The series of compositions A, B, C, D contain different weight concentrations of chromium $-9.9\%, 13.2\%, 14\%, 16\%$ and approximately the same composition of the other chemical elements - Si, B, Fe, Cu, Mo and etc. The composite mixture of series E (samples No and No 10) contains $20\%Cr$ and $80\%Ni$, ie. it does not include other elements present in the compositions of series A, B, C, D.

From each series two types of coatings are applied - without preliminary heat treatment of the substrate (cold HVOF process) and with preheating of the substrate in a thermal chamber at a temperature of $650°C$ for 60 minutes. Substrate heat treatment coatings are designated PHS [38].

All the coatings have been deposited upon a support of one and the same material - steel of chemical composition: $C - 0.15\%; S - 0.025\%; Mn - 0.8\%$; $P - 0.011\%; Si - 0.21\%; Cr - 0.3\%; Ni - 0.3\%$ and hardness $193.6 \div 219.5HV$. All coatings are applied on a substrate of the same material - steel with the above chemical composition: $C - 0.15\%; S - 0.025\%; Mn - 0.8\%; P - 0.011\%; Si - 0.21\%; Cr - 0.3\%; Ni - 0.3\%$ and hardness $193.6 \div 219.5HV$. The pad is a plate with dimensions: length 90 mm, width 20 mm and thickness 6 mm. After applying the coatings, 3 samples with dimensions of 30 mm $\times 20$ mm $\times 6$ mm were cut out of each plate, which are tested for erosion wear.

The particles in all the powder form composites have one and the same size $-45 \pm 2,5\mu$m.

Aiming at enhancement of the adhesion strength of the coatings the substrate is being treated in advance in three stages: cleaning, erosion under the effect of abrasive particles (blasting) and mechanical treatment. The cleaning is aimed at removal of the mechanical contaminants, adsorbed organic molecules, moisture and other components and it is carried out using a solvent. The extraction of the adsorbed gas molecules and elements in the depth of the surface layer is achieved by calcinations of the surface of the substrate with a flame jet up to $100°C$ at a distance of the nozzle 40 mm and angle $45°$ or by using vapour-flow apparatus. After this operation again the surface is cleaned with a solvent.

Table 10.1. Description, chemical composition, hardness and thickness of the tested coatings

Series	Sample	Coating designation	Description	Chemical com position, wt. %	Hard ness HRC	Thickness μm
A	1	NiBSi-9.9Cr	Coatings without heat treatment of the substrate	Cr : 9,9; Si : 3.1; B : 1.7; Fe : 3.2;	55+56 HRC	410-415
	2	NiBSi-9.9Cr : PHS	Coatings with heat treatment of the substrate	C : 0.35; Mo : 3; Cu : 3; Ni Balance	58-59 HRC	400-412
B	3	NiBSi-13.2Cr	Coatings without heat treatment of the substrate	Cr : 13.2; Si : 3.98; B : 2.79; Fe :	56+57 HRC	395-400
	4	NiBSi-13.2Cr PHS	Coatings with heat treatment of the substrate	4.6; Co : 0.03; C : 0.63; Ni : Balance	59+60 HRC	408-414
c	5	NiBSi-14Cr	Coatings without heat treatment of the substrate	Cr : 14; Si : 4.2; B : 2,9; Fe : 4,6;	57-58 HRC	395-406
	6	NiBSi-14Cr.PHS	Coatings with heat treatment of the substrate	C : 0.6; Mo : 2,5; Cu : 2,4; Ni : Balance	59-60 HRC	400+405
D	7	NiBSi-16Cr	Coatings without heat treatment of the substrate	Cr : 16; Si : 4; B : 3.4; Fe : 2.7;	58-59 HRC	394-405
	8	NiBSi-16Cr.PHS	Coatings with heat treatment of the substrate	C : 0.6; Mo : 3; Cu : 3; Ni : Balance	61-62 HRC	404-410
E	9	Ni80-20Cr	Coatings without heat treatment of the substrate		54-55 HRC	400-408
	10	Ni80-20Cr PHS	Coatings with heat treatment of the substrate	Cr : 20; Ni : 80	57-60 HRC	393+403

Wear of High-Technology Coatings, Deposited by High-Velocity Oxygen Flame (HVOF)
Determining the Influence of Chromium Concentration on the Erosive Wear of Ni-Cr-B-Si Coatings
Applied by Supersonic Flame Jet (HVOF)

Upon erosion of the surface of the substrate (blasting) one can achieve a specific level of the roughness of the substrate, which is of essential importance for the value of the adhesion strength of the coating. The abrasive material „Grit" is used, in accordance with the requirements of the ISO 11126 standard procedure, having grain size and composition of the abrasive material in the following percentage ratio: $3.15 \div 1.4 \text{ mm} - 9.32\%; 1.63 \div 0.5 \text{ mm} - 16.4\%; 1.4 \div 1.0 \text{ mm} - 15.8\%; 1.0 \div 0.63 \text{ mm} - 39.6\%; 0.5 \div 0.315 \text{ mm} - 9.32\%; 0.315 \div 0.16 \text{ mm} - 9.32\%$; particles of size below 0.15 mm of different fractions - up to 100% of the following chemical compounds: $SiO_2 - 41\%$, combined in the form of silicates; $Al_2O_3 - 8.3\%, MgO - 6.6\%, CaO - 5.5\%$ and $MnO - 0.4\%$.

The system for blasting has the following technical parameters: input pressure 8 atm; operating pressure in the nozzle -4 atm; diameter of the nozzle 7 mm; distance between the nozzle and the surface -30 mm; angle of interaction of the jet with the surface $-90°$.

The coatings have been deposited using the device MICROJET+Hybrid, which applies fuel mixture consisting of acetylene (propylene) and oxygen. The parameters of the technological regime of deposition of the coatings are listed in Table 10.2.

Prior to deposition of the coatings without thermal treatment (cold HVOF process) the surface of the substrate is heated by the flame up to temperature $200°C$, which is measured by Laser infrared thermometer INFRARED with an error of $0.5°C$.

The coating is deposited in several layers. In the case of the first layer the nozzle is situated at an angle of $45°$ and at a distance from the substrate 10 mm, while the consecutive layers - at a distance of 25 mm. Coatings have been obtained having thickness within the limits $393 \mu m$ up to $415 \mu m$. The thickness of the coatings has been measured using a portable device Pocket Leptoskop $2021Fe$ with an error of $1 \mu m$. Measurements were made at 10 points on the surface and the mean arithmetic value was accepted (Table 10.2). The error of the device is $1 \mu m$.

Table 10.2. Technological regime parameters for HVOF coating deposition

Parameter	Technological regime
Propylene/oxygen ratio	55/100,%
Jet velocity	1000 m/s
Distance 'nozzle-coating'	100 mm
Angle between nozzle and coating	90°
Aur pressure from compressor	5 bar
N, pressure in the proportioning device	4 bar
Velocity of powder material feeding	1.5 min^{-1}
Mass flowrate of the powder material	22 g/min

Wear of High-Technology Coatings, Deposited by High-Velocity Oxygen Flame (HVOF)
Determining the Influence of Chromium Concentration on the Erosive Wear of Ni-Cr-B-Si Coatings
Applied by Supersonic Flame Jet (HVOF)

After polishing all the surfaces of the coatings have the same roughness Ra = 0.450÷0.455 μm, which has been measured by recording of the profile diagram using profile-meter 'TESA Rugosurf 10-10G' with an error μm.

The hardness of the coatings has been measured using hardness-meter 'Bambino' based on the scale of Rockwel (HRC), whereupon the mean arithmetic value out of three measurements for each sample is used in order to eliminate the possible effects of segregation.

The erosion wear of the studied coatings has been accomplished by means of air stream, carrying abrasive particles in atmospheric environment. The functional scheme of the device is represented in Fig. 10.1.
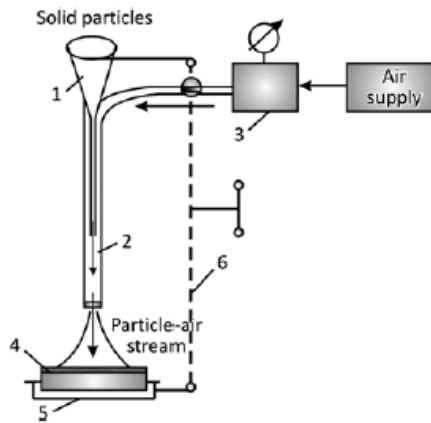
Fig. 10.1. Schematic diagram of erosive wear testing

The designation of this device is to produce bi-phase jet «air-abrasive particles» by independent setting and regulation of the parameters of the two separate stationary flows – air flow and abrasive mass flow and more specifically – the air pressure and the flow rate of the abrasive particles.

The abrasive material with defined flow rate is flowing out gravitationally from the chamber 1 and it passes into the mixing chamber 2, where it is being mixed with the incoming air stream having definite pressure. The bi-phase mixture jet «air-abrasive particles» flows out in the form of bi-phase stream and it interacts at preset angle á with the coating 4 of the sample, which is located in the holder 5. The holder 5 is attached to a stand, which enables regulation of the following parameters: distance between the nozzle and the surface of the sample, the angle of interaction á between the axis of the jet and the surface (jet angle).

The flowing out of the jet of abrasive particles from chamber 1 occurs at constant flow rate by means of an additional chamber containing a definite amount of abrasive particles, which is not represented in the scheme. The amount of

Wear of High-Technology Coatings, Deposited by High-Velocity Oxygen Flame (HVOF)
Determining the Influence of Chromium Concentration on the Erosive Wear of Ni-Cr-B-Si Coatings
Applied by Supersonic Flame Jet (HVOF)

abrasive materials, before putting it in the chamber 1, is being sieved using a set of sieves and dried up in a drying box to remove the moisture from the particles. The air flow from a cylinder of compressed air passes through pneumatic-presetting group, which comprises air filter and precipitator for air purification from mechanical particles, moisture and oil vapours; regulator and stabilizer of the pressure. The pressure is measured by a manometer, connected to a camera 3 after the pneumatic-presetting group.

The mass flow rate $\dot{m}_a$ of abrasive material having mass m_a in the device is determined by measuring the time interval t_a for its gravitational flowing out, i.e. without availability of air stream. It is calculated using the formula:

$$\dot{m}_a = \frac{m_a}{t_a} \qquad (10.1)$$

A minimum of 3 measurements is carried out and the mean arithmetic value is taken for the time interval t_a with an error of 0.1 s.

The methodology for studying the erosion wear and the erosion wear resistance using the above described device consists in measurement of the mass erosive wear as the difference between the mass of the sample before treatment and after treatment with bi-phase jet at the same preset parameters: distance between the nozzle and the surface, jet angle a, operating air pressure, type an average size of the abrasive particles, mass flow rate of the abrasive material $\dot{m}_a$, i.e.

$$m_e = m_e^o - m_e^i \qquad (10.2)$$

Having obtained the values of mass erosion wear m_e for each experiment one calculates further the parameters: rate of erosion $\dot{m}_e$, intensity of erosion i_e and erosion wear resistance I_e. The rate of erosion $\dot{m}_e$ represents the destructed mass of the coating per unit of time of the erosion process Δt, in our case it is 1 minute, i.e. it is measured in $\mathrm{mg/min}$:

$$\dot{m}_e = \frac{m_e}{\Delta t} \qquad (10.3)$$

The intensity of erosion i_e represents the ratio between the mass wear rate $\dot{m}_e$ and the mass flow rate $\dot{m}_a$ of the abrasive component in the jet, i.e.:

$$i_e = \frac{\dot{m}}{\dot{m}_a} \qquad (10.4)$$

The intensity of erosion is a non-dimensional quantity.

The erosion wear resistance I_e is determined as reciprocal value of the intensity of the wearing off process i_e. It is a non-dimensional quantity and it shows how many grams of abrasive mass m_a is necessary in order to destroy 1 gram of mass $\dot{m}_e$ on the surface of the sample for a definite period of time Δt of erosion, i.e.

Wear of High-Technology Coatings, Deposited by High-Velocity Oxygen Flame (HVOF)
Determining the Influence of Chromium Concentration on the Erosive Wear of Ni-Cr-B-Si Coatings
Applied by Supersonic Flame Jet (HVOF)

$$I_e = \frac{1}{i_e} = \frac{\dot{m}_a}{\dot{m}} \tag{10.5}$$

The relative erosion wear resistance $R_{i,j}$ is determined by the formula:

$$R_{i,j} = \frac{I_i}{I_j} \tag{10.6}$$

where I_e is the erosion wear resistance of the tested sample, determined based on equation (5), while I_j - wear resistance of the sample, assumed to be a standard for comparison, determined under the same conditions of the wearing off process.

Table 10.3. Parameters used in the erosive wear testing

Test parameter	Value
Solid particles material	Black corundum (Al2O3)
Maximal size of the particles	$600 \mu m$
Air stream pressure	0.1Mpa
Particles flow rate	166.67 g/min
Particles impact angle	90°
Distance between the sample and the nozzle	10 mm
Duration of the test	5minutes
Ambient temperature	24℃

The parameters of the experimental study of the erosion are represented in Table 10.3.

The mass of the samples is measured by electronic balance WP-S-180/C/2 with an accuracy of $0.1 mg$. Before each measurement the sample is cleaned using a solution, neutralizing the static electric charge, and then it is dried up.

10.3 EXPERIMENTAL RESULTS AND DISCUSSION

The experimental results on the mass erosion m_e have been obtained using the described methodology and device, the rate of erosion wear $\dot{m}_e$, the intensity i_e of the erosion, the absolute I_e and the relative $R_{i,j}$ erosion wear resistance for two values of the angle of interaction of the jet with the surface $\alpha - 90°$ and $60°$. The results are represented in Tables 10.4, 10.5 and 10.6.

Fig. 10.2 represents the diagram of the wear intensity for all the tested coatings at both angles of the jet. It can be seen that all the coatings at angle $90°$, i.e. in the case of perpendicular disposition of the jet axis with respect to the surface, display higher intensity of erosion. In this specific case the velocity of the separate particles has large value of its normal component and the destruction is under the impact of multiple bumps on the surface. The mechanism of weariness is prevailing, in which at the initial moment some sub-micro-cracks are occurring, which are growing up gradually into micro-cracks and at certain moment some particles are removed from the surface. The intensity of the wearing process in

Wear of High-Technology Coatings, Deposited by High-Velocity Oxygen Flame (HVOF)
Determining the Influence of Chromium Concentration on the Erosive Wear of Ni-Cr-B-Si Coatings
Applied by Supersonic Flame Jet (HVOF)

this case depends on the chemical composition of the coating and on the magnitude of the cohesion bonding between the particles of the coating. The greatest intensity of the wearing process at jet angle $90°$ is manifested by the coatings Nos 9 and 10 , which have only the elements nickel and chromium in their composition, and absence of the remaining elements - boron, silicon etc. The lack of such elements diminishes the plastic properties of the coatings and the prevailing mechanism is that of fragile destruction. At jet angle $60°$ the wear intensity is lower and this fact is explained by the appearance of tangential component in the velocity of the particles, which has smaller value and for the time interval of erosion it is not sufficient to cause micro-splitting effect of the surface by the particle.
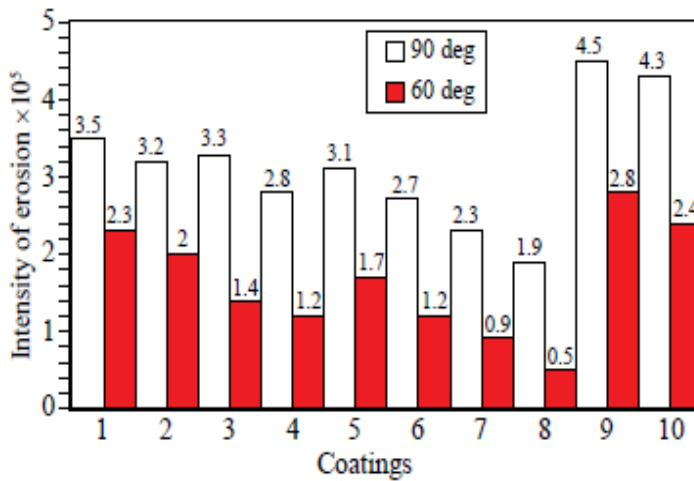

Fig. 10.2. A diagram of the intensity of erosion of the test coatings at an angle of interaction of the jet $90°$ and $60°$

Fig. 10.3 displays the influence of the angle of erosion upon the erosion wear resistance of the coatings in accordance with the results listed in Table 10.6. At jet angle $60°$ the wear resistance is growing up within the interval from 1.5 to 2.6 times for coatings without thermal treatment of the substrate and within the range 1.6 to 3.5 times for coatings with thermal treatment of the substrate. This effect is strongest -3.5 times for the coating No 8 having $16\%Cr$ and with preliminary thermal treatment of the substrate, and it is the weakest -1.5 times for the coating №1 having $9.9\%Cr$ without thermal treatment of the substrate.

Fig. 10.4 and Fig. 10.5 represent the diagrams for the influence of the thermal treatment of the substrate upon the erosion wear resistance at both jet angles.

Table 10.4. Erosive wear of the test coatings at the jet angle of contact with the $\alpha = 90°$

Sample	Coating designation	Mass wear, mg	Wear rate, mg/min	Intensity of erosion	Erosion wear resistance
1	NiBSi-9.9Cr	29.1	5.82	3.49×10^{-5}	2.8×10^4
2	NiBSi-9.9Cr:PHS	26.4	5.28	3.17×10^{-5}	3.2×10^4
3	NiBSi-13.2Cr	27.3	5.46	3.27×10^{-5}	3.1×10^4
4	NiBSi-13.2Cr:PHS	23.5	4.7	2.8×10^{-5}	3.6×10^4
5	NiBSi-14Cr	26.1	5.22	3.13×10^{-5}	3.2×10^4
6	NiBSi-14Cr:PHS	22.8	4.56	2.7×10^{-5}	3.7×10^4
7	NiBSi-16Cr	19.3	3.86	2.31×10^{-5}	4.3×10^4
8	NiBSi-16Cr:PHS	15.7	3.14	1.88×10^{-5}	5.3×10^4
9	Ni80-20Cr	37.8	7.56	4.54×10^{-5}	2.2×10^4
10	Ni80-20Cr:PHS	35.5	7.1	4.3×10^{-5}	2.3×10^4

Table 10.5. Erosive wear of the test coatings at the jet angle of contact with the $\alpha = 60°$

Sample	Coatig designation	Mass wear, mg	Wear rate, mg/min	Intensity of erosion	Erosion wear resistance
1	NiBSi-9.9Cr	19.4	3.88	2.33×10^{-5}	4.3×10^4
2	NiBSi-9.9Cr:PHS	17.0	3.4	2.0×10^{-5}	5.0×10^4
3	NiBSi-13.2Cr	11.4	2.28	1.36×10^{-5}	7.4×10^4
4	NiBSi-13.2Cr:PHS	9.9	1.98	1.2×10^{-5}	8.3×10^4
5	NiBSi-14Cr	13.9	2.78	1.67×10^{-5}	6.0×10^4
6	NiBSi-14Cr:PHS	9.8	1.96	1.2×10^{-5}	8.3×10^4
7	NiBSi-16Cr	7.7	1.54	0.9×10^{-5}	11.1×10^4
8	NiBSi-16Cr:PHS	4.5	0.9	0.54×10^{-5}	18.5×10^4
9	Ni80-20Cr	23.3	4.66	2.79×10^{-5}	3.6×10^4
10	Ni80-20Cr:PHS	19.6	3.92	2.4×10^{-5}	4.1×10^4

Table 10.6. Relative wear rate and the influences of angle and both influences of erosive wear rate of tested coatings

Sample	Coating designation	Wear resistance, min/mg		Relative wear resistance		
				Influence of angle	Influence (R) of substrate heating	
		$\alpha = 90°$	$\alpha = 60°$		$\alpha = 90°$	$\alpha = 60$
1	NiBSi-9.9Cr	2.8×10^4	4.3×10^4	$R_{60/90} = 1.5$	$R_{1.1} = 1$	$R_{1.1} = 1$
2	NiBSi-9.9Cr : PHS	3.2×10^4	5.0×10^4	$R_{60/90} = 1.6$	$R_{2.1} = 1.1$	$R_{2.2} = 1.2$
3	NiBSi-13.2Cr	3.1×10^4	7.4×10^4	$R_{60/90} = 2.4$	$R_{3.3} = 1$	$R_{3.3} = 1$
4	NiBSi-13.2Cr : PHS	3.6×10^4	8.3×10^4	$R_{60/90} = 2.3$	$R_{4.3} = 1.2$	$R_{4.3} = 1.1$
5	NiBSi-14Cr	3.2×10^4	6.0×10^4	$R_{60/90} = 1.9$	$R_{5.5} = 1$	$R_{5.5} = 1$
6	NiBSi-14Cr : PHS	3.7×10^4	8.3×10^4	$R_{60/90} = 2.2$	$R_{6.5} = 1.2$	$R_{6.5} = 1.4$
7	NiBSi-16Cr	4.3×10^4	11.1×10^4	$R_{60/90} = 2.6$	$R_{7.7} = 1$	$R_{7.7} = 1$
8	NiBSi-16Cr : PHS	5.3×10^4	18.5×10^4	$R_{60/90} = 3.5$	$R_{8.7} = 1.2$	$R_{8.7} = 1.7$
9	Ni80-20Cr	2.2×10^4	3.6×10^4	$R_{60/90}\ 1.6$	$R_{9.9} = 1$	$R_{9.9} = 1$
10	Ni80-20Cr : PHS	2.3×10^4	4.1×10^4	$R_{60/90} = 1.8$	$R_{10.9} = 1,1$	$R_{10.9} = 1,2$

Wear of High-Technology Coatings, Deposited by High-Velocity Oxygen Flame (HVOF)
Determining the Influence of Chromium Concentration on the Erosive Wear of Ni-Cr-B-Si Coatings
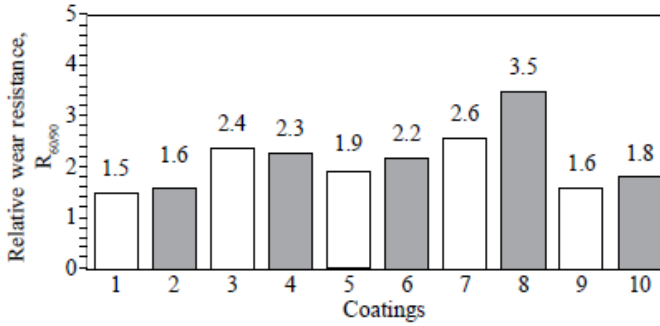*Applied by Supersonic Flame Jet (HVOF)*

Fig. 10.3. Diagram of the influence of the jet angle on the erosion wear resistance of the tested coatings
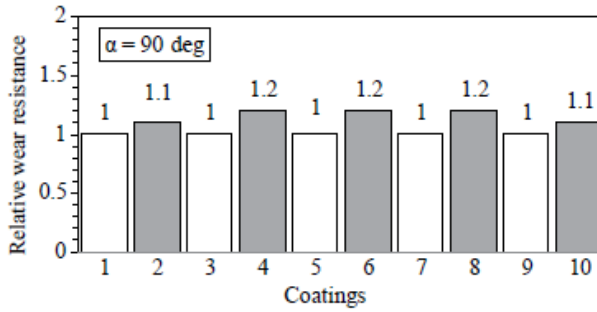

Fig. 10.4. Diagram of the influence of the heating of the substrate on the erosion wear resistance at a contact angle of the jet 90°
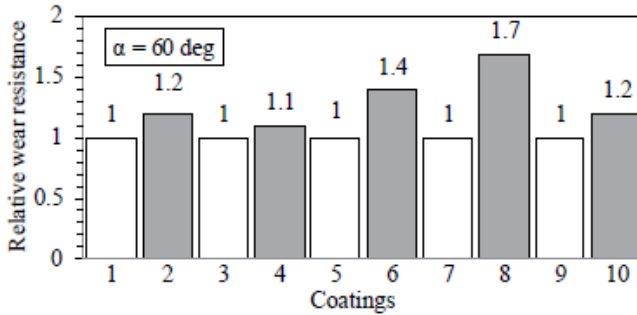

Fig. 10.5. Diagram of the influence of the heating of the substrate on the erosion wear resistance at a contact angle of the jet 60°

Wear of High-Technology Coatings, Deposited by High-Velocity Oxygen Flame (HVOF)
Determining the Influence of Chromium Concentration on the Erosive Wear of Ni-Cr-B-Si Coatings
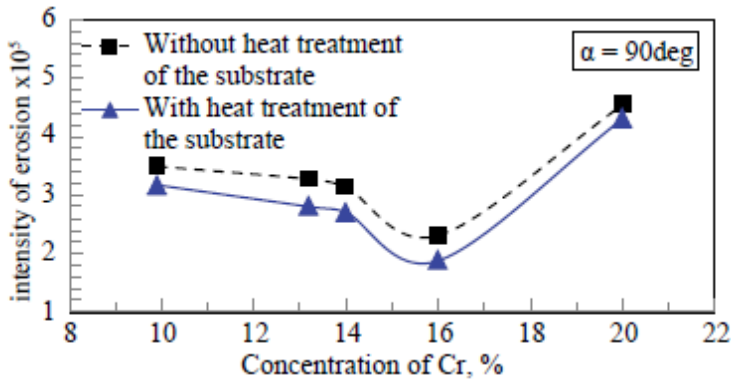*Applied by Supersonic Flame Jet (HVOF)*

Fig. 10.6. Dependence of the erosion intensity on the chromium concentration at a jet angle of 90°

For both jet angles all the tested coatings with thermal treatment of the substrate have better wear resistance than those of the coatings without thermal treatment of the substrate. The effect of thermal treatment of the substrate upon the wear resistance is greater at jet angle 60° and it is changing within the limits from 1.2 up to 1.7 times (Fig. 10.5). At jet angle 90° the increase in the erosion wear resistance is insignificant - from 1.1 to 1.2 times and it is almost one and the same for all the coatings (Fig. 10.4).
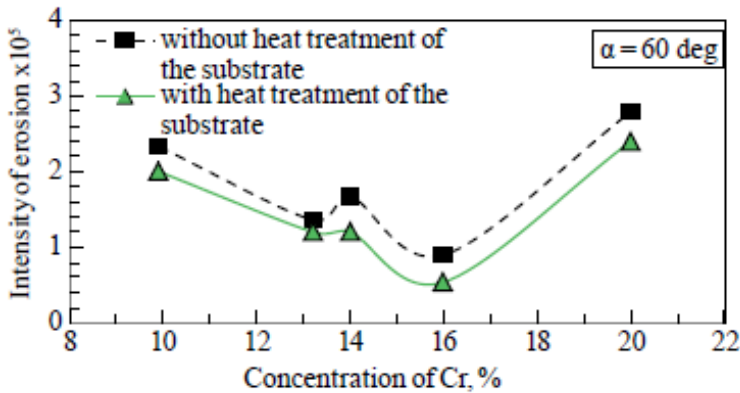

Fig. 10.7. Dependence of the erosion intensity on the chromium concentration at a jet angle of 60°
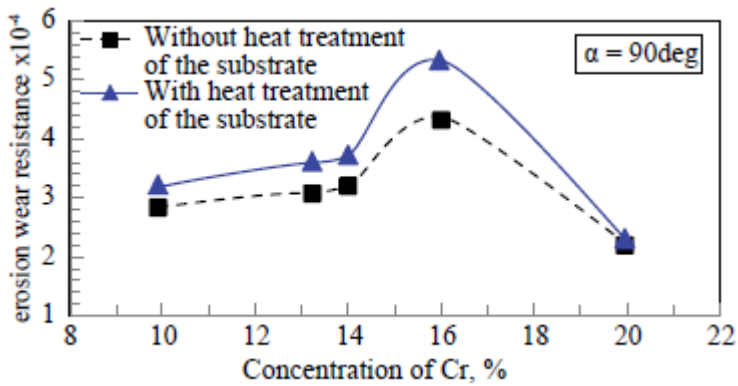
Wear of High-Technology Coatings, Deposited by High-Velocity Oxygen Flame (HVOF)
Determining the Influence of Chromium Concentration on the Erosive Wear of Ni-Cr-B-Si Coatings
Applied by Supersonic Flame Jet (HVOF)

Fig. 10.8. Dependence of the erosion wear resistanceon the chromium concentration at a jet angle of $90°$

Fig. 10.6 and Fig. 10.7 plot the dependences of the wear intensity as a function of the chromium concentration at both jet angles respectively for coatings without thermal treatment of the substrate and with thermal treatment of the substrate. It is seen that the dependence has non-linear character. Upon increasing the chromium concentration the erosion intensity is decreasing, and it reaches a minimal value for coatings having $16\%Cr$, and thereafter it grows up sharply for the coatings having $20\%Cr$, which do not contain the elements boron and silicon. At jet angle of $60°$ the curve has wave-like character, which is more clearly expressed for the coatings without thermal treatment of the substrate and containing $14\%Cr$ – one observes slight increase in the intensity of erosion (Fig. 10.7 - the dotted line).
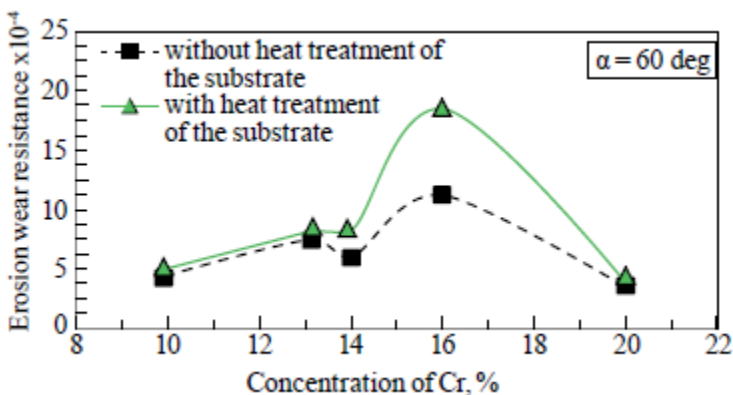

Fig. 10.9. Dependence of the erosion wear resistanceon the chromium concentration at a jet angle of $60°$
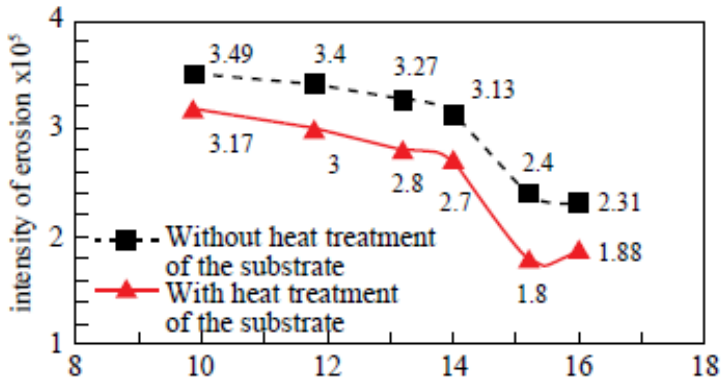
Wear of High-Technology Coatings, Deposited by High-Velocity Oxygen Flame (HVOF)
Determining the Influence of Chromium Concentration on the Erosive Wear of Ni-Cr-B-Si Coatings
Applied by Supersonic Flame Jet (HVOF)

Fig. 10.10. Dependence of the erosion inte nsity on chromium
concentration in the range from 9.9% to 16% at a jet angle of $90°$

The dependence of the erosion wear resistance on the chromium concentration is reciprocal with respect to the curve of the intensity of erosion. For both jet angles $90°$ and $60°$ this dependence is shown in Figs. 10.8 and 10.9 for all the tested coatings.

The coatings containing the greatest chromium concentration display lower erosion wear resistance. At jet angle $\alpha = 90°$ the wear resistance reaches values equal to the wear resistance of coatings having the lowest chromium content 9.9% (Fig. 10.9), while at $\alpha = 60° -$ smaller values (Fig. 10.8).

Regression Models. Measurements were made at 10 points on the surface and the mean arithmetic value was accepted (Table 10.1). The accuracy of the device is $1\mu m$. The experimental curve of the dependence of the erosion intensity on the chromium concentration in the interval for two angles of interaction of the jet with the surface $-90°$ and $60°$ is considered (Fig. 10.6 and Fig. 10.7).

The section of the curve $w > 16\%$ is not considered, because it includes coatings No 9 and No 10 (Ni80-20Cr and Ni80-20Cr: PHS) with different chemical composition from the other coatings. These coatings contain only nickel (80%) and chromium (20%), which does not give us reason to analyze them in parallel with the other coatings.

Experimental results for the intensity of erosion at a jet angle of $90°$ and $60°$ are represented in Table 10.7 and Table 10.8.

Based on the regression analysis, analytical dependences of the intensity of erosion on the chromium concentration were obtained, represented as secondand third-degree polynomials.

Table 10.7. Intensity of erosion at different chromium concentration, % at a jet angle of 90°

w, Concentration of Cr, (%)	9.9	11.8	13.2	14.0	15.2	16.0
i_e, intensity of erosion without heat treatment of the substrate	3.49×10^{-5}	3.4×10^{-5}	3.27×10^{-5}	3.13×10^{-5}	2.4×10^{-5}	2.31×10^{-5}
i_e, intensity of erosion with heat treatment of the substrate	3.17×10^{-5}	3.0×10^{-5}	2.8×10^{-5}	2.7×10^{-5}	1.8×10^{-5}	1.88×10^{-5}

Table 10.8. Intensity of erosion at different chromium concentration, % at a jet angle of 60°

w, Concentration of Cr, (%)	9.9	11.8	13.2	14.0	15.2	16.0
i_e, intensity of erosion without heat treatment of the substrate	2.33×10^{-5}	1.8×10^{-5}	1.36×10^{-5}	1.67×10^{-5}	1.2×10^{-5}	0.9×10^{-5}
i_e, intensity of erosion with heat treatment of the substrate	2.0×10^{-5}	1.6×10^{-5}	1.2×10^{-5}	1.2×10^{-5}	0.6×10^{-5}	0.54×10^{-5}

Wear of High-Technology Coatings, Deposited by High-Velocity Oxygen Flame (HVOF)
Determining the Influence of Chromium Concentration on the Erosive Wear of Ni-Cr-B-Si Coatings
Applied by Supersonic Flame Jet (HVOF)

For coatings without heat treatment of the substrate at jet angle 90° the dependence has the following form:

$$i_e(w) = a_3 w^3 + a_2 w^2. \tag{10.7}$$

The results are represented in the next Fig. 10.12.

The Adjusted R Square is 0.7454 and it shows that 74.54% of the variance of the intensity of erosion is predictable from chosen factors (w^3, w^2), which are adequately included in the model. The value of the significance F with significance level 0.05 is $0.000146 < 0.05 (0.0146\% < 5\%)$, i.e., the results are reliable (statistically significant) and the model is adequate. P-values of the coefficients of the regression equations with level of significance 0.05 are smaller than 0.00017, i.e., they are smaller than 0.05, which means that the coefficients are statistically significant, and the adequacy of the model is confirmed.
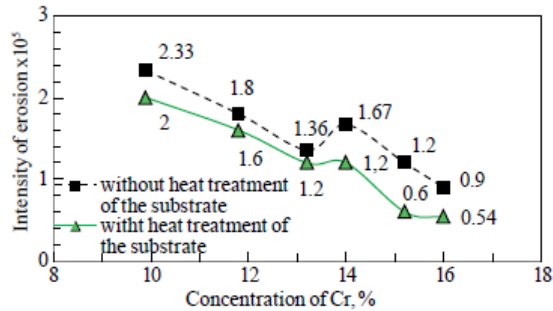

Fig. 10.11. Dependence of the erosion intensity on chromium concentration in the range from 9.9% to 16% at a jet angle of $60°$
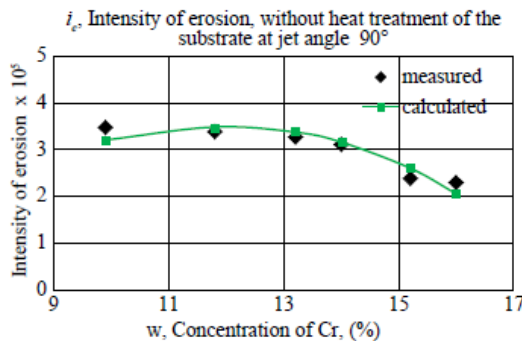

Fig. 10.12. Analytical dependences of the intensity of erosion on the chromium concentration for coatings without heat treatment at jet angle $90°$, $i_e(w) = 0.00000004053535w^3\ 0.000000729229w^2$

Wear of High-Technology Coatings, Deposited by High-Velocity Oxygen Flame (HVOF)
Determining the Influence of Chromium Concentration on the Erosive Wear of Ni-Cr-B-Si Coatings
Applied by Supersonic Flame Jet (HVOF)

For coatings with heat treatment of the substrate at jet angle of $90°$ the dependence has the following form

$$i_e(w) = b_2 w^2 + b_1 w.$$ (10.8)
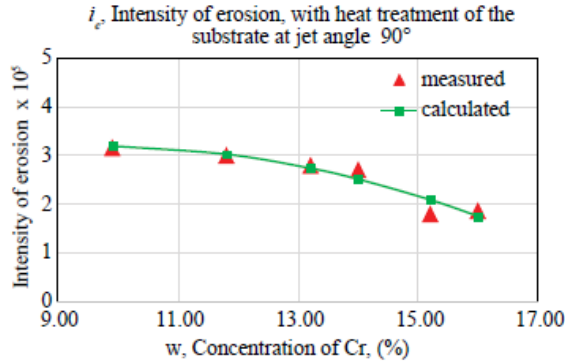
The results are represented in the next Fig. 10.13.

Fig. 10.13. Analytical dependences of the intensity of erosion on the chromium concentration for coatings with heat treatment at jet angle 90°, ie(w) = –0.000000349986w² + 0.000006699146w
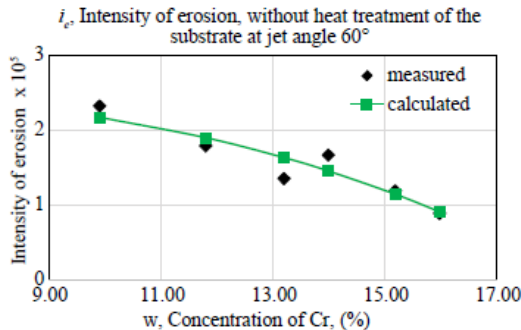

Fig. 10.14. Analytical dependenc- i_e, Intensity of erosion, without heat treatment of the es of the intensity of erosion substrate at jet angle $60°$ on the chromium concentration for coatings without heat treatment at jet angle $60°$, $i_e(w) = -0.000000004054378w^3 + 0.0000257484$

The Adjusted R Square is 0.7457 and it shows that 74.57% of the variance of the intensity of erosion is predictable from chosen factors (w^2, w), which are adequately included in the model. The value of the significance F with significance level 0.05 is $0.0001306 < 0.05(0.01306\% < 5\%)$, i.e., the results are

Wear of High-Technology Coatings, Deposited by High-Velocity Oxygen Flame (HVOF)
Determining the Influence of Chromium Concentration on the Erosive Wear of Ni-Cr-B-Si Coatings
Applied by Supersonic Flame Jet (HVOF)

reliable (statistically significant) and the model is adequate. P-values of the coefficients of the regression equations with level of significance 0.05 are smaller than 0.00033, i.e., they are smaller than 0.05, which means that the coefficients are statistically significant, and the adequacy of the model is confirmed.

For coatings without heat treatment of the substrate at jet angle of $60°$ the dependence has the following form

$$i_e(w) = c_3 w^3 + c_0. \tag{10.9}$$

The results are represented in the next Fig. 10.14.

The Adjusted R Square is 0.8426 and it shows that 84.26% of the variance of the intensity of erosion is predictable from chosen factor (w^3), which is adequately included in the model. The value of the significance F with significance level 0.05 is $0.0062 < 0.05(0.62\% < 5\%)$, i.e., the results are reliable (statistically significant) and the model is adequate. P-values of the coefficients of the regression equations with level of significance 0.05 are smaller than 0.0063, i.e., they are smaller than 0.05, which means that the coefficients are statistically significant, and the adequacy of the model is confirmed.

For coatings with heat treatment of the substrate at jet angle 60˚ the dependence has the following form:

$$i_e(w) = d_2 w^2 + d_1 w. \tag{10.10}$$
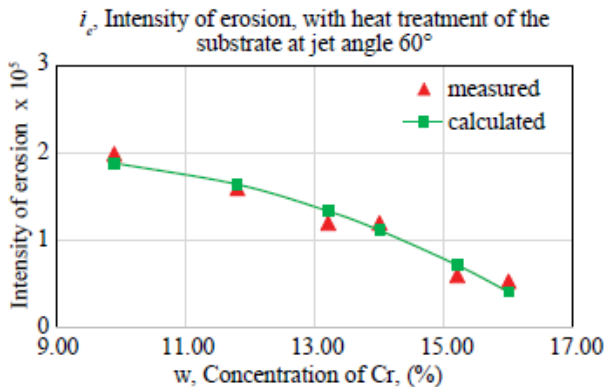
The results are represented in the next Fig. 10.15.

Fig. 10.15. Analytical dependences of the intensity of erosion on the chromium concentration for coatings with heat treatment at jet angle $60°, i_e(w) = -0.0000000270476968w^2 + 0.0000045861326w$

Wear of High-Technology Coatings, Deposited by High-Velocity Oxygen Flame (HVOF)
Determining the Influence of Chromium Concentration on the Erosive Wear of Ni-Cr-B-Si Coatings
Applied by Supersonic Flame Jet (HVOF)

The Adjusted R Square is 0.7411 and it shows that 74.11% of the variance of the intensity of erosion is predictable from chosen factors (w^2, w), which are adequately included in the model. The value of the significance F with significance level 0.05 is $0.0003885 < 0.05 (0.03885\% < 5\%)$, i.e., the results are reliable (statistically significant) and the model is adequate. $\square$-values of the coefficients of the regression equations with level of significance 0.05 are smaller than 0.00024, i.e., they are smaller than 0.05, which means that the coefficients are statistically significant, and the adequacy of the model is confirmed.

10.4 CONCLUSIONS

The present research work represents comparative results for erosion wear and erosion wear resistance of coatings, deposited by supersonic flame jet (HVOF), which contain composites $\text{Ni} - \text{Cr} - \text{B} - \text{Si}$ having various chromium concentrations $9.9\%; 13.2\%; 14\%; 16\%$ and 20%, at identical size of the particles $45\mu\text{m}$ and the same content of the remaining elements boron and silicon. The coating, prepared to have 20%Cr, does not contain the elements B and Si. Upon using each one powder composition coatings have been prepared without preliminary thermal treatment of the substrate and with preliminary thermal treatment of the substrate up to $650\degree\text{C}$. The coatings have been tested in identical regime of erosion using air stream, carrying abrasive particles under the same conditions - nature, sizes and velocity of the particles, duration of erosion, air pressure, distance between the nozzle and the surface, angle of the jet axis with respect to the surface.

Results have been obtained about the dependence of mass wear; the intensity of erosion and the erosion wear resistance on the chromium concentration in the coatings without and with thermal treatment of the substrate at two jet angles $60\degree$ and $90\degree$.

It has been established that:

- For all the coatings the preliminary thermal treatment of the substrate leads to decrease in the wear intensity, i.e. increase in the erosion wear resistance.
- The jet angle influences the erosion wear resistance of all the coatings. At jet angle of $60\degree$ the wear resistance grows up within the interval from 1.5 to 2.6 times for coatings without thermal treatment of the substrate and within the interval from 1.6 to 3.5 times for coatings with thermal treatment of the substrate in comparison with the wear resistance at jet angle of $90\degree$. This effect is greatest -3.5 times for the coating №8 having 16% Cr. At jet angle of $90\degree$ the wear resistance increases up to 10% and this increase is one and the same for all the coatings.
- The dependence of the erosion wear resistance on the chromium concentration has strongly non-linear character. The wear resistance is growing up with the increase in the chromium concentration and it reaches a maximum in the case of coatings having 16%Cr with thermal treatment of the substrate at jet angle of $60\degree$.

Wear of High-Technology Coatings, Deposited by High-Velocity Oxygen Flame (HVOF)
Determining the Influence of Chromium Concentration on the Erosive Wear of Ni-Cr-B-Si Coatings
Applied by Supersonic Flame Jet (HVOF)

- The wear resistance of the coatings, containing the highest chromium concentration -20%, but not containing the elements boron and silicon, is lower or almost equal to the wear resistance of coatings having the lowest chromium concentration -9.9%.

Regression models were obtained for the erosion intensity for two angles of the jet $60°$ and $90°$ for coatings without heat treatment and for coatings with heat treatment of the substrate.

REFERENCES

1.   Bhushan B. Principles and Applications of Tribology. New York: John Wiley & Sons; 2013.
2.   Cotell CM, Sprague JA. Preface. - In: ASM Handbook, Surface Engineering, ASM International, Metals Park. 1994;5.
3.   Martin PM. Introduction to Surface Engineering and Functionally Engineered Materials. Hoboken: John Wiley & Sons; 2011.
4.   Kandeva M, Vencl A, Karastoyanov D. Advanced Tribological Coatings for Heavy-Duty Applications: Case Studies, Monographia, ISBN: 978-954-322-858-4, Academy Publishing House, Sofia, Bulgaria. 2016;147.
5.   Kandeva M, Kalitchin ZH. Svoboda P, Sovilj-nikic S. General Methodology for Studying the Tribological Processes on the Basis of the Communicative Potential, J. Balk. Tribol. Assoc. 2019;25(2):432.
6.   Kandeva M, Karastoyanov D, Ivanova B, Asenova E. Tribological Interactions of Spheroidal Graphite Cast Iron Micro alloyed with TIN, Monography, ISBN: 978- 954-322-861-4, Academy Publishing House, Sofia, Bulgaria. 2016;160.
7.   Kandeva M, Penyashki T, Kostadinov G, Kalichin ZH. Abrasive and Erosion Wear of Composite NiCrSiB Coatings Inflicted with Subsonic Flammable Structure Through a Cold Process, International Conference on Tribology (ROTRIB'19), IOP Conf. Series: Materials Science and Engineering. 2020;724:012014.
8.   Kandeva M, Svoboda P, Kalitchin ZH, Penyashki T, Kostadinov G. Wear of Gas-Flame Composite Coatings with Tungsten and Nickel Matrix. Part II. Erosive Wear, J. Environ. Prot. Ecol. 2019;20(3):1292.
9.   Penyashki T, Kostadinov G, Radev D, Kandeva M. Comparative Studies of Tribological Characteristics of Carbon Steels with Gas Flame Coatings from New Multi-component Carbide Composite Materials, Oxid. Commun. 2019;42(1):74.
10.   Vencl AL, Bobic I, Bobic B, Jakimovska K, Svoboda P, Kandeva M. Erosive Wear Properties of ZA-27 Alloy-Based Nanocomposites: Influence of Type, Amount, and Size of Nanoparticle Reinforcement, Friction. 2019;7:340.
11.   Kandeva M, Penyashki T, Kostadinov G, Kalitchin ZH, Kaleicheva J. Wear of Electroless Nickel-Phosphorus Composite Coatings with Nanodiamond Particles, J. Environ. Prot. Ecol. 2018;19 (3):1200.
12.   Kandeva M, Grozdanova T, Karastoyanov D, Ivanov PL, Kalichin ZH. Tribology Study of High-Technological Composite Coatings Applied Using

Wear of High-Technology Coatings, Deposited by High-Velocity Oxygen Flame (HVOF)
Determining the Influence of Chromium Concentration on the Erosive Wear of Ni-Cr-B-Si Coatings
Applied by Supersonic Flame Jet (HVOF)

High Velocity Oxyfuel (HVOF), 9th International Conference on Tribology, BalkanTRib17, IOP Conf. Series: Mater. Sci. Eng. 2018;295:012025.

13. Kovac P, Jesic D, Sovilj-nikic S, Kandeva M, Kalitchin ZH, Gostimirovic M, et al. Energy Aspects of Tribological Behaviour of Nodular Cast Iron, J. Environ. Prot. Ecol. 2019;19(1):163.

14. Vencl N, Vaxevanidis M, Kandeva: A Bibliometric Analysis of Scientific Research on Tribology of Composites In Southeastern Europe, International Conference on Tribology (ROTRIB'19), IOP Conf. Series: Materials Science and Engineering, 724012012 .
DOI: 10.1088/1757-899X/724/1/012012 (2020)

15. Holmberg K, Matthews A. Coatings Tribology: Properties, Mechanisms, Techniques and Applications in Surface Engineering. Amsterdam: Elsevier; 2009.

16. Petrov T, Tashev P, Kandeva M. Wear Resistance of Surface Layers Modified with AL_2O_3 and TiCN Nanopowders Weld Overlaid Using TIG and ITIG Methods, J. Balk. Tribol. Assoc. 2016;22(1):304.

17. An Introduction to Thermal Spray. Brochure, Oerlikon Metco, Winterthur; 2015.
Available:http://www.oerlikon.com / metco).

18. Schorr B, Stein KJ, Marder A. Characterization of Thermal Spray Coatings. Materials Characterization. 1999;42:93.

19. Vaxevanidis N, Vencl AL, Assenova E, Kandeva M, Psyllaki P. Scientific Literature on Thermal Spray Coatings from Southeastern Europe: A Ten Years Bibliometric Analysis, FME Transactions. 2019;47:649.

20. Vencl: Optimization of the Deposition Parameters of Thick Atmospheric Plasma Spray Coatings, J. Balk. Tribol. Assoc. 2012;18(2):405.

21. Kandeva M, Zadorozhnaya E, Kalitchin ZH, Svoboda P. Tribological Studies Of High Velocity Oxy-Fuel (HVOF) Superalloy Coatings, J. Balk. Tribol. Assoc. 2018;24(2):411).

22. Rukhande SW, Rathod WS. Tribological behaviour of plasma and HVOF-sprayed NiCrSiBFe coatings. Surface Engineering. 2020;36(7):745-55.

23. Castro RD, Rocha AD, Mercado Curi EI, Peruch F. A comparison of microstructural, mechanical and tribological properties of WC-10Co4Cr-HVOF coating and hard chrome to use in hydraulic cylinders. American Journal of Materials Science. Rosemead, CA. 2018;8(1):15-26.

24. Wang S, Ma C, Walsh FC. Alternative tribological coatings to electrodeposited hard chromium: a critical review. Transactions of the IMF. 2020;98(4):173-85.

25. Kandeva M, Grozdanova T, Karastoyanov D, Ivanov P, Kalichin ZH. Tribology Study of High-Technological Composite Coatings Applied Using High Velocity Oxy-Fuel, IOP Conference Series: Materials Science and Engineering, 295, (1), Art. No 012025 , ISSN:1757-8981, 9th International Conference on Tribology, Balkantrib 2017; Cappadocia, Nevsehir; Turkey; 13 September 2017 through 15 September 2017; Code 135934(2018).

26. Guilemany JM. J. NIN: Thermal spraying methods for protection against wear. - In: Mellor, B. G (Ed.), Surface Coatings for Protection against Wear, Cambridge, Woodhead Publishing. 2006;249.

Wear of High-Technology Coatings, Deposited by High-Velocity Oxygen Flame (HVOF)
Determining the Influence of Chromium Concentration on the Erosive Wear of Ni-Cr-B-Si Coatings
Applied by Supersonic Flame Jet (HVOF)

27. Pawlowski L. The Science and Engineering of Thermal Spray Coatings. Chichester: John Wiley & Sons; 2008.
28. Bahadur S, Badruddin R. Erodent particle characterization and the effect of particle size and shape on erosion. – Wear. 1990;138:189.
29. Goodwin JE, Sage W, Tilly GP. Study of erosion by solid particles. - Proceedings of the Institution of Mechanical Engineers. 1969;184 (1):279.
30. Kandeva M, Grozdanova T, Karastoyanov D, Assenova E. Wear Resistance of WC/Co HVOF-Coatings and Galvanic Cr Coatings Modified by Diamond Nanoparticles, 13th International Conference on Tribology ROTRIB'16, Galați, Romania, IOP Conf. Series: Materials Science and Engineering. 2017;174:012060.
    DOI:10.1088/1757-899X/174 (1) 012060(2016)
31. Czuprynski: A. Properties of Al_2 O_3/TiO_2 and ZrO_2/CaO flame sprayed coatings, Spajanie Materiałów Konstrukcyjnych. 2017; 2:32.
32. Czuprynski A, Górka J, Adamiak M, Tomiczek B. Testing of Flame Sprayed Al2O3 Matrix Coatings Containing TiO, Arch. Metall. Mater. 2016;6:1363.
33. Czuprynskki A. Flame Spraying of Aluminum Coatings Reinforced with Particles of Carbonaceous Materials As an Alternative for Laser Cladding Technologies, Materials. 2019;12:3467.
34. Kulu P, Pihl T. Selection criteria for wear resistant powder coatings under extreme erosive wear conditions, Journal of Thermal Spray Technology. 2002;11:517.
35. Lalit Thakur L, Arora N. A Study on Erosive Wear Behavior of HVOF Sprayed Nanostructured WC-CoCr Coatings, Journal of Mechanical Science and Technology. 2013;27.
36. Kandeva M, Kalitchin ZH, Stoyanova YA. Influence of Chromium Concentration on the Abrasive Wear of Ni-Cr-B-Si Coatings Applied by High-Velocity Oxygen Fuel, Metals. 2021;915.
37. Kulu P, Zimakov S. Wear Resistance of Thermal Sprayed Coatings on the Base of Recycled Hardmetal, Surface and Coatings Technology. 2000;130:46.
38. Miguel Ángel Reyes-mojena, Mario Sánchez-orozco, Hipólito Carvajal-fals, Roberto Sagaró-Zamora, Carlos Roberto Camello-lima: A Comparative Study on Slurry Erosion Behavior of HVOF Sprayed Coatings, Dyna. 2017;84.

COMPETING INTERESTS

Authors have declared that no competing interests exist.
_____

REFERENCES

1. Jost P. Some economic factors of tribology. Proceedings of the JSLE-ASLE Elsever, Amsterdam; 1976.
2. Frene J, Nicolas D, Degueurce B, Berthe D, Godet M. Lubrification hydrodynamidue, Paliers et Butees. Paris: Edutions Eyrolles; 1990.
3. Hutchings I, M, TIBOLOGY. Friction and wear of engineering materials. London: Edward Arnold; 1992.
4. Bowden FP, Tabor D. The friction and lubrication of solids, Oxford at the clarendon Press; 1964.
5. Moore DF. Principles and application of Tribology. Oxford: Pergamon Press; 1975.
6. Moore D. The friction and lubrication of elastomers. Pergamon Press; 1977.
7. Gras R, Tribologie. Principes et solutions industrielles, L'usinenouvelle. Dunod; 2008.
8. Kandeva M. The interdisciplinary paradigm of tribology. J Balk Tribol Assoc. 2008;14(4):421-30.
9. Kandeva M. On the law of Contact Gap Change. Belgrade (Serbia), Proceedings, 2001, Seventh Yugoslav Tribol Conference – YUTRIB, ISBN: 86-902487-1-4; '01. p. 5.21-3.
10. Stachowiak G, Batchelor A. Engineering tribology. Elsevier; 2014.
11. Vencl A, Manić N, Popovic V, Mrdak M. Possibility of the abrasive wear resistance determination with scratch tester. Tribol Lett. 2010;37(3):591-604.
12. Braithwaite E. Solid Lubricants and surfaces. Oxford: Pergamon Press; 1972.
13. Tashev Pl. Introduction of nanoparticles in the liquid phase during welding, Publishing House of BAS "Prof. Marin Drinov",. Sofia ISBN: 978-619-245-065-6; 2020 (in Bulgarian).
14. Penyashki T, Kostadinov G, Kandeva M, Radev D. Electrospark and gas-flame layering. Opportunities and applications [monograph] Company R, editor. Sofia, ISBN: 978-954-92236-9-9; 2020 (in Bulgarian).
15. Wood RJKMR. Tribology of thermal-sprayed coatings. In: Roy M, editor, Surface engineering for enhanced performance against wear. Wien: Springer; 2013. p. 1-43.
16. Pawlowski L. The science and engineering of thermal spray coatings. Chiches ter: John Wiley & Sons; 2008.
17. Kandeva M, , AlKarastoyanov, Al D. Vencl, advanced tribological coatings for heavy-duty applications: case studies, Prof. Marin Drinov publishing house of Bulgarian Academy of Sciences, Sofia, 2016.
18. Practical applications of gas-thermal technologies for the application of protective coatings, Guide for Engineers, LLC. Therm Spray Technol. 2007. (in Russian).
19. Kiselev VS, Nagorny DA, Mankovsky SA. Carrying out of the automated electric drive for the process of supersonic gas-powder Cladding// International Sci-entific and Practical Conference of Students. Post-graduetes and young scientists" modern techniques and

technologies"(MTT). Tomsk: Tomsk Polytechnic University. Tomsk: TPU Press. 2007;51-53.

20. GOST 28844-90, Gas-thermal and reducing coatings, General requirements.

21. Available: http://www.gordonengland.co.uk/hvof.htm.

22. Available: http://www.tspc.ru/tech/HVOF.php.

23. Barbezat G, Nicol AR, Sickinger A. Abrasion, erosion and scuffing resistance of carbide and oxide ceramic thermal sprayed coatings for different applica-tions. Wear. 1993;162-164(A):529-37.

24. Oksa M, Turunen E, Suhonen T, Varis T, Hannula S-P. Optimization and characterization of high velocity oxy-fuel sprayed coatings, Techniques. materials. Coatings. 2011;1(1):17-52.

25. Liu Y, Fischer TE, Dent A. Comparison of HVOF and plasma-sprayed alumina/titania coatings – microstructure, mechanical properties and abrasion behaviour, Surface and Coatings Technology. 2003;167(1):68-76.

26. Oksa M, Turunen E, Suhonen T, Varis T, Hannula S-P. Optimization and characterization of high velocity oxy-fuel sprayed coatings, Techniques. materials. Coatings. 2011;1(1):17-52.

27. Vaksevanidis N, Vencl A, Asenova E, Kandeva M, Psilaki P. Scientific literature on thermal spray coatings from southeastern Europe: A ten years bibliometric analysis. FME Trans. 2019;47(3):649-57, ISSN: 1451-2092.

28. Cabral-Miramontes JA, Gaona-Tiburcio C, Almeraya-Calderón F, Estupiñan-Lopez FH, Pedraza-Basulto GK, Poblano-Salas CA. Parameter studies on high-velocity oxy-fuel spraying of CoNiCrAlY coatings used in the aeronautical industry. Int J Corros. 2014;2014:Article ID 703806.

29. Chivavibul P, Watanabe M, Kuroda S, Kawakita J, Komatsu M, Sato K et al. Effect of powder characteristics on properties of warm-sprayed WC-Co coatings. J Therm Spray Technol. 2010;19(1-2):81-8.

30. Vencl A. Optimization of the deposition parameters of thick atmospheric plasma spray coatings. J Balk Tribol Assoc. 2012;18(3):405-14.

31. Peichev I, Kandeva M, Assenova E, Pojidaeva V. About the deposition of superalloys by means of supersonic HVOF process. Proceedings, 91-97, 12th International Conference on Tribology – SERBIATRIB'11, Kragujevac (Serbia). p. 11-13.05.2011.

32. About thermal spray [poster]. Duiven: Flame Spray Technologies. Available: http://www.fst.nl.

33. Kandeva M, Ivanova B, Pozhidaeva V, Karastoyanov D, Javorova J. Compos-ite coatings to improve durability of the working body of the drill. – Proceedings of 5th World Tribol Congress (WTC 2013), Turin (Italy), 08-13.09.2013:Paper 1251.

34. Kandeva M, Karastoyanov D, Vencl A, Peichev I, Ivanova B, Assenova E. Wear-resistance of composite coatings deposited by gas-flame supersonic HVOF process. Proceedings of the XIV international scientific conference "tribology and reliability," Saint Petersburg, Russia; 2014;307-21.

35. Kandeva M, Grozdanova T. Effect of Vibration Velocity on the Wear Under Conditions of Abrasive Friction. Proceedings, 14th International Conference on Tribology SERBIATRIB'15, Belgrade, Serbia. 2015;272-8.
36. Kandeva M, Ivanova B, Pozhidaeva V, Karastoyanov D, Javorova J. Compos-ite coatings to improve the durability of the working body of the drill. – Proceedings of 5th World Tribol Congress (WTC 2013), Turin (Italy), 08-13.09.2013:Paper 1251.
37. Kandeva M, Penyashki T, Kostadinov G, Nikolova M, Grozdanova T. Wear resistance of multi-component composite coatings applied by concentrating energy flows, 16th International Conference on Tribology SERBIATRIB '19. may 15-17 2019, Proceeding on Engineering Sciences;1:1, 197-207, ISSN: 2620-2832.
38. Penyashki T, Kandeva M, Kostadinov G, Dimitrova E, Mortev I. Considerations for the selection of materials for electrical spark and gas flame spraying deposition on structural steels, 16th International Conference on Tribology SERBIATRIB '19. may 15-17 2019, Proceeding on Engineering Sciences;1:1, 212-226, ISSN: 2620-2832.
39. Penyashki T, Kostadinov G, Radev D, Kandeva M. Comparative studies of tribological characteristics of carbon steels with gas flame coatings from new multi-component carbide composite materials. Oxid Commun. 2019;42(1):74-90.
40. Kandeva M, Svoboda P, Kalitchin Zh, Penyashki T, Kostadinov G. Wear of gas-flame composite coatings with tungsten and nickel matrix. Part I. Abrasive wear. J Environ Prot Ecol. 2019;20(2):811-22.
41. Kandeva M, Svoboda P, Kalitchin Zh, Penyashki T, Kostadinov G. Wear of gas-flame composite coatings with tungsten and nickel matrix. Part II. Erosive wear. J Environ Prot Ecol. 2019;20(3):1292-302.
42. Kandeva M, Grozdanova T, Karastoyanov D, Ivanov PI, Zh K. Tribology study of high-technological composite coatings applied using high velocity oxyfuel (HVOF). Mater Sci Eng, 9th International Conference on Tribology, Balkan TRib17, IOP Conference Series. 2018;295:012025.
43. Kandeva M, Zadorozhnaya E, Kalitchin Zh, Svoboda P. Tribological studies of high Ve-locity oxy-fuel (HVOF) superalloy coatings. J Balk Tribol Assoc. 2018;24(3):411-28.
44. Kandeva M, Grozdanova T, Karastoyanov D, Ivanova B, , AlJakimovska, Al K. Vencl, wear under vibration conditions of spheroidal graphite cast iron microalloyed by Sn. J Balk Tribol Assoc. 2016;22(2A):1729-40.
45. Kandeva M, Ivanova B, Karastoyanov D, Grozdanova T, Assenova E. Abrasive wear of high velocity oxygen fuel (HVOF) superalloy coatings under vibration load. Mater Sci Eng, 13th International Conference on Tribology ROTRIB`16, (2016), Galați conference Series. 2017;1, 174:012010.
46. Kandeva M, Kalitchin Z, Stoyanova Y. Influence of chromium concentration on the abrasive wear of Ni-Cr-B-Si coatings applied by supersonic flame jet (HVOF). Metals. 2021;11(6):915.
47. Kandeva M, Kalitchin Zh, Stoyanova Y. Influence of chromium concentration on the erosive wear of Ni-Cr-B-Si coatings applied by supersonic flame jet (HVOF). J Balk Tribol Assoc. 2021;27(6):977-96.

48. Kandeva M, Gidikova N, Valov R, Petkov V, Kalchevska K, Torbova M. Wear resistance of chromium composite galvanic coating modified with Nanodiamond particles. Proceedings of the 9th international conference THE – "A" coating in manufacturing engineering, Oct 3-5, Thessaloniki, Greece, ISBN 978-960-98780-5-0; 2011.

49. Petkov V, Valov R, Simeonova S, Kandeva M. Characteristics and properties of chromium coatings with diamond nanoparticles deposited directly on aluminum alloys. Arch Foundry Eng. 2020;20(4):115-20.

50. Petkov V. Chrome plating with diamond nanoparticles deposited on metal alloys, Publishing House of BAS "Prof. Marin Drinov",. Sofia ISBN: 978-619-245-135-6; 2021 (in Bulgarian).

51. Kandeva M, Grozdanova T, Karastoyanov D, Assenova E. Wear resistance of WC/Co HVOF-coatings and galvanic Cr Coatings modified by diamond nanoparticles. Mater Sci Eng, 13th International Conference on Tribology ROTRIB'16, (2016), Galați Conference Series. 2017;1(174):012060.

52. Kandeva M. The contact approach in engineering tribology, TU-Sofia Publishing

53. House, ISBN: 978-954-438-986-4; 2012 (in Bulgarian).
_____

Biography of author(s)

Mara Kandeva

Faculty of Industrial Engineering, Tribology Center, Technical University – Sofia, 8, Kl. Ohridski Blvd, 1756 Sofia, Bulgaria.

Research and Academic Experience: Lecturer of "Bachelor" and "Master" students in the following disciplines: Technical Mechanics, Theoretical Mechanics, Dynamics and Tribology of Machines, Tribology and Lubricants, Engineering Triboecology, Micromechanics, and Nanotribology. Head of Ph.D. students in tribology. Head of national and international projects in the field of tribology. President of the Society of Tribologists in Bulgaria. Member of the editorial board of the International Journal of the Balkan Tribological Association.

Research Area: Fundamental research in tribology: development of an interdisciplinary paradigm of tribology and a new contact approach for the study of contact interactions in tribosystems.

Applied tribological studies:

- Friction, abrasive, and erosion wear of high-tech coatings applied by supersonic flame jet;
- Friction, abrasive, and erosion wear of chemical nickel coatings modified with nanosized particles of diamond, silicon carbide, and boron nitride.
- The influence of metal-plating additives on the antifriction and anti-wear properties of mineral and biodegradable oils;
- Friction, abrasive, and erosion wear of biodegradable materials obtained by 3D printing;
- Research and technologies for restoration of automobile air filters without dismantling the filter element.

Number of Published papers: 11 books: monographs and textbooks; six patents; over 300 scientific publications.

Special Award: Gold badge "Prof. Dr. Asen Zlatarov" of the Federation of Scientific and Technical Unions in Bulgaria; Diploma for "Tribologist of the Year" of the Society of Tribologists in Bulgaria.

Zhetcho Kalitchin
SciBulCom2 Ltd., 2A, Yakubitza Str., 1164 Sofia, Bulgaria.

Research and Academic Experience: PhD thesis and assoc. prof. in the Institute of Organic Chemistry of the Bulgarian Academy of Sciences.

Professor in the Publishing House "SciBulCom" Ltd.

Research Area:

- Investigation of the mechanism of oxidation of organic compounds, antioxidants, and catalysts by chemiluminescence. Research in the field of a new contact approach for the study of contact interactions in tribosystems;
- Risk assessment in the insurance industry and in the protection of the environment;
- The influence of metal-plating additives on the antifriction and anti-wear properties of mineral and biodegradable oils;
- Friction, abrasive and erosion wear of biodegradable materials obtained by 3D printing;

Number of Published papers: 170 papers and 3 books.

Any other remarkable point(s): Deputy Editor-in-Chief of 3 scientific journals indexed in SCOPUS and one of them in Web of Science.

Yana Stoyanova (Associate Professor)
Faculty of Industrial Engineering, Tribology Center, Technical University – Sofia, 8, Kl. Ohridski Blvd, 1756 Sofia, Bulgaria.

Research and Academic Experience: Lecturer of "Bachelor" and "Master" students in the following disciplines: Risk Management, Big Data, Data Mining, Modelling the Spread of Pollutants in the Environment.

Research Area: Differential Equations, Asymptotic Methods, Synthesis and Analysis of Mechanisms, Analysis of Mechanical Systems, Modeling of Processes in Ecology, Risk Analysis and Management, Data Mining.

Number of Published papers: Four patents; over 65 scientific publications.
_____

London   Tarakeswar